T H E U N I V E R S I T Y O F M I C H I G A N

MEDICAL SCHOOL
Department of Physical Medicine and Rehabilitation
Orthetics Research Project

Technical Report No. 5

CHARACTERISTICS OF THE BRAIDED FLUID ACTUATOR

H. F. Schulte, Jr.
D. F. Adamski
J. R. Pearson

ORA Project 04468

under contract with:

OFFICE OF VOCATIONAL REHABILITATION
DEPARTMENT OF HEALTH, EDUCATION, AND WELFARE
CONTRACT NO. 216
WASHINGTON, D.C.

administered through:

OFFICE OF RESEARCH ADMINISTRATION ANN ARBOR

November 1961

TABLE OF CONTENTS

TABLE OF CONTENTS (Concluded)

LIST OF ILLUSTRATIONS

LIST OF ILLUSTRATIONS (Continued)

LIST OF ILLUSTRATIONS (Continued)

LIST OF ILLUSTRATIONS (Continued)

LIST OF ILLUSTRATIONS (Continued)

LIST OF ILLUSTRATIONS (Continued)

LIST OF ILLUSTRATIONS (Concluded)

NOMENCLATURE

A_s = Pressure stable cross-sectional area of a BFA, i.e., when T = 0. Cross-sectional area of a pneumatic cylinder the force output of which is compared to the ideal output of a BFA ($in.^2$)

$B = \left(\frac{\cos \theta_o}{L_o}\right)^2$

$C = (1 - BL^2)^{1/2}$

D = Ideal maximum diameter of the braided sheath when fully compressed (in.)

D_o = Diameter of a BFA at its free length, i.e., the fabricated diameter of the braided sheath (in.)

D_s = Pressure stable diameter of a BFA, i.e., when T = 0 (in.)

E = Absolute usable excursion of a BFA, $|L_m - L_s|$ (in.)

F = Total circumferential force (tensile) in the walls of a BFA, assuming that they are an integral unit composed of the braided sheath and elastic inner tube (F' + F") (lb)

F' = Circumferential force (tensile) in the walls of the elastic inner tube (lb)

F" = Circumferential force (tensile) in the strands of the braided sheath (lb)

L = Length of a BFA at any value of θ (in.)

L_c = Cut-off length. The absolute maximum length to which an actual BFA can be elongated, i.e., when P = 0 (in.)

L_h = Straight length of a single strand of material in the braided sheath (in.)

L_m = Maximum working length. Maximum recommended usable length of a BFA (in.)

L_o = Free length of a BFA, i.e., the fabricated length (in.)

L_s = Pressure stable length of a BFA, i.e., when T = 0 (in.)

M = Mass of gas (CO_2) consumed by a particular BFA at standard atmospheric conditions (oz)

N = Normal force between the sheath and elastic inner tube and between the strands of the sheath due to the internal pressure acting on these surfaces. Normal means at a right angle to the surface (lb)

P = Total internal pressure which activates a BFA ($P' + P''$) (psig)

P' = A partial pressure which maintains force equilibrium in the elastic inner tube at a given configuration of a BFA (psig)

P'' = A partial pressure, acting on the internal surface area of a BFA, which creates the force N the vector resolution of which is the force F" (psig)

T = Total tensile force output of a BFA (lb)

T_f = Fraction of the total tensile force output of a BFA due to frictional effects (lb)

T_{max} = Theoretical maximum force output of a BFA (lb)

T_p = Fraction of the total force output of a BFA due to the action of an internal pressure (lb)

T_r = Fraction of the total tensile force output of a BFA due to the action of the rubber inner tube (lb)

T' = Theoretical tensile force output of a pneumatic cylinder having a cross section equal to the stable cross section of a BFA (lb)

U = $(u_t + u_s)$ (dimensionless)

V = Volume of gas consumed by a particular BFA at standard atmospheric conditions ($in.^3$)

W = Flat width or width of a BFA when flattened against a level surface (in.)

Z = Fabricated circumference of the braided sheath (in.)

d = Diameter of a BFA at any value of θ (in.)

d_o = Mean unelongated diameter of the elastic inner tube, i.e., when P = 0. For practical purposes this diameter is identically equal to D_o

k_e = Elastic constant of the rubber inner tube. This parameter is assumed equal in both the axial and circumferential directions (lb/in.^{2})*

m = Number of strands in the braided sheath

n = Number of spiral turns made by a single strand in the helical (braided) sheath

t_f = Frictional forces created within a BFA (lb)

t_p = Force of pressure acting on the ends of a BFA (lb)

t_r = Axial retractive force of the rubber inner tube (lb)

t_t = Total axial component of the force (tensile) in the braided sheath (lb)

u_s = Coefficient of friction between the strands of the braided sheath (dimensionless)

u_t = Coefficient of friction between the strands of the braided sheath and the elastic inner tube (dimensionless)

θ = Fabricated helix angle of the braided sheath. The angle between an elemental length of a strand forming the helix and the longitudinal axis of a BFA (degrees)

θ_c = Cut-off angle. The lower limit of θ due to binding the crossed strands in the braided sheath (degrees)

θ_m = Helix angle of a BFA at L_m (degrees)

θ_o = Helix angle of a BFA at L_o (degrees)

θ_s = Pressure stable helix angle, i.e., when T = 0 (degrees)

*See page 106 and 107; also Appendix D, page 123.

I. INTRODUCTION

In 1955 Dr. J. L. McKibben, a physicist, devised a simple yet versatile gas-operated device for externally powering orthetic devices used by physically disabled individuals. Technically, the McKibben Artificial Muscle is an actuator or transducer which can use either gas or liquid as its working fluid. It belongs in the general category of pressure-actuated devices, of which pistons and bellows are other examples. The "muscle" consists of a straight piece of hollow braided sleeving, a gas-tight inner elastic tube, and suitable end closures for external attachment and pressurization. When inflated, the outer sleeve tends to increase its diameter which in turn tends to decrease its axial length. Dr. McKibben's device can be conveniently described as a Braided Fluid Actuator, or BFA.

The theory and a working model of the device (which consisted of a 6-in. length of 3/8-in.-diam. Penrose drainage tubing inserted in a braided nylon parachute cord) were presented in 1957 at the Rancho Los Amigos Hospital in Downey, California. There, development of the BFA into a practical source of orthetic power was undertaken by a staff of orthotists under the direction of Dr. V. L. Nickel. The basic elements of one of the first practical actuators as developed at the Rancho Hospital are illustrated in Fig. 1.

In March, 1958, the National Foundation for Infantile Paralysis (now the National Foundation) sponsored a conference on the McKibben Artificial Muscle at the Rancho Hospital, to present the results and ideas of those concerned with development and application of the device, and to stimulate new ideas and interest on the part of those attending.

A review of the 1958 conference proceedings indicated that information contained in the report[1] was insufficient to design a satisfactory orthetic system. As a consequence, a measurement and analysis program using BFA's supplied by Rancho was initiated at The University of Michigan to provide the desired information. The early work was supported by funds from the National Foundation, with Dr. D. G. Dickinson, Medical Director of The University of Michigan Children's Rehabilitation Service, as project director. Later the program was broadened and support was provided by the Office of Vocational Rehabilitation, Department of Health, Education, and Welfare, with Dr. J. W. Rae, Jr., of The University of Michigan Orthetics Research Project, as project director. A preliminary report of this work was presented at the Lake Arrowhead Conference on the Application of External Power in Prosthetics and Orthotics, in September, 1960.[7]

This report discusses the various types of BFA's developed as of July, 1960, defines the physical parameters of their construction, describes their operating characteristics, and recommends certain improvements in their design.

It is hoped that the information which follows will assist in the effective utilization of the BFA as well as stimulate evaluation of current actuators and development of other sources of power for orthetic devices. In addition, the nomenclature defined herein is presented for consideration as a standard means of measuring and describing various parameters of the BFA.

At the outset of this work, it seemed clear that too little was known about BFA characteristics to expect optimum or perhaps even reasonable utilization of the BFA in powering a useful orthetic device. The human motor system consists of a matrix of articulated levers moved by means of muscles. Because the effective lever arms through which the muscles act are short in proportion to the resistive lever-arm length, the muscles are required to generate large retractive forces to provide adequate response speed and force output. The forces developed by muscles are not constant throughout their excursion, but vary at different lengths, becoming less as they shorten and greater as they lengthen. These force variations are not observed in ordinary movements because of the existence of compensatory body mechanisms which maintain relatively constant moments around joints by variations in effective lever arms or through integrated motions of contiguous joints.[2] These relationships must be appreciated and accounted for in any truly useful design of an orthetic device.

When an assistive device uses external power, additional problems arise because of the force-versus-excursion characteristics of the BFA. As shown later, the BFA excursion curves are remarkably similar to those of human muscle. This is sometimes advantageous and sometimes not, depending on the application. The main point is that the designer must deal with the BFA characteristics as presented herein, and use all his ingenuity to devise a brace-BFA system which provides satisfactory function while making good use of the available power.

To determine the type of data needed to achieve these aims, the design of a functional arm brace system was undertaken. The first system of this type (Fig. 2) required two identical actuators, one anterior and one posterior, of the upper-arm section of the brace. The actuators were connected together by a flexible cable which passed over a pulley pivoted at the shoulder joint. This was necessary because the anterior actuator had a fixed point of attachment on the forearm section of the brace, and when lifting the patient's arm, plus the weight equivalent of a full glass of water as a useful load, one actuator of the type available at the time could not provide the required contraction to permit motion through the standard 135° of arm flexion. It was possible to eliminate the posterior actuator by designing a sliding point of attachment for the anterior actuator as shown in Fig. 3. The variable lever arm which resulted compensated for the decrease in force output of the actuator as it contracted, thereby matching the output load moment at the elbow joint. Work on the brace was discontinued at this point since the experiment clearly defined the type of performance data required for satisfactory application of the actuator.

A. GENERAL DESCRIPTION OF THE BFA

The BFA consists essentially of two parts: a contractive element and a fluid retainer. The contractive element is composed of strands of nylon fibers woven over a cylindrical form in a double criss-cross pattern to form a tubular braid similar to the familiar "Chinese Finger Trap." The fluid retainer consists of a thin-walled rubber tube sealed with metal ends to form a balloon-type chamber. One of the ends is fabricated with fittings containing a hole through which fluid can enter. Reference is again made to Fig. 1, page 6. Figure 4 is a photograph of one of the first actuators. The rubber tube fitted with the end pieces is placed within the nylon braid. The braid is tied in place with nylon thread. The retainer rings are then placed over the threaded ends and secured in place with nuts to form a single unit, thus completing the actuator.

Inflating the device with a fluid causes a simultaneous diametral expansion and axial contraction. Since the strands of the nylon braid form criss-cross helixes, the increase in diameter caused by internal pressure decreases the lead of the helix and thus reduces the over-all length of the device. The action is analogous to that of scissors in which the handle-to-tip distance decreases while the tip-to-tip distance increases as the scissors are opened (see Fig. 5).

In the BFA, the axial contraction causes an axial tensile force to be exerted when the ends are secured in place or otherwise restrained from free movement such as when lifting a weight or powering an orthetic device. This force varies as the actuator contracts, decreasing as it shortens and increasing as it lengthens, provided the fluid is contained in a closed system. The result is similar to the force excursion characteristics of human muscles.

B. DESCRIPTION OF A BASIC BFA ORTHETIC SYSTEM

A complete basic orthetic system for the BFA consists of the actuator and its hardware, an orthetic device, a harness and a paralytic, as shown schematically in Fig. 6. The paralytic uses human muscle power to actuate the control valve through the harness, thus releasing fluid energy which activates the BFA. The actuator converts fluid energy to mechanical energy which activates the orthetic device, thus providing the paralytic with a useful motion. After each cycle of use the gas is exhausted to the atmosphere. The patient may use residual power of afflicted or unafflicted muscles to activate the control valve, depending on his capabilities and the design of the harness. When unafflicted muscles are used, the point of control for the valve is in practice usually located remotely from the orthetic device. The virtue of this practice is doubtful.

The basic hardware of the BFA system consists of a gas cylinder, pressure regulator, control valve, and a supply line. The general relationship of these items in a system in which the control valve is connected directly to the

pressure regulator is shown in Fig. 7. The only difference in a system involving a remotely located control valve is a supply line connecting the valve to the regulator. A brief description of each of the above mentioned components follows.*

1. Gas cylinder.—The cylinder is a high-pressure, seamless steel container, production tested to 3000 psi and approved by the Federal ICC. Cylinders are available in various sizes having a gross weight range of approximately 1 lb 13 oz to 8 lb, and containing from 2 to 56 oz of liquid carbon dioxide (CO_2). The liquid occupies 68% of the total volume of a cylinder regardless of its size. Normal working pressure within the cylinder is 850 pounds per square inch gauge pressure (psig) at 70°F. The cylinders are equipped with a positive acting shut-off-valve containing "O" ring seals in which a safety valve consisting of a soft metal disk is incorporated. This disk will rupture and empty should the pressure within the cylinder reach 2100 psig.** The shut-off valve is used primarily for filling the tank and attaching it to the regulator. It is kept closed when not in use to prevent complete drainage of the cylinder should a slow leak develop in the system.

2. Pressure regulator.—The regulator reduces the high pressure in the cylinder to a usable output pressure. It is designed to reduce pressures of up to 3000 psig to a range from 0 to 90 psig. Like the cylinder, it is approved by the Federal ICC.

3. Control valve.—There are three types of valves currently in use, all having common control positions, viz: hold, exhaust, and fill. The hold position does not require the exertion of physical effort by the patient; the fill and exhaust positions require the application of force and excursion. The position of exhaust is intermediate between the hold and fill positions. Valves may be directly connected to the regulator or remotely connected by a supply line as previously mentioned. Types of valves available and their recommended applications are:

(a) Lever type.—Has been used for activation with the toes by wheel chair patients. Requires 4 oz of activation force at a maximum excursion of 3/8 in. It is recommended that the patient should be capable of

---

*The components described here and completed BFA's can be obtained from the Orthopedic Supply Co., 9126 E. Firestone Ave., Downey, California. The gas cylinders and pressure regulator can also be obtained from Beacon Devices, Inc., 78 Oliver St., North Tonawanda, New York.

**At 850 psig and 70°F, carbon dioxide exists as a liquid and vapor. When it is confined to a constant volume (as in the steel cylinders), the pressure increases as the temperature increases. A temperature of 120°F is required to develop a pressure of 2100°F within the cylinder. Thus there is little likelihood that the safety disk will rupture in ordinary use. The temperature can reach 120°F in the trunk of a car or in a car with the windows rolled up on a hot summer day.

applying twice the required force.

(b) Slide type (spring return).—Generally harnessed to a shoulder or chest strap and activated by shoulder adduction or chest expansion. Activation force is 12 oz at a maximum excursion of 1/4 in.

(c) Slide type (spring return—attached to the regulator).—Generally harnessed to a shoulder strap and activated by shoulder elevation. Screws directly into the regulator and eliminates the supply line between valve and regulator required by the above valves. It can be used by both wheel-chair and ambulatory patients. The control cable and its housing are incorporated as part of the valve. Activation force is 12 oz at an excursion of 1/2 in.

(d) Solenoid Slide type.—The switch which controls the solenoid requires a force of 1/2 oz at an excursion of 1/8 in. to activate it. The solenoid is driven by a 12-v d-c source supplied by a commercial converter which plugs into a standard 115-v a-c wall socket. The valve is used primarily for wheel-chair patients due to the relatively high weight and low useful lifetime of a portable 12-v source of power.

4. Harness.—As in ordinary orthesis, the manner in which the valves are harnessed to the patient is flexible. For most situations standard orthetic harnessing procedures can be used which make the use of the BFA quite versatile.

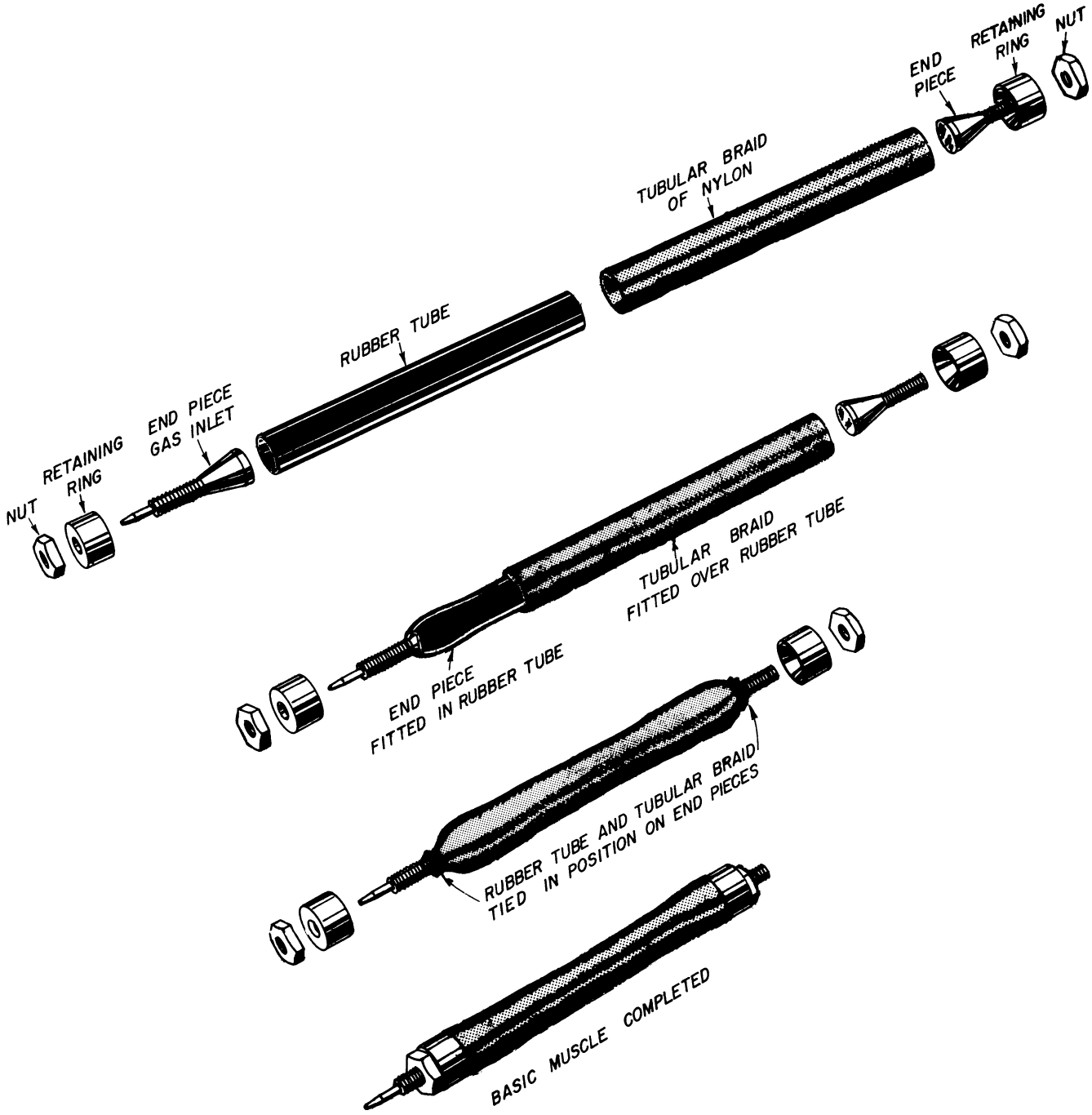

Fig. 1. Elements and assembly sequence of the first practical BFA.

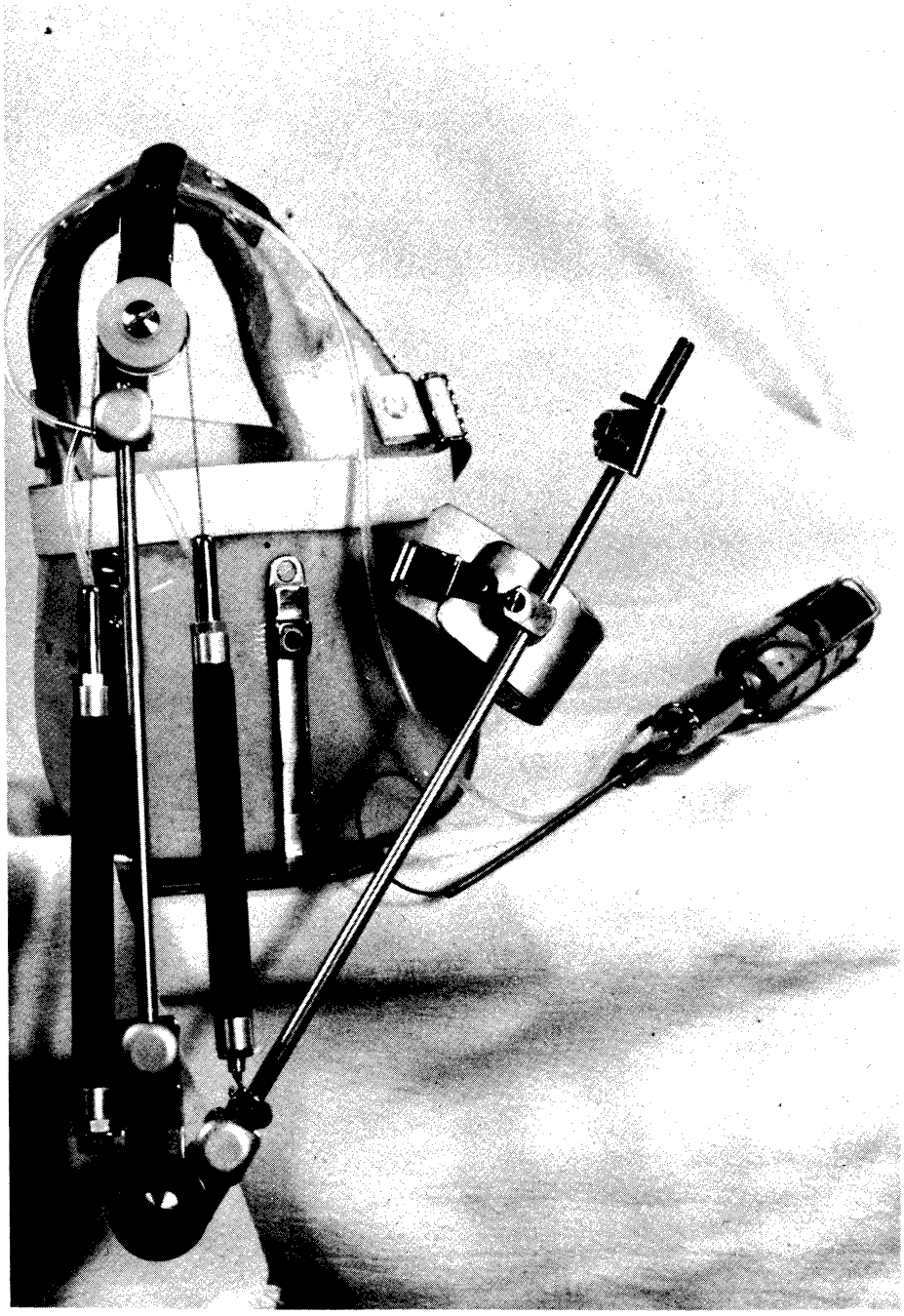

Fig. 2. First prototype design of the BFA powered functional arm brace.

(a) Extended position.

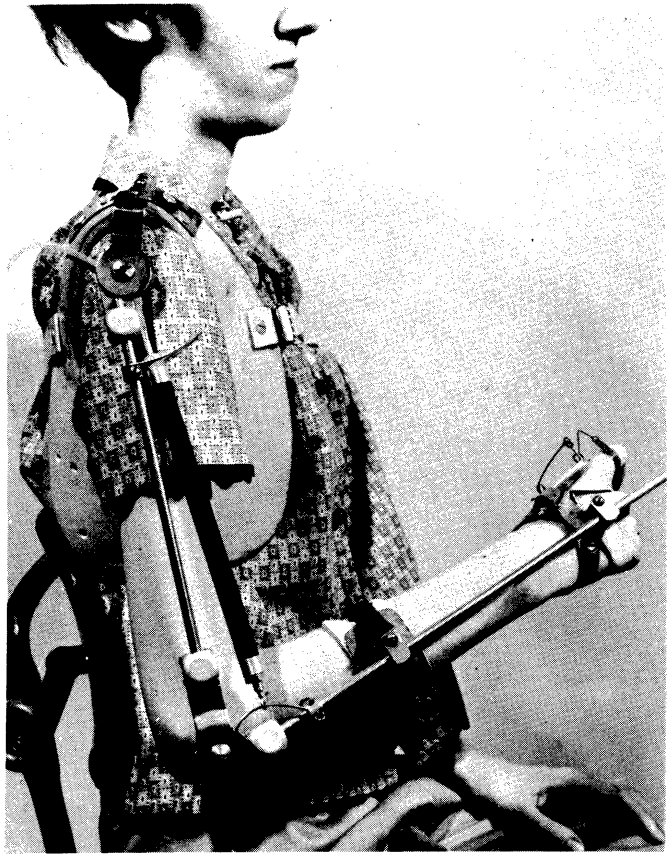

(b) Flexed position.

Fig. 3. Second prototype design of the BFA powered functional arm brace. Introduction of the simple slider mechanism at the elbow joint allowed elimination of the posterior actuator of the first design shown in Fig. 2.

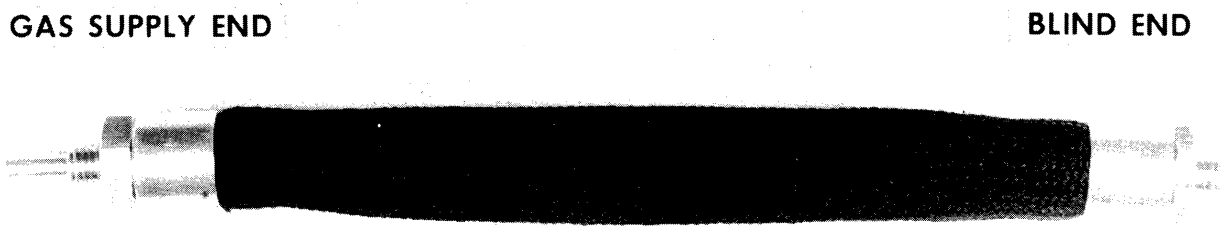

Fig. 4. The BFA as a completed unit.

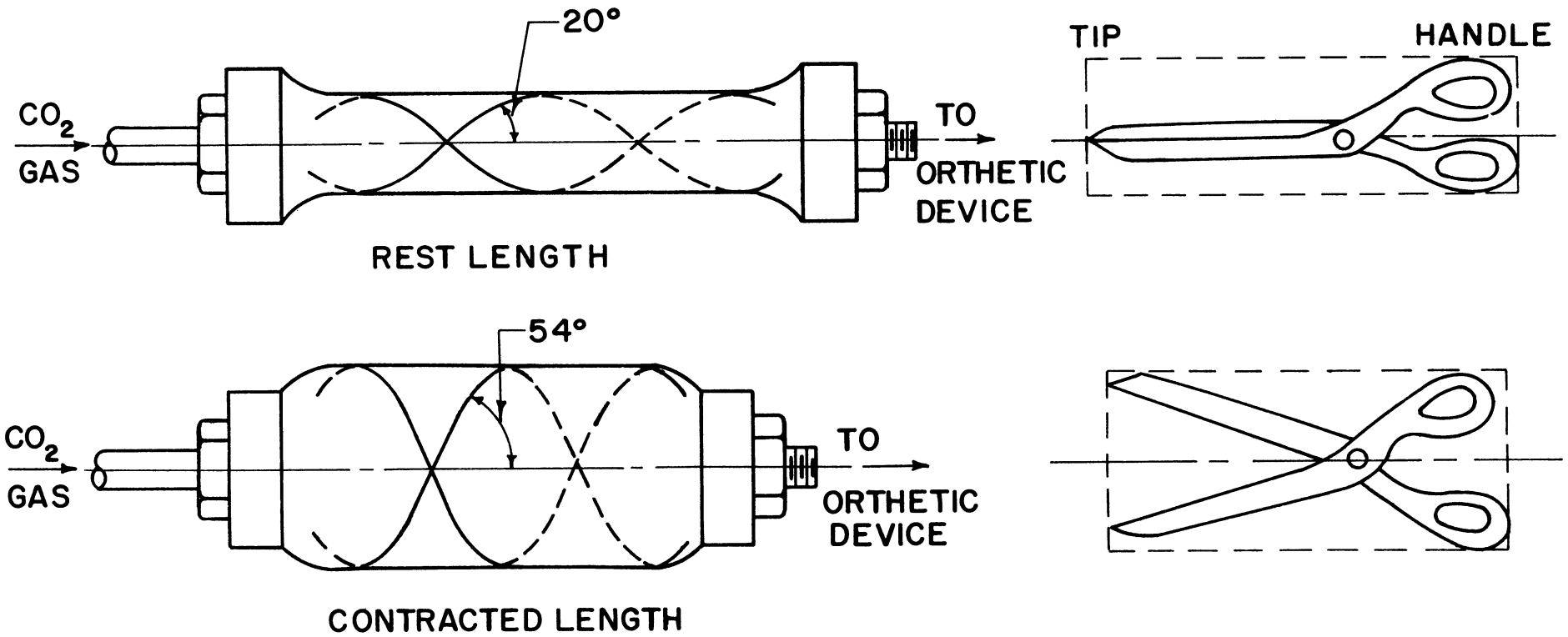

Fig. 5. Action of the BFA when inflated and its scissor analogy.

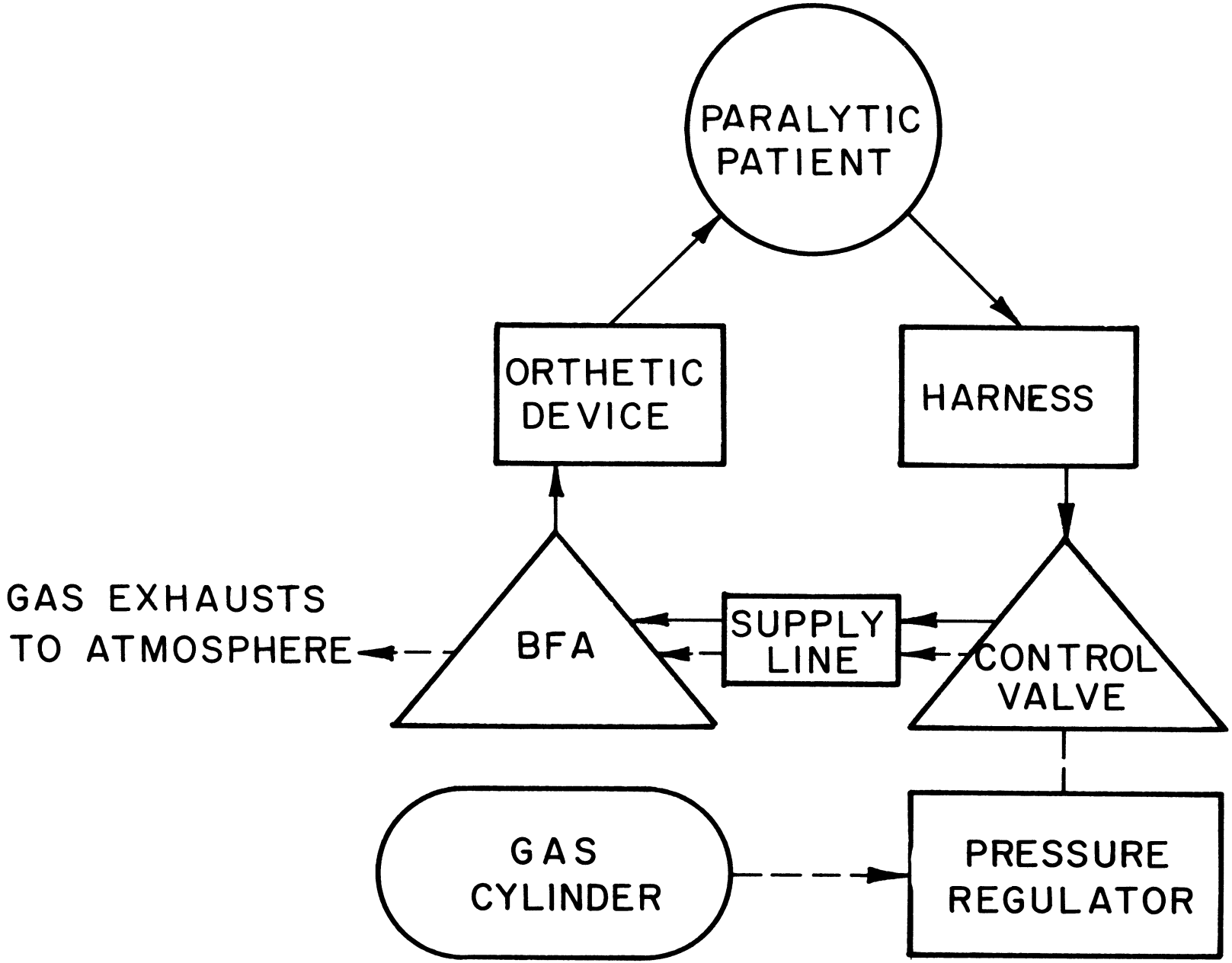

Fig. 6. Schematic of a basic orthetic system for the BFA. Solid arrows indicate flow of power in the system. Dashed arrows indicate flow of gas through the system.

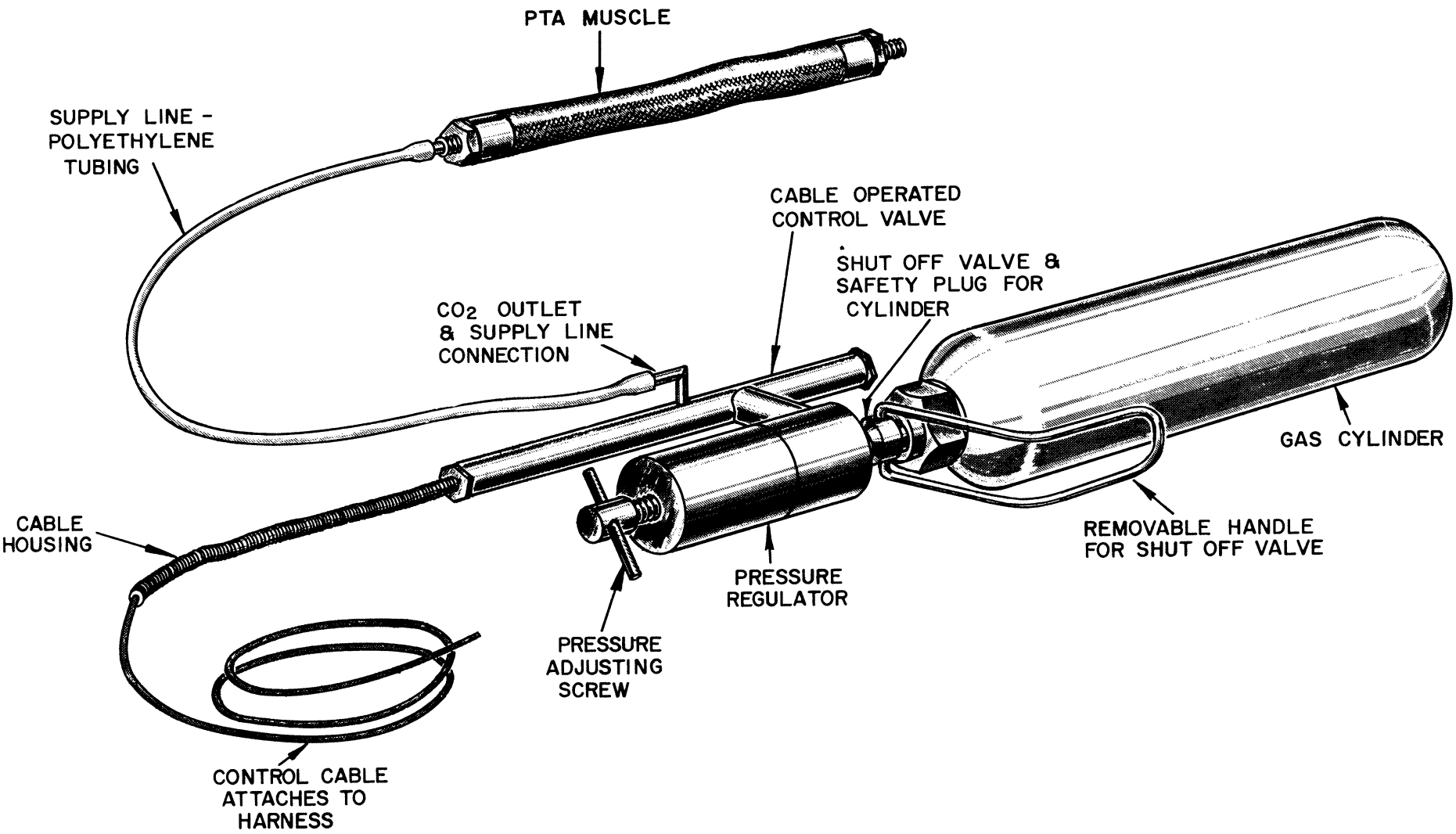

Fig. 7. Basic hardware of the BFA system. The harness (not shown) depends on the particular application.

II. DESCRIPTIVE PARAMETERS OF THE BFA'S BASIC ELEMENTS

The following parameters are defined to aid in comparing and identifying the several types of actuators studied in this report. Figure 8 illustrates the interrelationship of these parameters.

A. THE BRAIDED TUBULAR SHEATH

1. Flat width (W).—Width of the braid when flattened against a level surface. For practical purposes, this is one-half the circumference (Z) of the braided sheath in its tubular shape,

$$Z = 2W$$

and

$$D_o = \frac{2W}{\pi}$$

where D_o is the woven diameter of the braided sheath.

2. Fiber.—The basic element used in weaving the sheath. Two types of fibers have been used, one consisting of an untwisted yarn, the other of twisted yarn.

3. Strand.—The major element used in weaving the sheath. It consists of one or more fibers either lying side by side or twisted together.

4. Types of weave.—The type of weave is defined by the type of strand irrespective of the type of fiber. There are two types in use, one involving a single, the other a double crossing of the strands.

5. Pic.—The distance from point to point in a longitudinal direction along the sheath of a single diamond of the diamond-shaped pattern formed by the crossing of the strands. These are measured per linear inch of the sheath and are designated as pics per inch.

6. Weave tightness.—The distance between the strands of a given weave type. It is characterized by the amount of void space between the diamonds of the weave pattern. A given weave type can have fewer or more pics per inch depending on its tightness. In this respect, the size of the strand dictates the maximum upper limit of the pics per inch for a given type of weave.

7. Helix angle (θ_o).—The angle between an elemental length of a strand

forming the helix of the braid and the longitudinal axis of the sheath.

B. THE ELASTIC INNER TUBE

The inner tube of the first usable actuator was composed of standard latex surgical tubing. However, in areas where the smog content of the air is high, such as in Southern California, this material was found to deterioate rapidly. To eliminate this problem, a special tubing composed of a mixture of latex rubber and carbon black was substituted. This tubing is fabricated by dipping a 0.50 in. diam mandrell in the rubber mixture. The wall thickness of the tubing is controlled by the time length of dip. Several wall thicknesses, ranging from 0.01 to 0.02 in. have been tried. The 0.02 in. wall has proved to be the most satisfactory.

C. THE END ELEMENTS

Two types of ends have been designed, one consisting of male and female cones bolted together, the other, of male and female cylinders pressed or "crimped" together. In both types the male element fits inside the ends of the rubber inner tube and braided sheath, while the female element fits over the assembly thus formed and forces it against the male element, sealing the ends. The two types of ends are shown assembled in Fig. 9. Engineering drawings of both the gas supply and blind elements for both types of ends are presented in Appendix C.

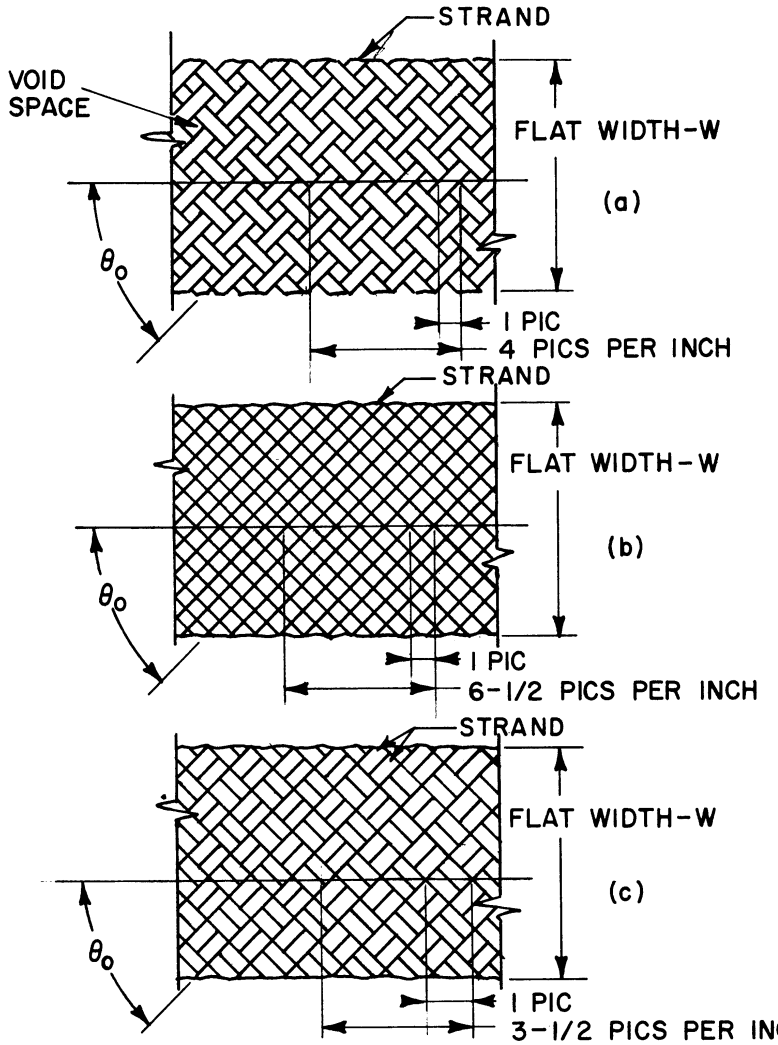

Fig 8. Parameters of the braided tubular sheath. (a) The single crossed strand loose weave type. The strands consist of a single fiber of untwisted nylon yarn. (b) The single crossed strand tight weave type. The strands consist of two fibers of twisted nylon yarn. (c) The double crossed strand tight weave type. The strands are the same as in (b).

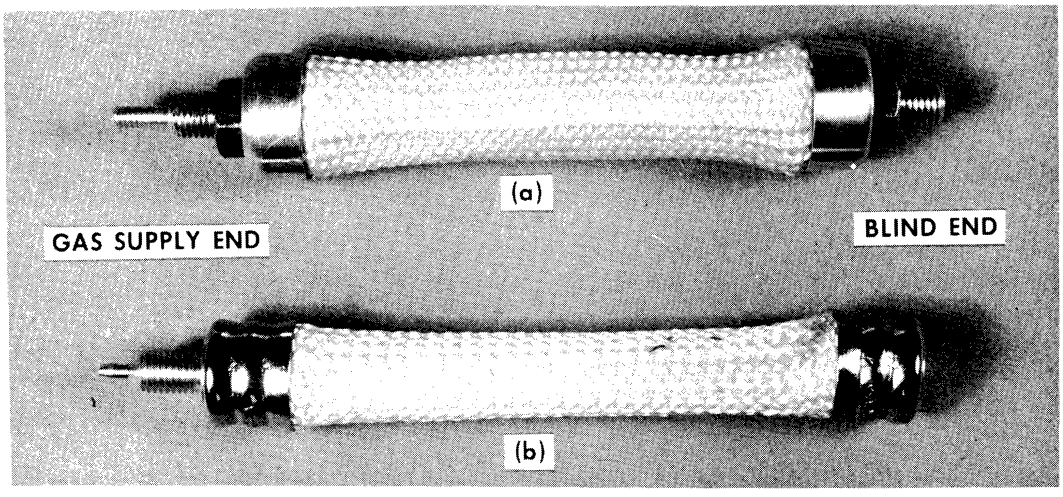

Fig. 9. End types. (a) Male and female cones bolted together; (b) male and female cylinders crimped together.

III. DESCRIPTIVE PARAMETERS OF THE BFA FOR USE IN ORTHETIC DESIGN

To define conveniently the force-excursion characteristics of the actuator, the following parameters are defined.

A. PRESSURE STABLE ANGLE (θ_s)

This is the angle of weave when the force output of the actuator becomes zero. Theoretically the value of this angle is 54°44' (see Fig. B-4 p. 115). In practice this value deviates significantly from the theoretical due to the finite thickness of the strands and frictional effects in the sheath.

B. PRESSURE STABLE LENGTH (L_s)

This is the length measured from the inside edges of the end elements when the force output of the actuator becomes zero. This is the minimum length the actuator can assume under the action of an internal pressure.

C. PRESSURE STABLE DIAMETER (D_s)

This is the diameter of the actuator when the force output becomes zero, the maximum diameter which can be attained. In design work it is significant in allowing proper clearance for the actuator.

D. FREE LENGTH (L_o)

This is the length of the actuator when it is free from all external forces and internal pressure. It can also be referred to as the fabricated length and is measured from the inside edges of the end elements.

E. CUT-OFF ANGLE (θ_c)

This is the lower limit of θ due to binding of the crossed strands in the braided sheath. This angle occurs at the maximum extension of the actuator (i.e., when the internal pressure is zero and an external force is applied to it). It is a function of the weave tightness and strand thickness.

F. CUT-OFF LENGTH (L_c)

This is the maximum length of the actuator (measured from the inside edge of the end elements) when the internal pressure is zero and an external force is applied to it. This length is a function of θ_m, and, therefore, depends directly on the strand thickness and weave tightness.

G. MAXIMUM WORKING LENGTH (L_m)

This is the maximum recommended usable length of the actuator. This length is somewhat less than L_c. It is chosen to prevent excessive wear of the braided sheath and rubber inner tube due to high stress concentration at their junction with the end elements. It is also measured from the inside edges of the end elements.

H. ABSOLUTE USABLE EXCURSION (E)

This is the absolute difference between the maximum working length (L_m) and the pressure stable length (L_s) in inches.

Specific values of the parameters thus far defined for the various types of actuators developed and tested as of July, 1960, are presented in Table I along with identifying code numbers based on the type of weave.

Correlation analysis of the data presented in the next section allowed the forcing of a linear relationship between the pressure stable length (L_s), the maximum working length (L_m), and the free length (L_o) for the two W-1 types and the W-2 type actuators. These relationships are shown in Fig. 10. The data have been extrapolated to an 8-in. free length which is the probable maximum length that will be used in orthetic design. The absolute usable excursion (E) is the vertical distance between the two curves. Figure 11 is an alignment chart developed from Fig. 10. This chart allows the four variables L_s, L_m, L_o, and E to be read directly, provided one of the four variables is known. The forcing of a relationship between these parameters for the W-3, W-4, and W-3I actuators was not investigated.

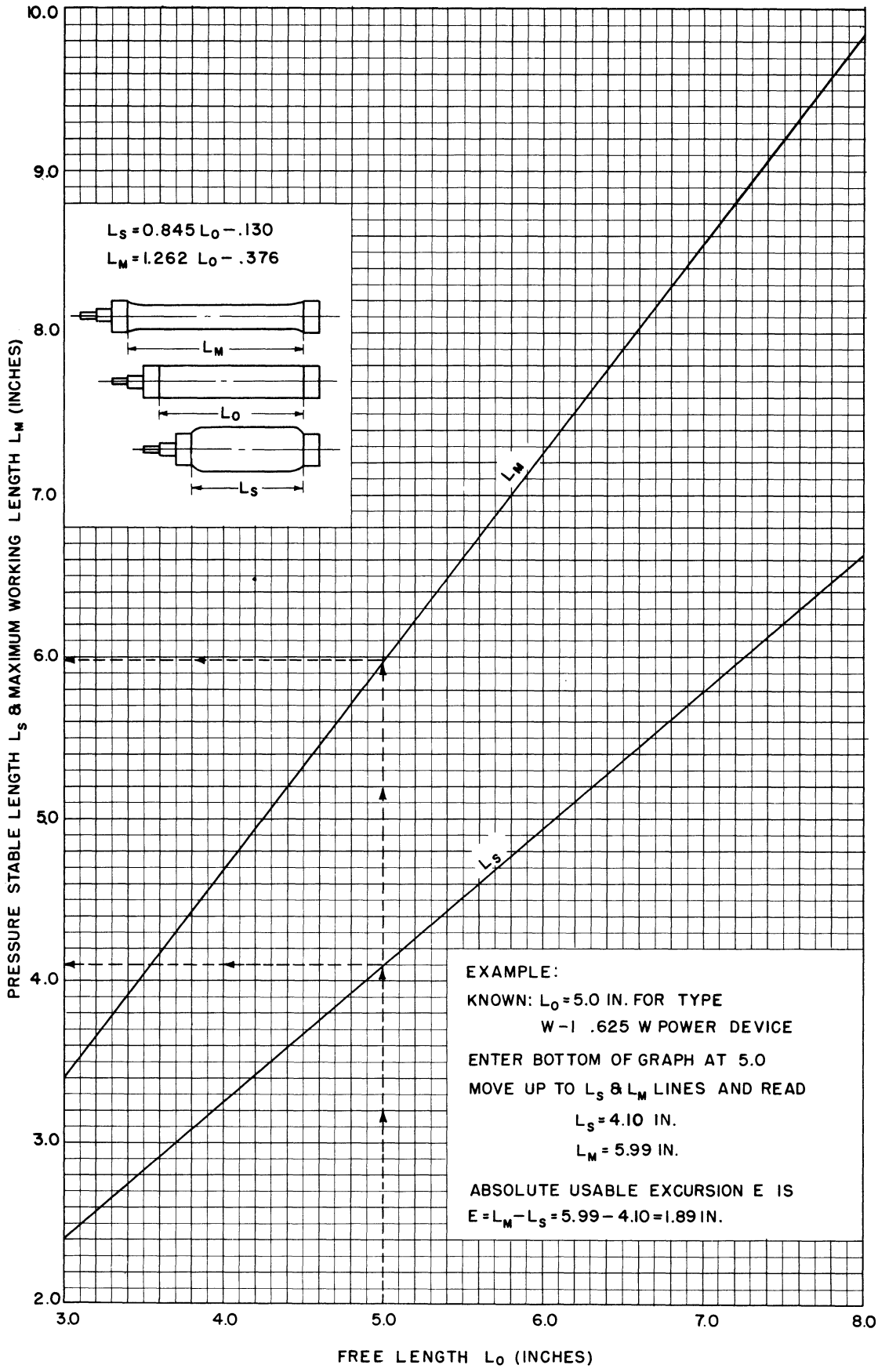

Fig. 10. Pressure stable length and maximum working length as a function of free length for the W-1 and W-2 type BFA's of any flat width.

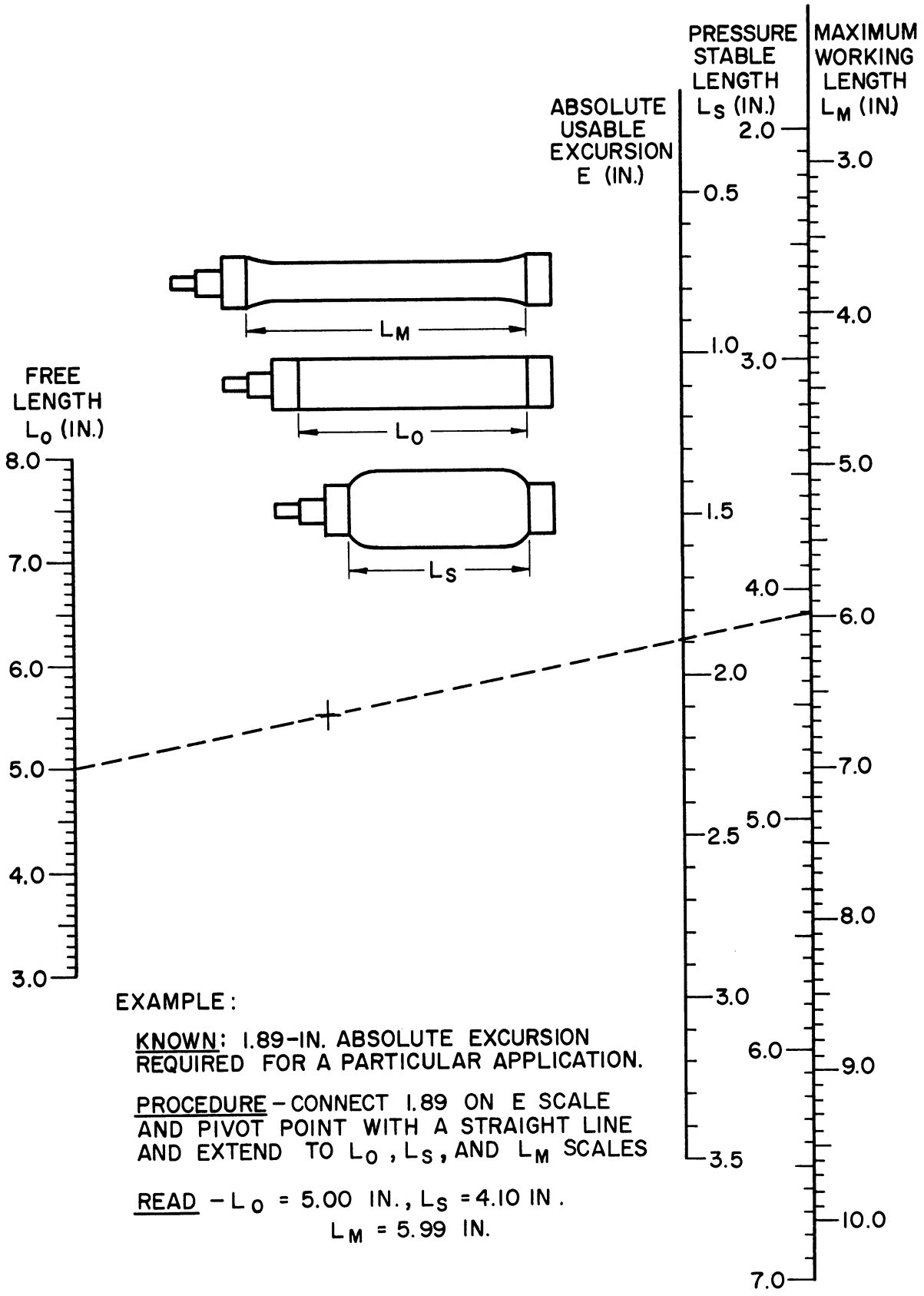

Fig. 11. Alignment chart relating free length, absolute usable excursion pressure stable length and maximum working length for the W-1 and W-2 type BFA's of any flat width.

IV. FABRICATION DETAILS

Construction of the W-1, W-2, and W-3 actuators has been illustrated in Fig. 1 (page 6). Figure 12 shows the construction of the W-4 type. The female-end elements of this actuator consist of standard hose fittings crimped with a commercial tool for this purpose. Construction of the W-3I type of actuator is the same as for the W-4 type except that the rubber tubing and helical sheath are dipped in liquid latex rubber to form a single integral unit. The dipping is carried out while the rubber tube and helical sheath are stretched over a cylindrical form called a mandrell. The length of the time that the mandrell is in the liquid latex determines the thickness of material deposited.

TABLE I

CODE NUMBERS AND PARAMETERS OF THE BFA

Code No.	Parameters of Helical Sheath						Parameters of Inner Tube			Type of Ends	Rubber Impregnated
	Weave Type	Type of Fibers	Type of Strand	Flat Width (W), in.	Helix Angle, θ_o, °	Pics, in.	Material	Flat Width, in.	Wall Thickness, in.		
W-1	Single criss-cross, tight	Twisted nylon yarn dyed black	Double fiber twisted together	.625	40°	20	Commercial latex rubber surgical tubing			Male and female cones, bolted	No
W-1	Single criss-cross, tight	Twisted nylon yarn dyed black	Double fiber twisted together	.700	40°	20	Commercial latex rubber surgical tubing			Male and female cones, bolted	No
W-2	Double criss-cross, tight	Twisted nylon yarn dyed black	Double fiber twisted together	.950	40°	14	Commercial latex rubber surgical tubing			Male and female cones, bolted	No
W-3	Single criss-cross, very loose	Untwisted nylon yarn bleached white	Untwisted yarn	.950	25°	7	Commercial latex rubber surgical tubing			Male and female cones, bolted	No
W-4	Single criss-cross, loose	Untwisted nylon yarn bleached white	Untwisted yarn	.750	40°	9	Latex rubber carbon black dip fabricated	.50	.020	Male and female cylinders, crimped	No
W-3I	Single criss-cross, very loose	Untwisted nylon yarn bleached white	Untwisted yarn	.950	25°	7	Latex* rubber carbon black dip fabricated	.50	.020	Male and female cylinders, crimped	Yes

*Bonded to the helical sheath by dipping together to form an integral unit.

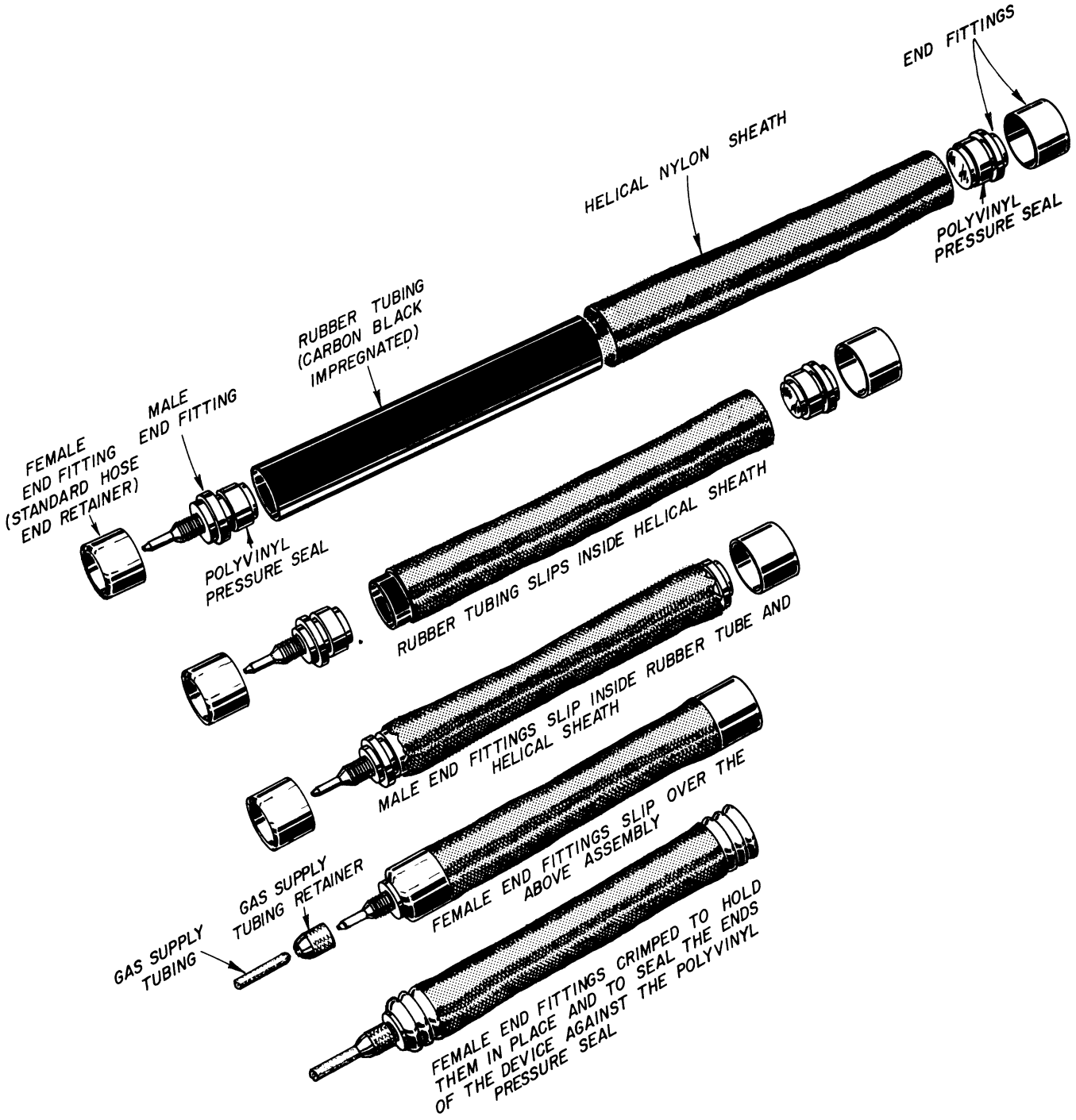

Fig. 12. Construction of the W-4 type BFA.

V. EMPIRICAL CHARACTERISTICS

A. ISOMETRIC TENSILE FORCE—LENGTH CHARACTERISTICS

Empirical isometric* tensile force—length characteristics of the BFA's tested are presented in the following two series of graphs. The first series (Figs. 13—24 and 26—28) present tensile force output plotted against length as a function of pressure. The pressure ranges from 0 to 90 psig in 10-psig increments for the W-1 and W-2 actuators, and 0 to 60 psig in 10-psig increments for the W-4 and W-3I actuators. The second series (Figs. 30—44) presents the same data in a different manner, viz: force output versus pressure as a function of length. The advantage of the second series is evident in that the characteristics plotted in this manner have a linear relationship. Each series is divided into identically structured subgroups which consist of the characteristics of a power device of a particular weave type, flat width, and free lengths of 3, 4, and 5 in. Figures 25 and 29 indicate the variation of the pressure stable diameter (D_S) with changes of pressure for the W-4 and W-3I actuators. Similar curves are not shown for the W-1, W-2, and W-3 actuators since D_S is essentially constant for these devices.

The curves indicate four general characteristics common to all actuators.

1. The useful excursion is limited and directly proportional to the free length (L_O) (i.e., the greater L_O, the greater the excursion).

2. Tensile force output is a direct function of the flat width (W) or the woven diameter of the braided sheath (D_O).

3. Tensile force output is a direct function of internal pressure (P).

4. The tensions developed are not constant throughout the range of excursion but vary from a maximum at the maximum working length (L_m) to zero at the pressure stable length (L_S).

---

*The term isometric refers to the manner in which the curves were developed. Each actuator was tested by applying a given internal pressure at a particular length within the range from the maximum working length (L_m) to the pressure stable length (L_S) without allowing it to shorten (see Appendix A). The actuator generates force (tension), but does no external work. This type of action is commonly spoken of as "isometric."

B. GAS-CONSUMPTION CHARACTERISTICS

Gas consumption as a function of internal pressure for the BFA's tested is presented in Figs. 45—59. The gas used was carbon dioxide (CO_2). The charts indicate total volume in cubic inches ($in.^3$), corrected to standard atmospheric conditions (14.7 $lb/in.^2$ and 77°F or 760 mm Hg and 25°C), consumed by a given actuator on contracting from any initial length to any final length, the initial and final lengths lying in the range between the maximum working length (L_m) and the pressure stable length (L_s). Grouping is the same as for the isometric tensile force—length characteristics. Pressures vary in 20-psig increments starting with 20 psig in all cases and range to the same upper limits as for the force characteristics.

The following characteristics are common to all actuators.

1. Gas comsumption is a direct function of the free length (L_o), i.e., the greater L_o, the more gas consumed per cycle of contraction.

2. Gas consumption is a direct function of flat width (W) or the woven diameter of the braided sheath (D_o) for a given free length (L_o).

3. Gas consumption is a direct function of internal pressure.

4. The amount of gas consumed is not constant throughout the range of excursion but varies from a minimum at the maximum working length (L_m) to a maximum at the pressure stable length (L_s).

Since the gas-supply cylinders are filled on a weight basis, it is of interest to be able to convert the gas-consumption characteristics to this basis so that the number of cycles to be expected from a given size of gas-supply cylinder can be approximated. This conversion can be accomplished by use of the formula

$$M = 1.04 \times 10^{-3} V$$

where:

M = The weight in ounces (oz) at standard atmospheric conditions.

V = The volume in cubic inches ($in.^3$) at standard atmospheric conditions.

Use of this formula to convert the data is illustrated in Fig. 59 which indicates the total weight of gas (at standard atmospheric conditions) consumed by a given actuator on contracting from any initial length to any final length, the initial and final length lying in the range between the maximum working length (L_m) and the pressure stable length (L_s). By reading directly from this type of graph, the weight consumed on contracting to a given length (the range of

contraction is governed by the orthetic device and its constraints) one can find (by dividing the volume read into the total weight of gas in the supply cylinder) the number of flexions that can be expected for a given BFA system per supply cylinder. This calculation does not include the weight of gas wasted in the supply lines for a particular system. This weight is assumed to be small in comparison to that required by the actuator. However, a certain allowance is included in the data since a 2-ft length of small bore tubing (0.031 ID) was used in the test setup.

C. SIGNIFICANT FEATURES OF THE EMPIRICAL CHARACTERISTICS

1. Figures 13—21.—This group of graphs representing the W-1 and W-2 actuators shows a marked similarity in respect to the following specific points:

(a) All curves regardless of pressure converge to a given length.

(b) The point of convergence of these curves occurs at zero force output for the three sizes of actuators represented. For this reason the length of the device at the point of convergence has been designated the pressure stable length (L_S).

(c) A maximum length is reached for each weave type beyond which the absolute excursion of the actuators does not increase. This length has been designated as the cut-off length (L_C). L_C is not indicated on the figures since repeated cycling of the actuators to this length has proved detrimental to their life. To eliminate this problem, a length somewhat less than L_C, designated as the maximum working length (L_m), has been indicated. It is recommended that in using the actuators L_m is not exceeded.

(d) The free length (L_O) lies approximately midway between L_S and L_m. The relationship of L_O to L_m is significant since to obtain maximum absolute excursion and force output when applying the actuators, L_m and not L_O should be used as the length at which excursion begins.

(e) The diameter at the pressure stable length, designated as the pressure stable diameter (D_S), is a constant independent of pressure for a particular weave type and flat width.

(f) Each figure has a zero-pressure curve which indicates the force output of the actuator when no internal pressure is applied to it. This zero-pressure curve is due to the elasticity of the latex rubber inner tube and binding of the strands in the braided sheath as the actuator is elongated from its free length (L_O) to the cut-off length (L_C) or

preferably the maximum working length (L_m). Note that in each figure this curve does not start at the L_o indicated but at a slightly less length, because the original experimental data are represented in these curves, and in some instances the actual free length of the actuator tested was slightly less than that indicated. This deviation could not be avoided, and it is within probable manufacturing tolerances should the BFA be produced in quantity.

The effect of the zero-pressure curve on the isometric tensile force—length characteristics of the actuator is similar to that of the passive tension curve on the total isometric tensile output of the human muscle as discussed in Klopsteg and Wilson.[2] Figure 60 shows this similarity. The developed tension (Δ curve) for the BFA shown in this figure represents only the force developed due to the internal pressure. The curve is obtained by subtracting the zero-pressure curve from the total force curve at a given pressure. Developed force curves are not presented in Figs 13—24 and 26—28 since it is the total force which is of interest in design, i.e., the zero-pressure tensile force output can be used to overcome the weight of human limbs or the force of return springs which may be used in orthetic devices, thus leaving the developed force to do a useful task.

2. Figures 22—25.—The characteristics for the W-4 actuator are different from those of the W-1 and W-2 types in the following respects.

(a) The curves converge at a length corresponding to a negative force output as opposed to the convergence at zero force output for the W-1 and W-2 actuators. Since the pressure stable length (L_s) has been defined as occurring at zero force output, the W-4 actuator has a variable L_s which is an inverse function of pressure, i.e., the larger the pressure, the smaller L_s becomes.

(b) The maximum working length (L_m) is equal to the free length (L_o) since the braided sheath and inner tube tend to pull out of the end elements causing the actuator to burst violently if elongated beyond this point.

(c) The pressure stable diameter (D_s) is variable and a function of pressure. This relationship is shown in Fig. 25. Note that at low pressure D_s is less than the maximum diameter of the metal end elements, because the free-length diameter (D_o) of the braided sheath is less than the diameter of the ends as seen in Fig. 61.

(d) The pressure is limited to 60 psig since above this value the helical sheath and rubber inner tube tend to pull out of the end elements due to the high force output.

3. Figures 26—29.—Characteristics of the W-3I actuator are similar in all respects to those of the W-4 type. The force output is limited to a maximum of 70 lb regardless of pressure, since above this value there is a tendency for the impregnated helical sheath to separate from the end elements.

4. Figures 30—38.—These characteristics correspond to those of Figs. 13—21. Values of L_s and L_m are taken from Fig. 10. Absolute excursion (E) is measured from the pressure stable length (L_s). The free length (L_o) is designated by the dashed lines. The close coincidence between the data and the straight lines shown is indicated in Fig. 30 where the data points are designated by dots. This close correspondence holds for virtually all types of actuators tested. Not only do these plots show a linear relationship; but further:

(a) The lines of variable excursion from lengths of L_s to L_o pass through the origin or point of zero pressure zero force.

(b) At excursions above L_o the lines intersect the force axis at increasing values as the excursion approaches L_m. This phenomenon is apparently related to the fact that the zero-pressure curves of Figs. 13—21 influence the force output at other pressures. However, the forces indicated by these intersections do not correspond to those of the zero-pressure curves since they are extensions of the pressurized data. No attempt has been made to plot the zero-pressure curves on this set of diagrams.

5. Figures 39—41.—These curves are derived from Figs. 22—24. The lines of absolute excursion differ from those of Figs. 30—38 in that the absolute excursion (E) is measured from L_m and not L_s since this is the only fixed reference length for this actuator (i.e., L_s is a variable as previously discussed). Significant characteristics of these graphs are:

(a) The absolute excursion lines do not intersect the origin or the tensile force axis since the zero-pressure curve does not influence the characteristics of the actuator as seen from Figs. 22—24.

(b) The absolute excursion lines intersect the pressure axis at various points since L_s is a function of pressure. The relationship between L_s (or E) and P is shown on each figure. That L_s is a variable is important since the usable excursion decreases as the pressure decreases. This phenomenon does not exist for the W-1 and W-2 actuators.

(c) The absolute excursion is not zero at zero pressure since a small finite portion of the internal pressure is required to overcome the elasticity of the rubber inner tube. This phenomenon did not occur for the W-1 and W-2 actuators since the wall thickness of the latex

rubber tube used was thinner and therefore required less pressure to overcome the elasticity.

6. Figures 42—44.—The linear characteristics of the W-31 actuator are similar in all respects to those of the W-4 actuator.

7. Figures 45—52.—In these graphs (representing the gas-consumption characteristics for the W-1 and W-2 actuators) the following points should be noted.

(a) The abscissas or length axes are the same on both the tensile force—length and gas-consumption characteristics; therefore the pressure stable lengths (L_s), free lengths (L_o), and maximum working lengths (L_m) are the same on both sets of curves.

(b) The curves indicate a near linear relationship between successive increases in pressure at a given length. This indicates that (as for the tensile force—length characteristics) these characteristics could be represented as straight lines by plotting gas consumption against pressure as a function of absolute excursion. A representative plot of this type for the W-2 actuator is Fig. 62.

8. Figure 53—58.—Comments concerning the gas-consumption characteristics for the W-1 and W-2 actuators apply equally to the W-4 and W-31 types represented by these graphs. Note that the pressure stable lengths (L_s) for these actuators are not constant as for the W-1 and W-2 type. This phenomenon has been discussed in connection with the tensile force—length characteristics (page 29). Comparing these figures to Figs. 45—52, it is apparent that size for size the W-31 and W-4 actuators consume more gas than the W-1 and W-2 types in respect to both changes in length and internal pressure. Also, the slope of the curves for the W-1 and W-2 actuators are generally less than for the W-31 and W-4 types, indicating that the relative amount of gas consumed on contracting over a given range is greater for the W-31 and W-4 actuators. These characteristics result because the latter devices undergo greater changes in diameter as they contract. A direct comparison between the W-31 and W-4 actuators is not possible since data were obtained only for a single diameter different for each type of actuator.

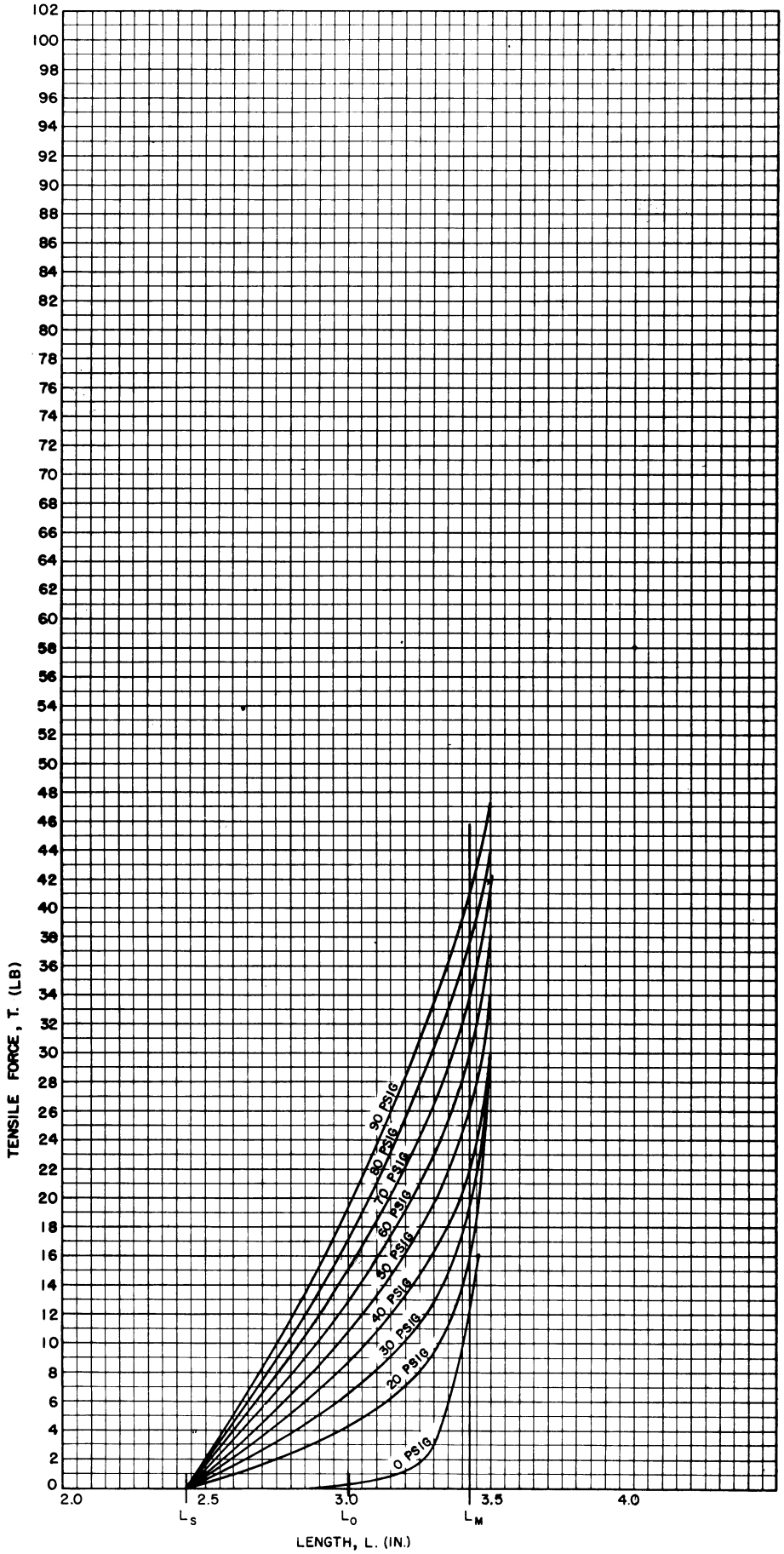

Fig. 13. Isometric tensile force—length characteristics as a function of pressure for the W-1 type BFA: L_O = 3.00 in., W = .63 in., D_S = .48 in.

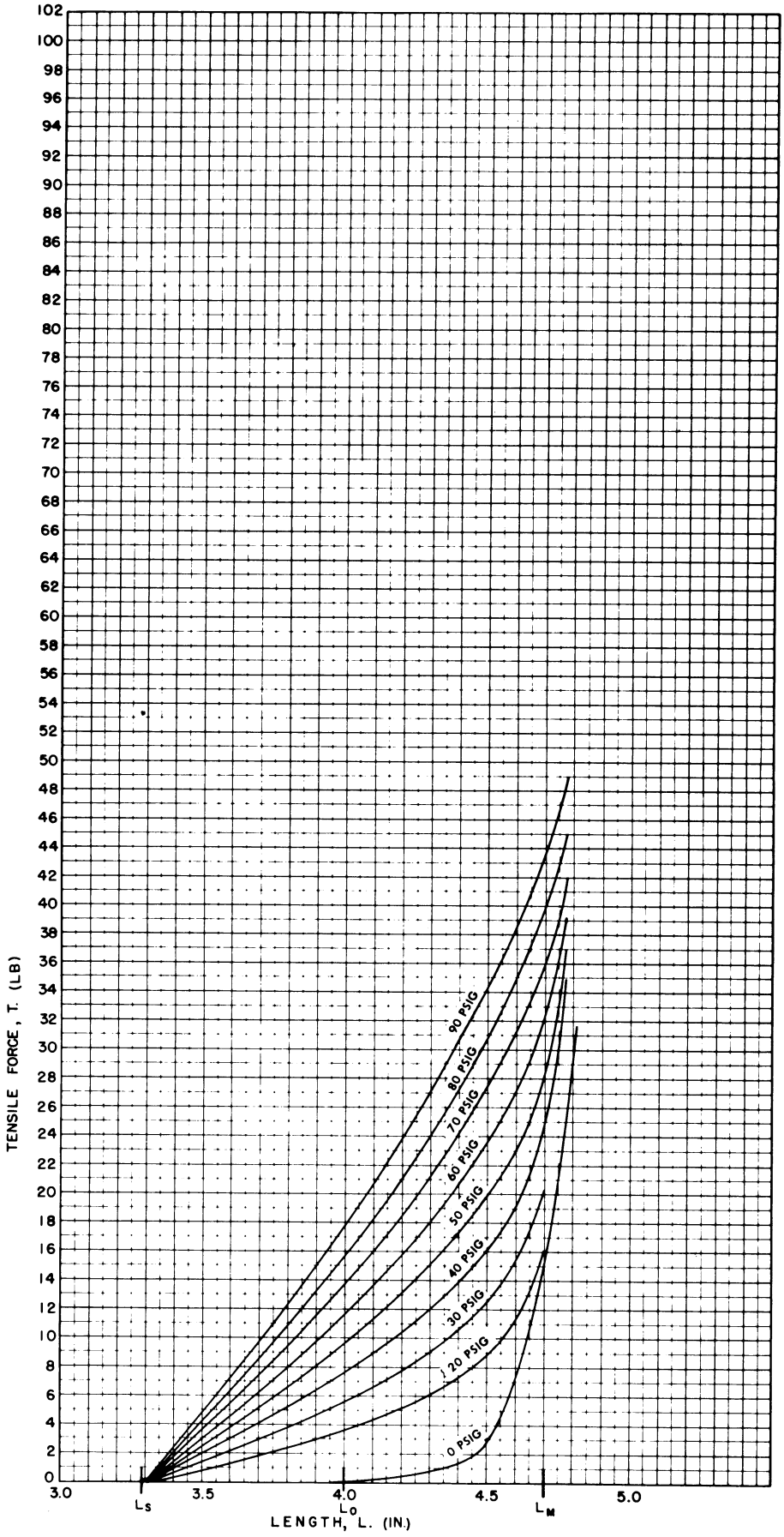

Fig. 14. Isometric tensile force—length characteristics as a function of pressure for the W-1 type BFA: L_o = 4.00 in., W = .63 in., D_s = .48 in.

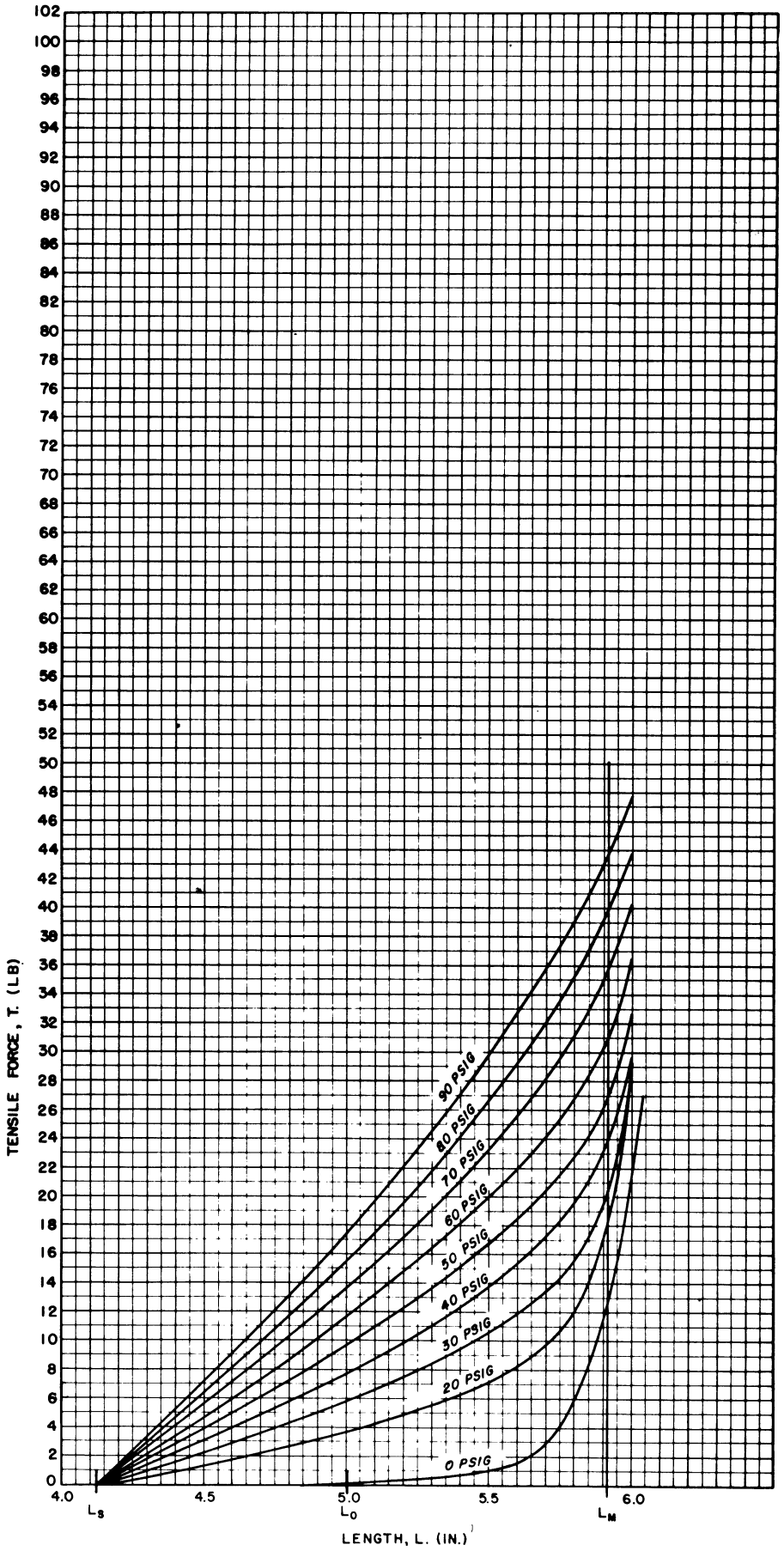

Fig. 15. Isometric tensile force—length characteristics as a function of pressure for the W-1 type BFA: L_o = 5.00 in., W = .63 in., D_s = .48 in.

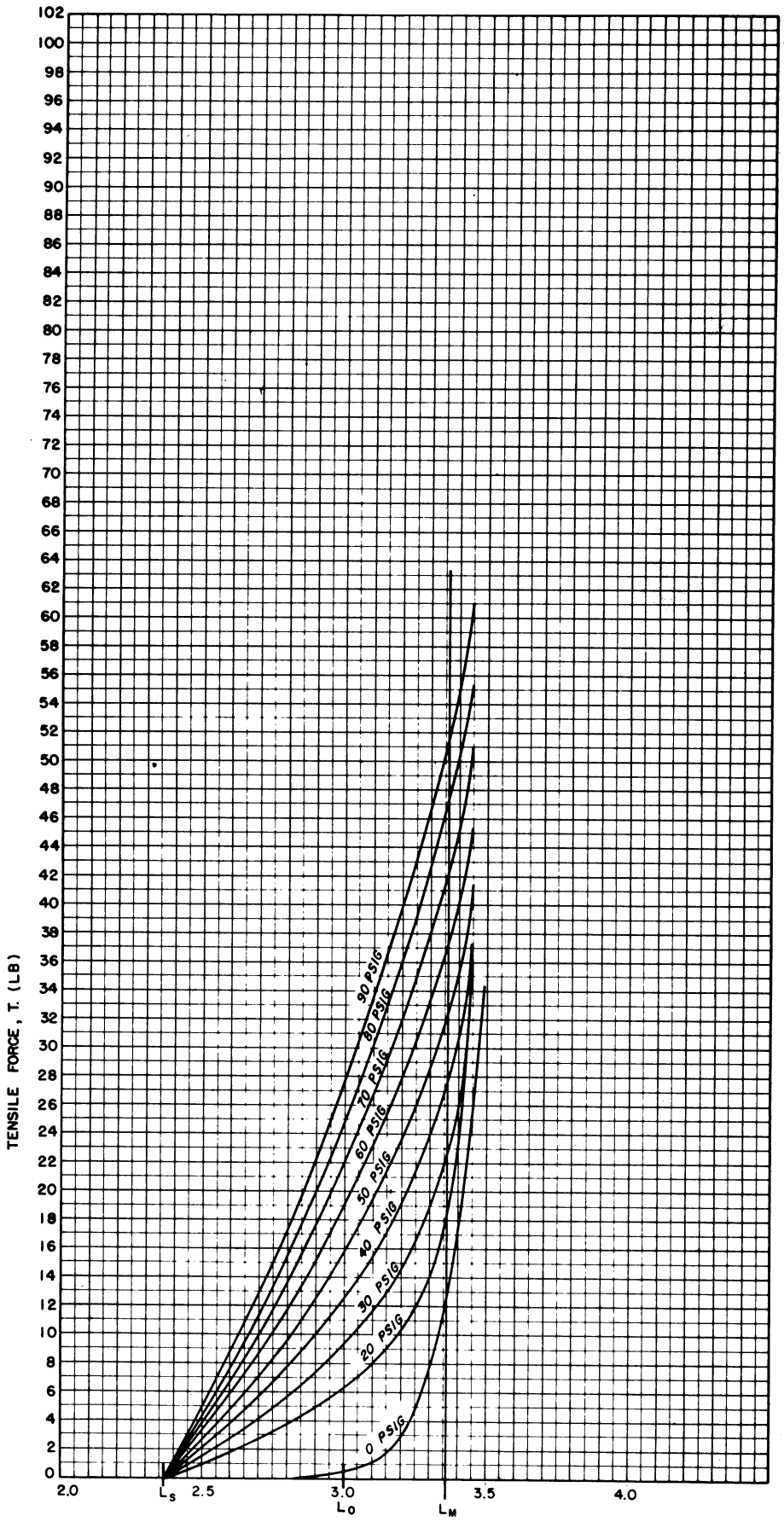

Fig. 16. Isometric tensile force—length characteristics as a function of pressure for the W-1 type BFA: L_O = 3.00 in., W = .70 in., D_S = .57 in.

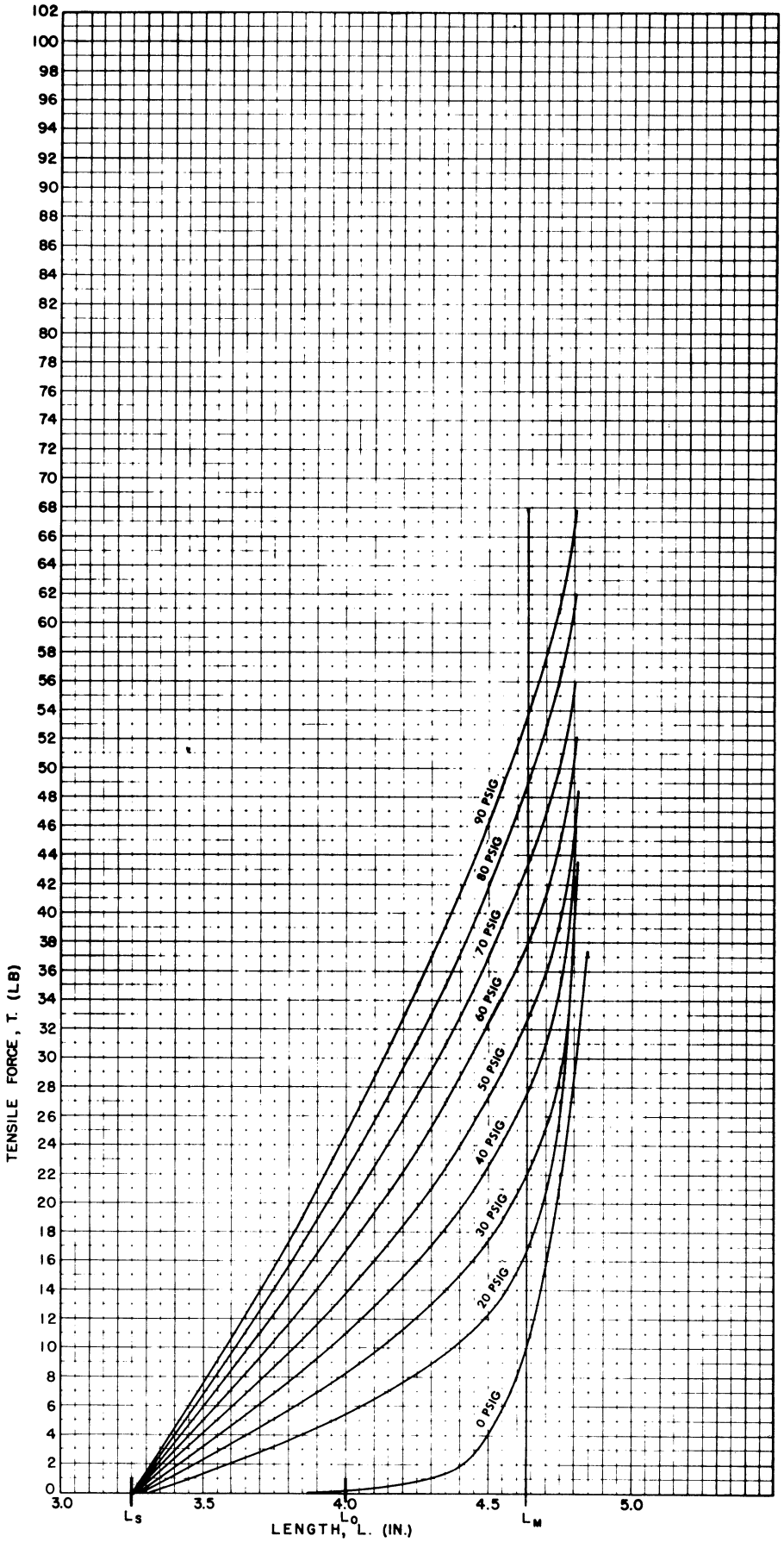

Fig. 17. Isometric tensile force—length characteristics as a function of pressure for the W-1 type BFA: L_O = 4.00 in., W = .70 in., D_S = .57 in.

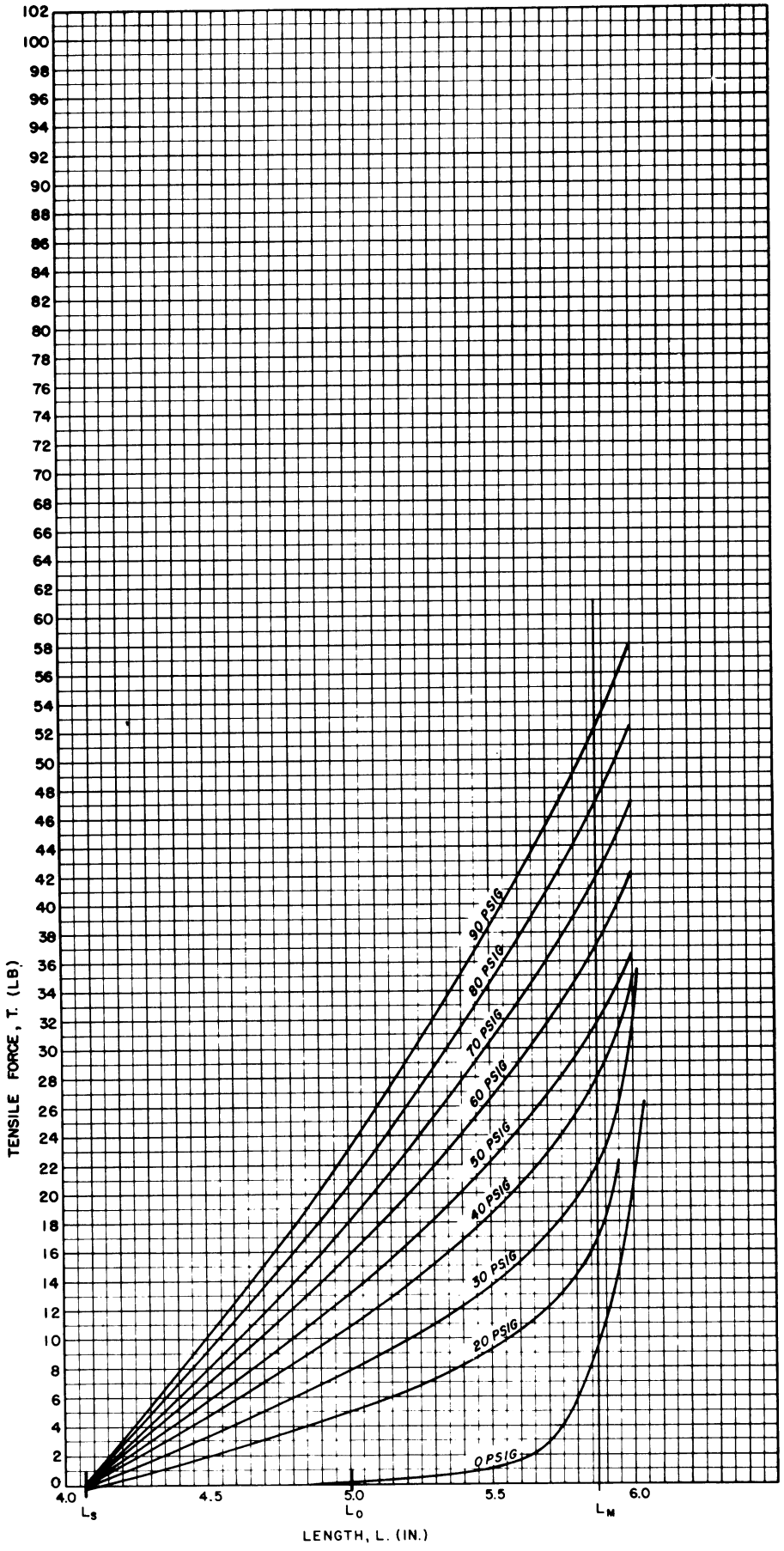

Fig. 18. Isometric tensile force—length characteristics as a function of pressure for the W-1 type BFA: L_o = 5.00 in., W = .70 in., D_s = .57 in.

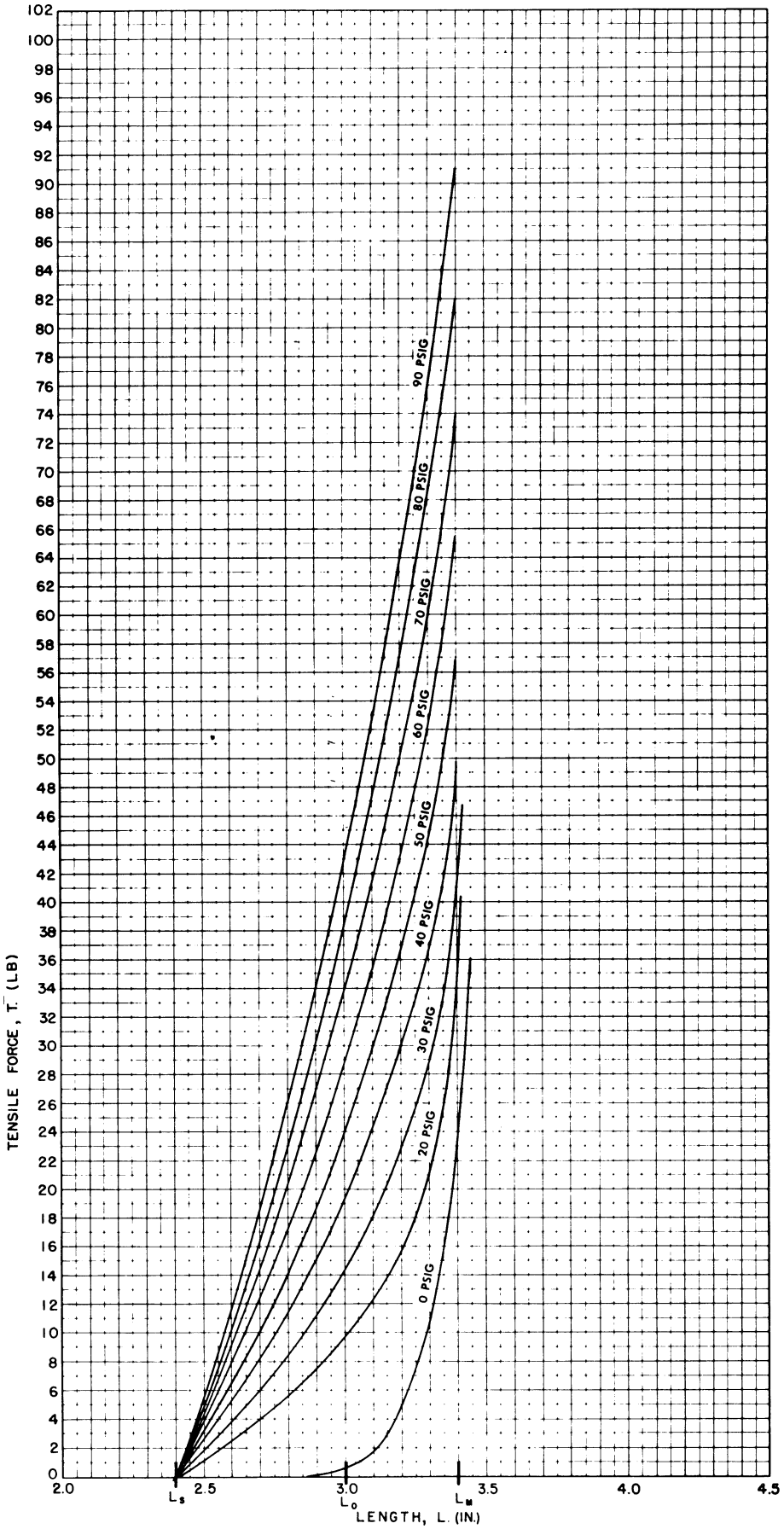

Fig. 19. Isometric tensile force—length characteristics as a function of pressure for the W-2 type BFA: L_o = 3.00 in., W = .95 in., D_s = .72 in.

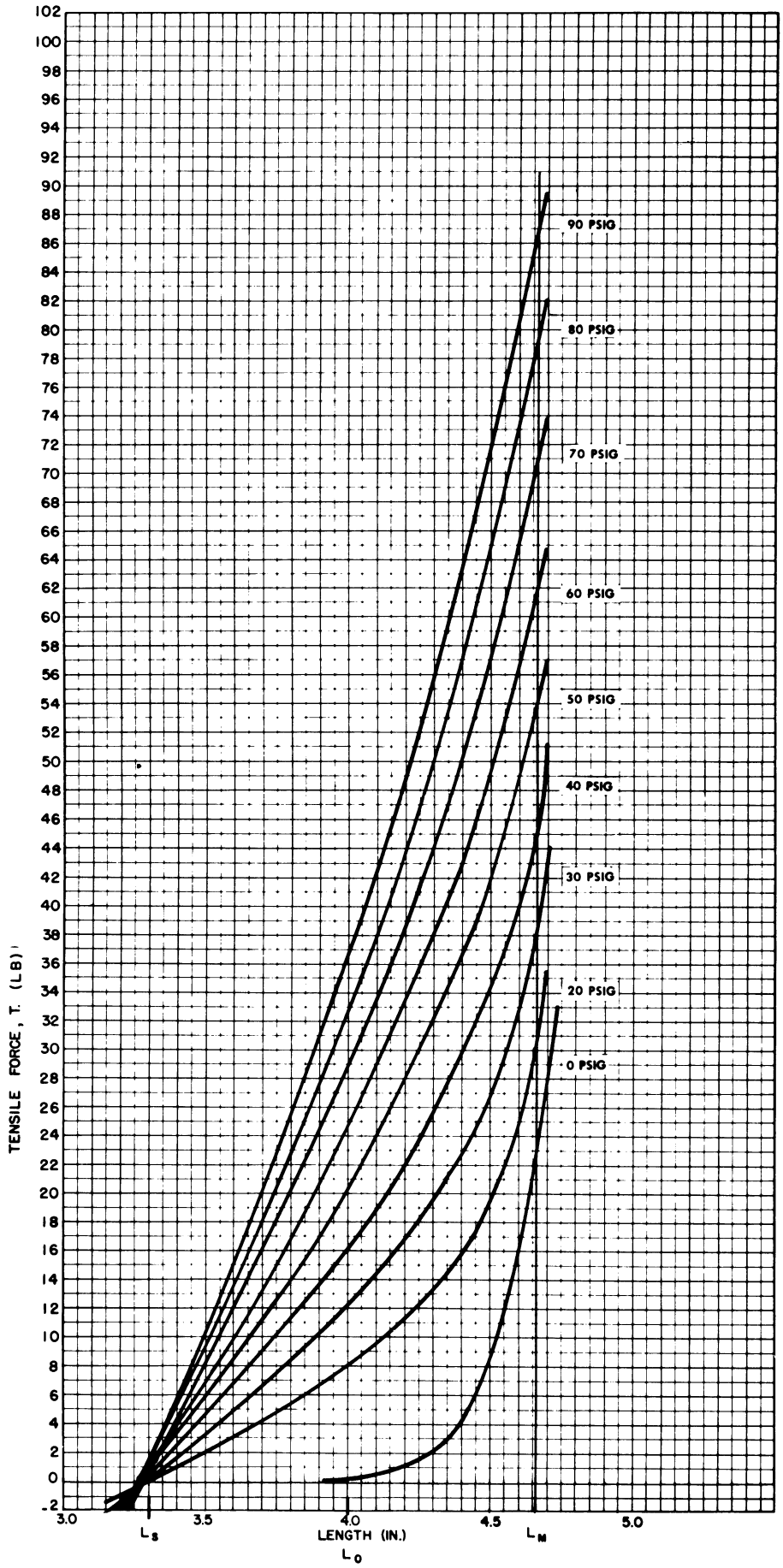

Fig. 20. Isometric tensile force—length characteristics as a function of pressure for the W-2 type BFA: L_o = 4.00 in., W = .95 in., D_s = .72 in.

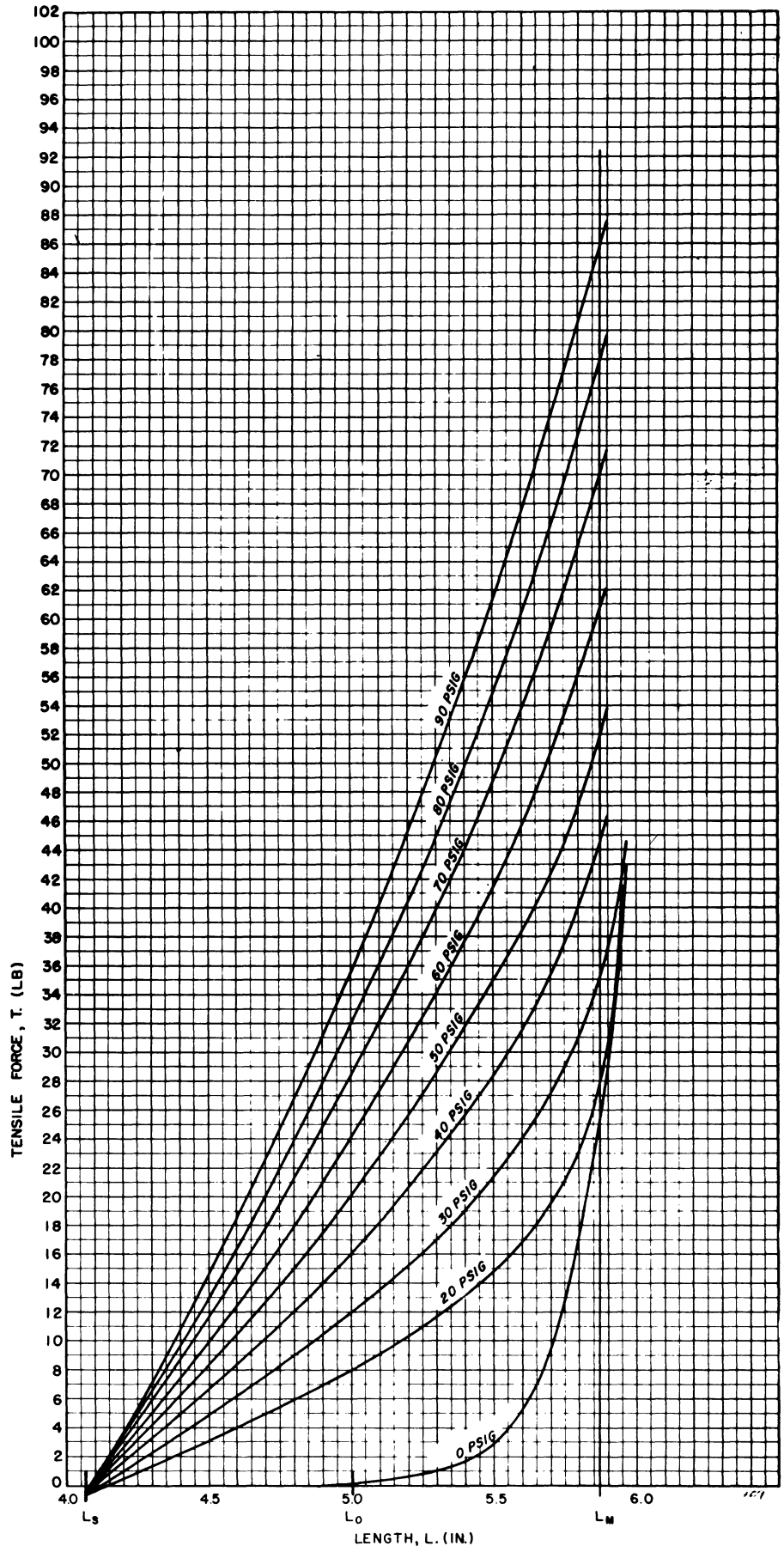

Fig. 21. Isometric tensile force—length characteristics as a function of pressure for the W-2 type BFA: L_o = 5.00 in., W = .95 in., D_s = .72 in.

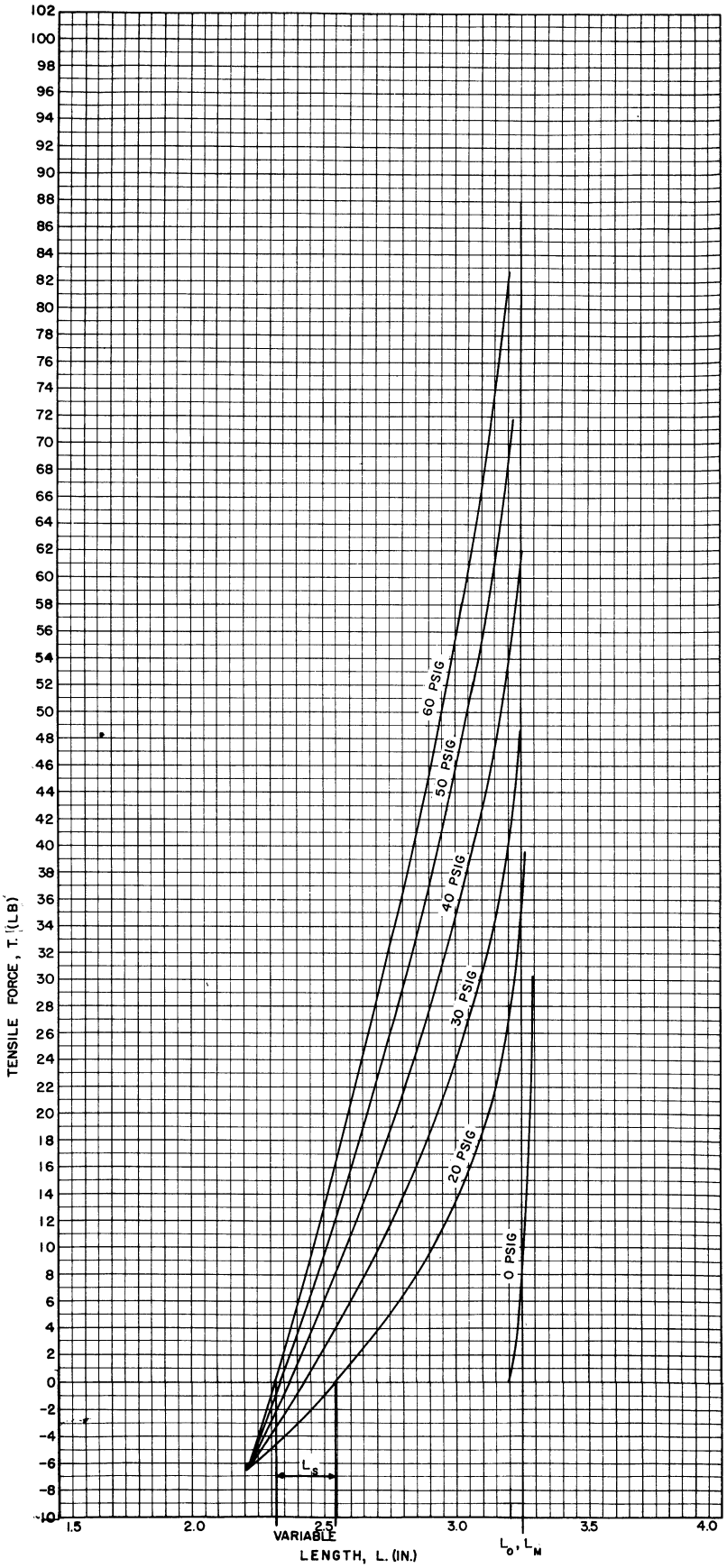

Fig. 22. Isometric tensile force—length characteristics as a function of pressure for the W-4 type BFA: L_o = 3.00 in., W = .75 in.

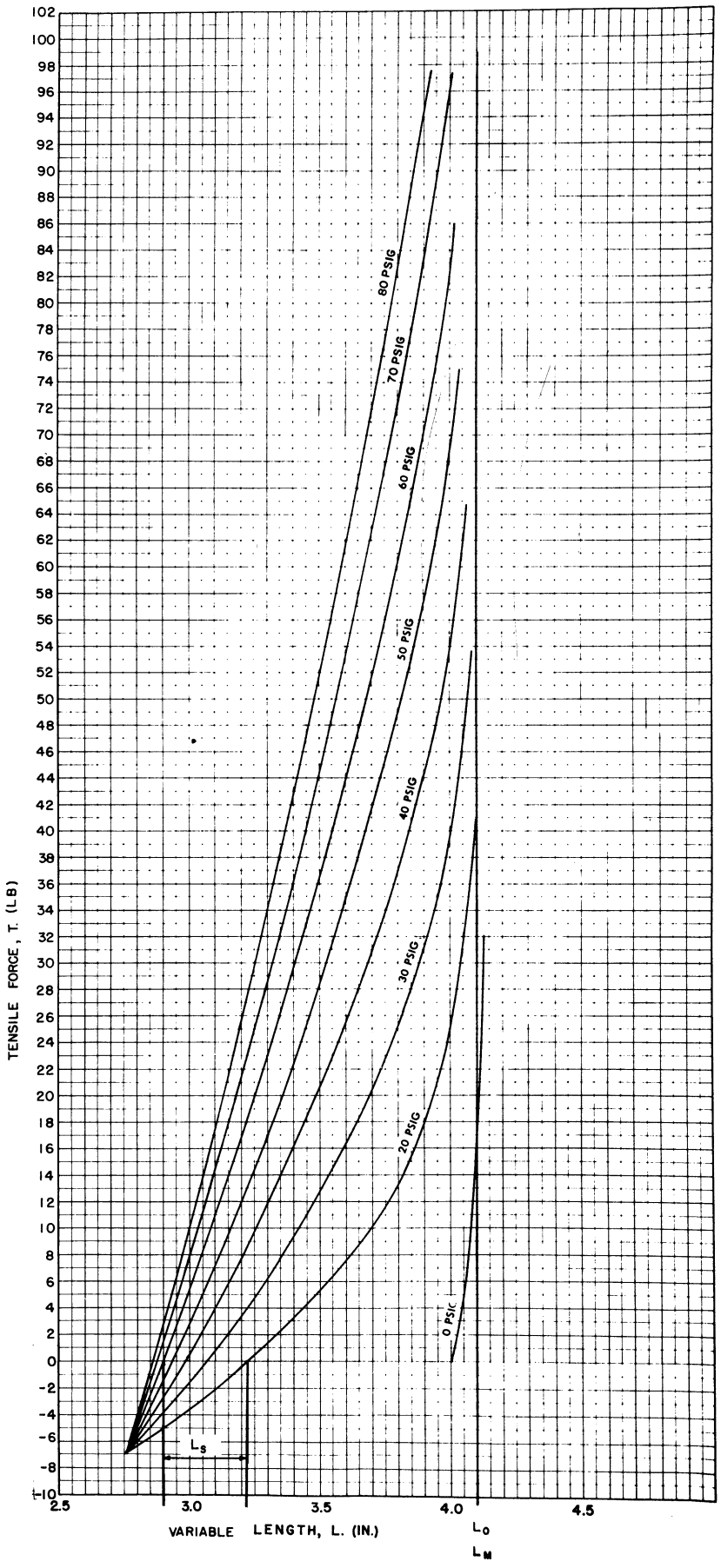

Fig. 23. Isometric tensile force—length characteristics as a function of pressure for the W-4 type BFA: L_o = 4.00 in., W = .75 in.

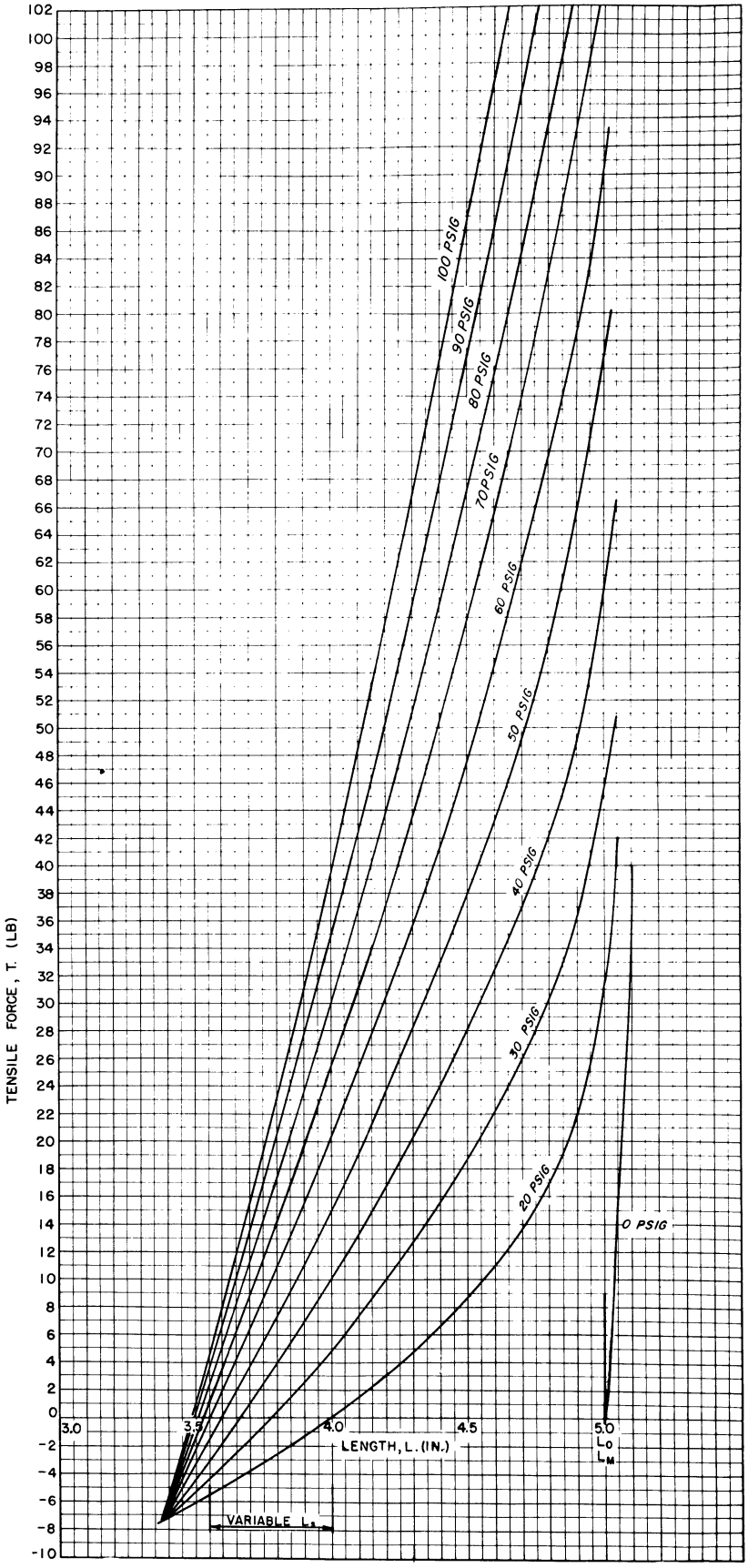

Fig. 24. Isometric tensile force—length characteristics as a function of pressure for the W-4 type BFA: L_o = 5.00 in., W = .75 in.

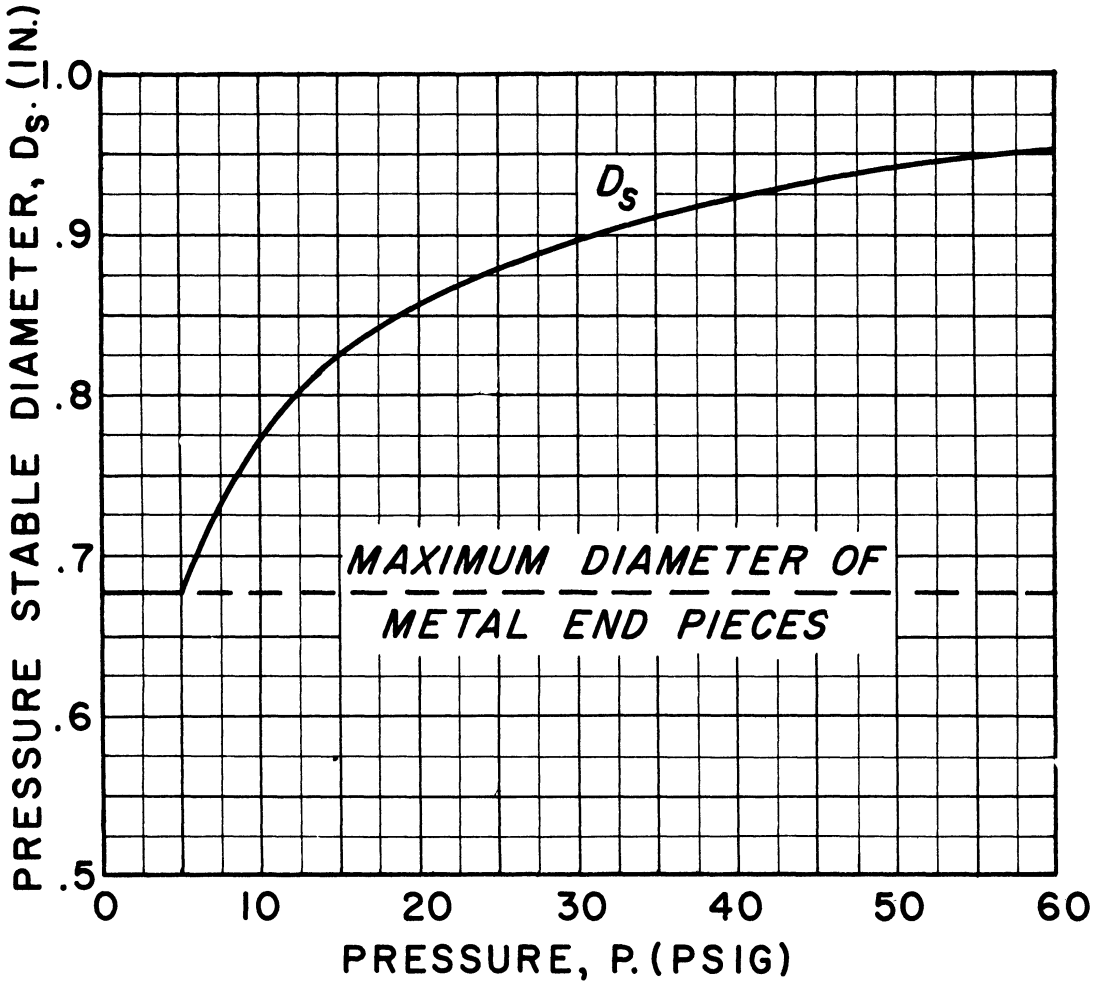

Fig. 25. Pressure stable diameter as a function of pressure for the W-4 type BFA. Flat width W = .95 in.

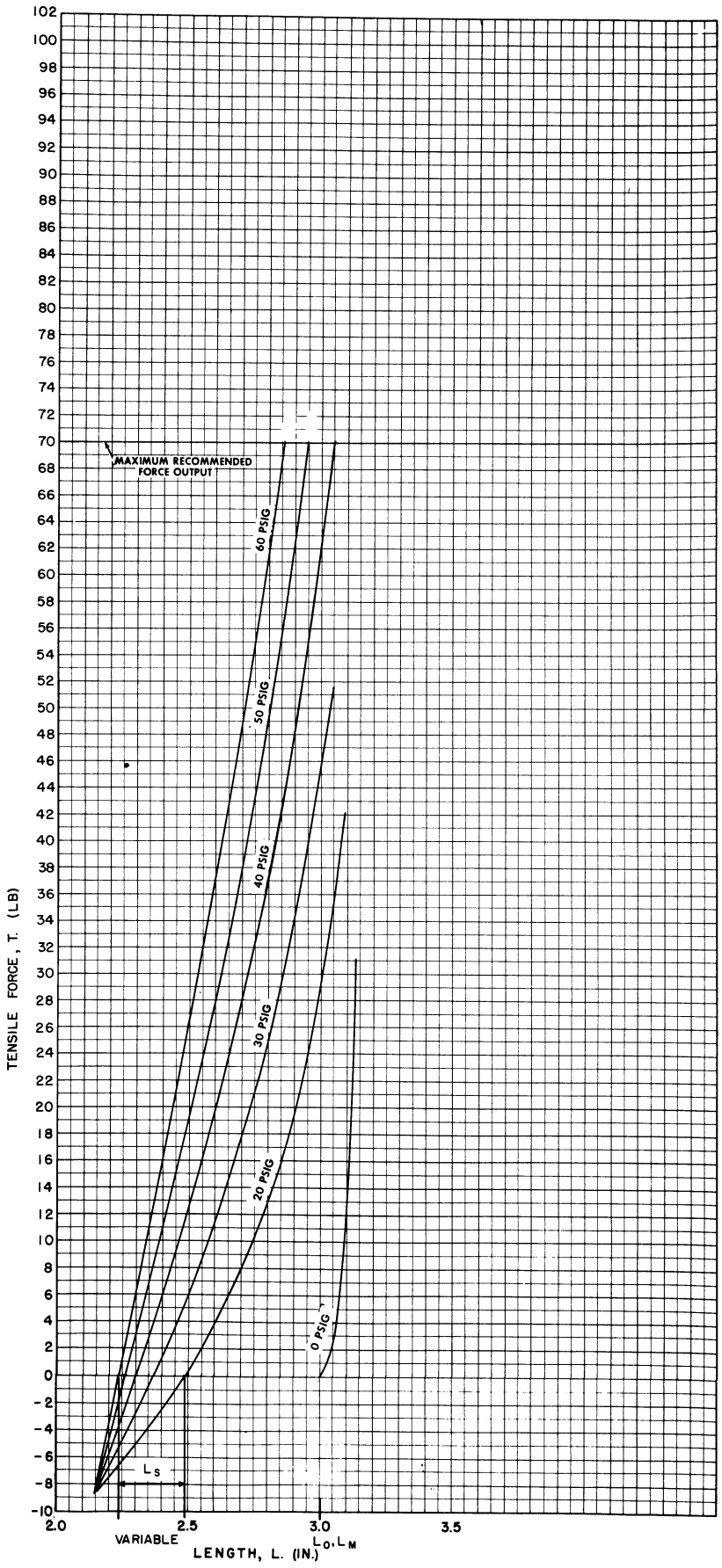

Fig. 26. Isometric tensile force—length characteristics as a function of pressure for the W-3I type BFA: L_o = 3.00 in., W = .95 in.

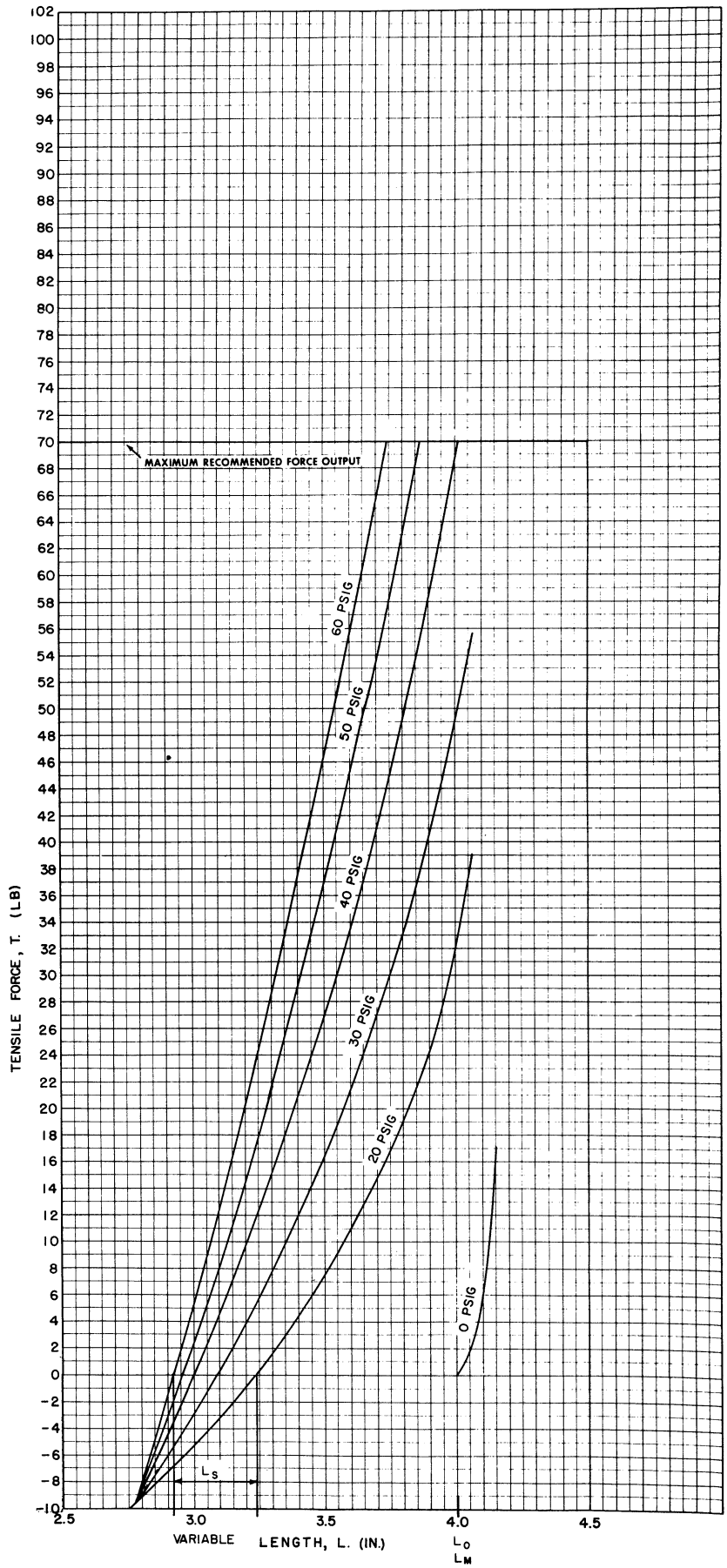

Fig. 27. Isometric tensile force—length characteristics as a function of pressure for the W-3I type BFA: L_o = 4.00 in., W = .95 in.

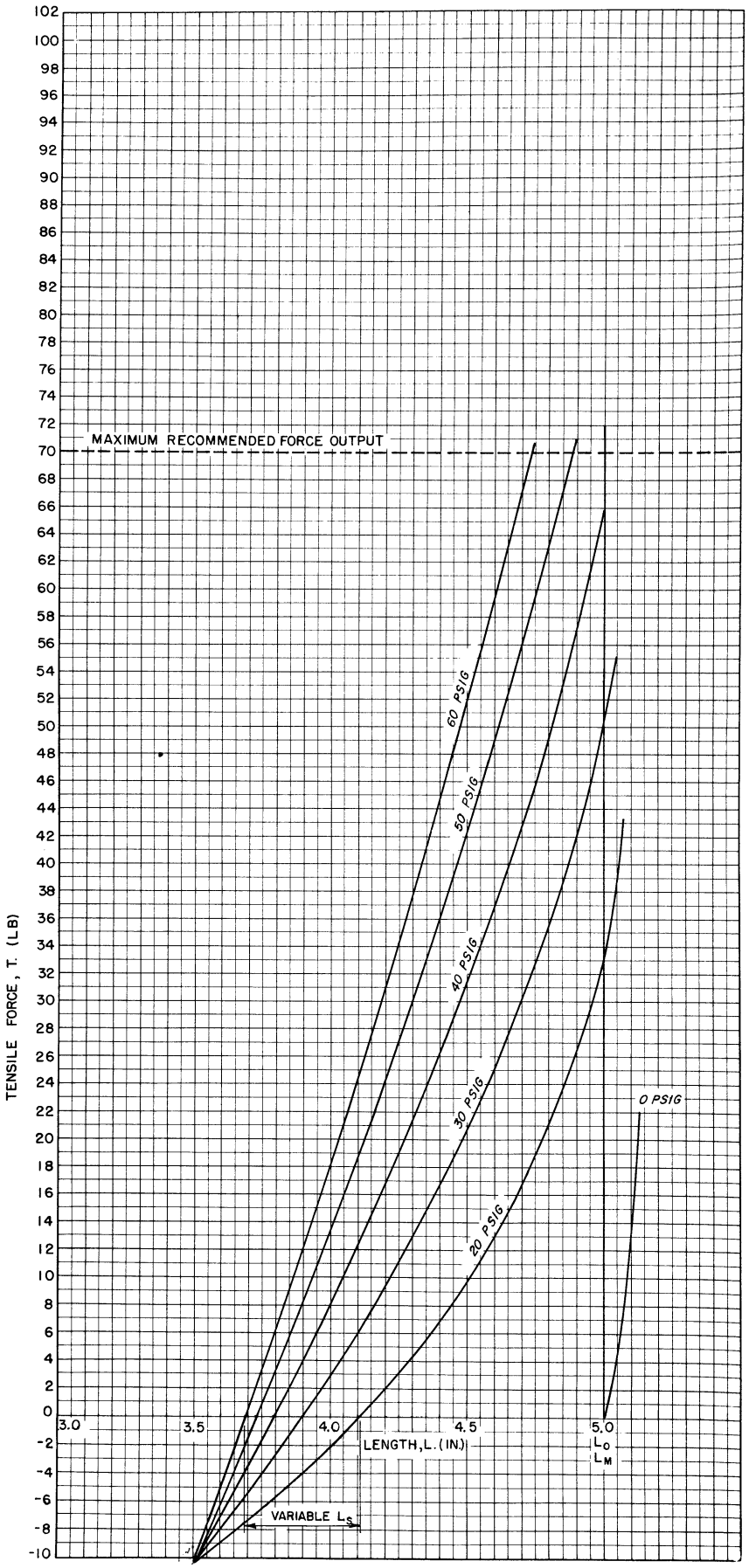

Fig. 28. Isometric tensile force—length characteristics as a function of pressure for the W-3I type BFA: L_o = 5.00 in., W = .95 in.

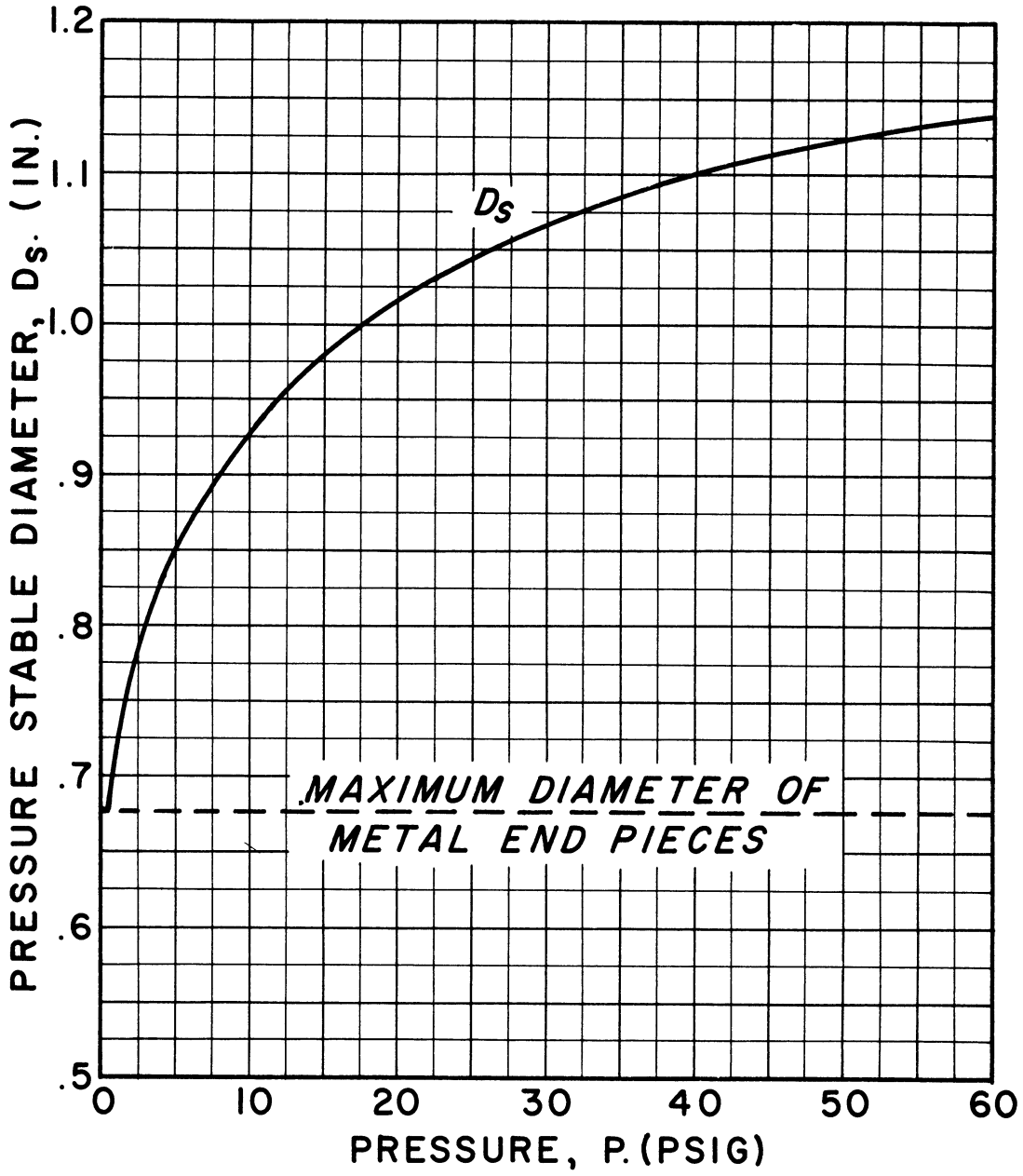

Fig. 29. Pressure stable diameter as a function of pressure for the W-3I type BFA. Flat width W = .95 in.

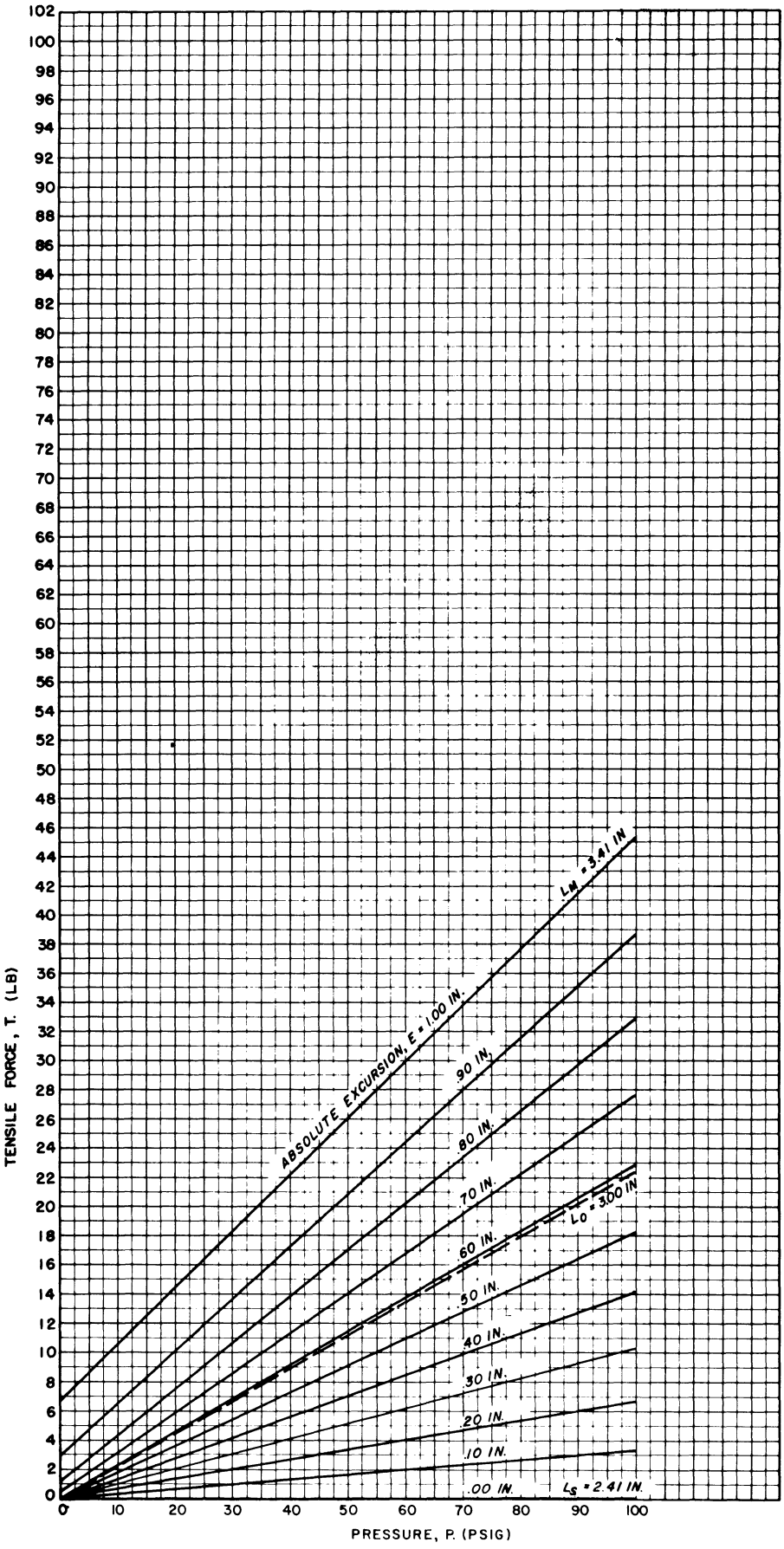

Fig. 30. Isometric tensile-force pressure characteristics as a function of absolute excursion for the W-1 type BFA: L_o = 3.00 in., W = .63 in., D_s = .48 in.

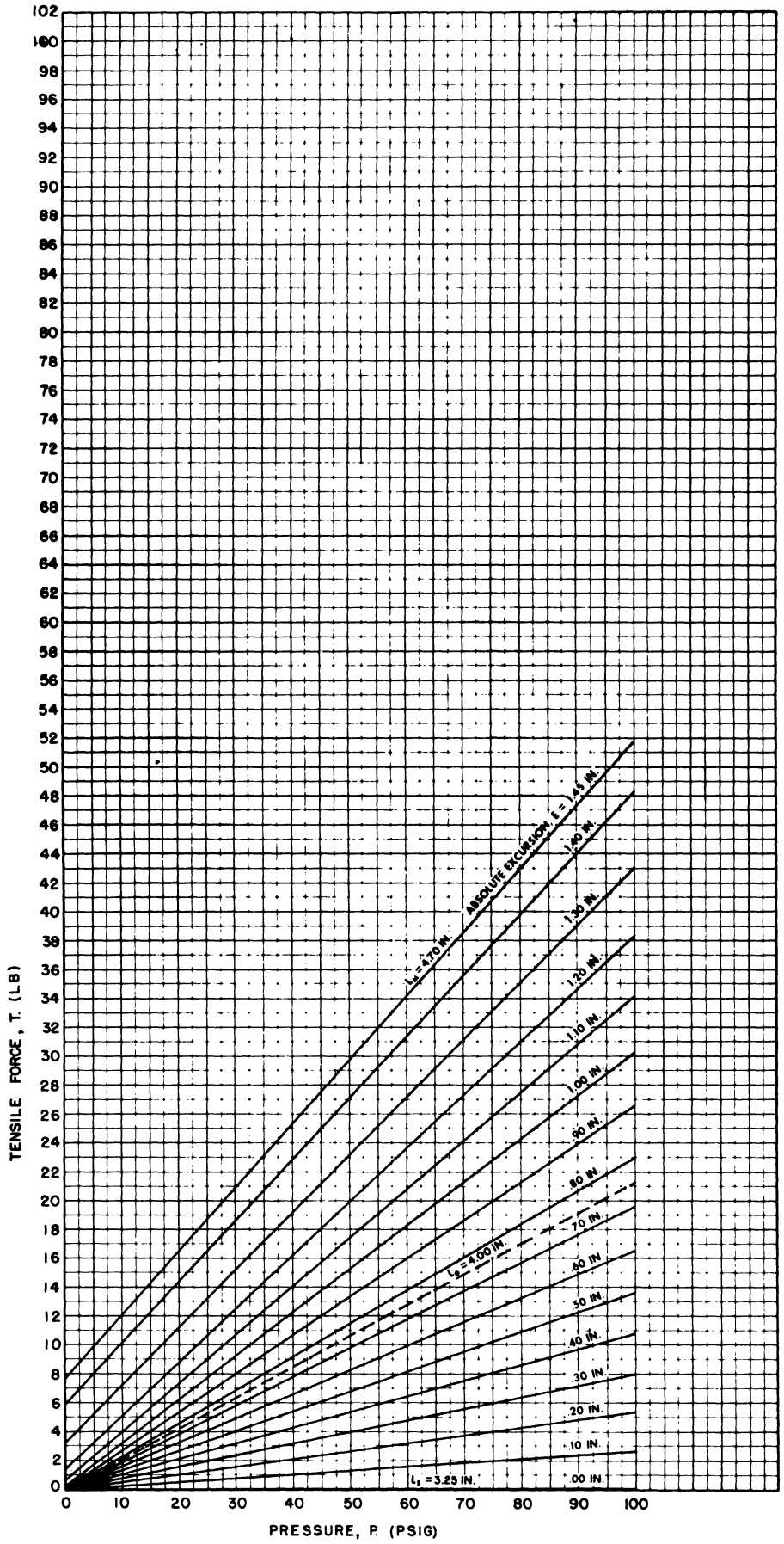

Fig. 31. Isometric tensile force-pressure characteristics as a function of absolute excursion for the W-1 type BFA: L_o = 4.00 in., W = .63 in., D_s = .48 in.

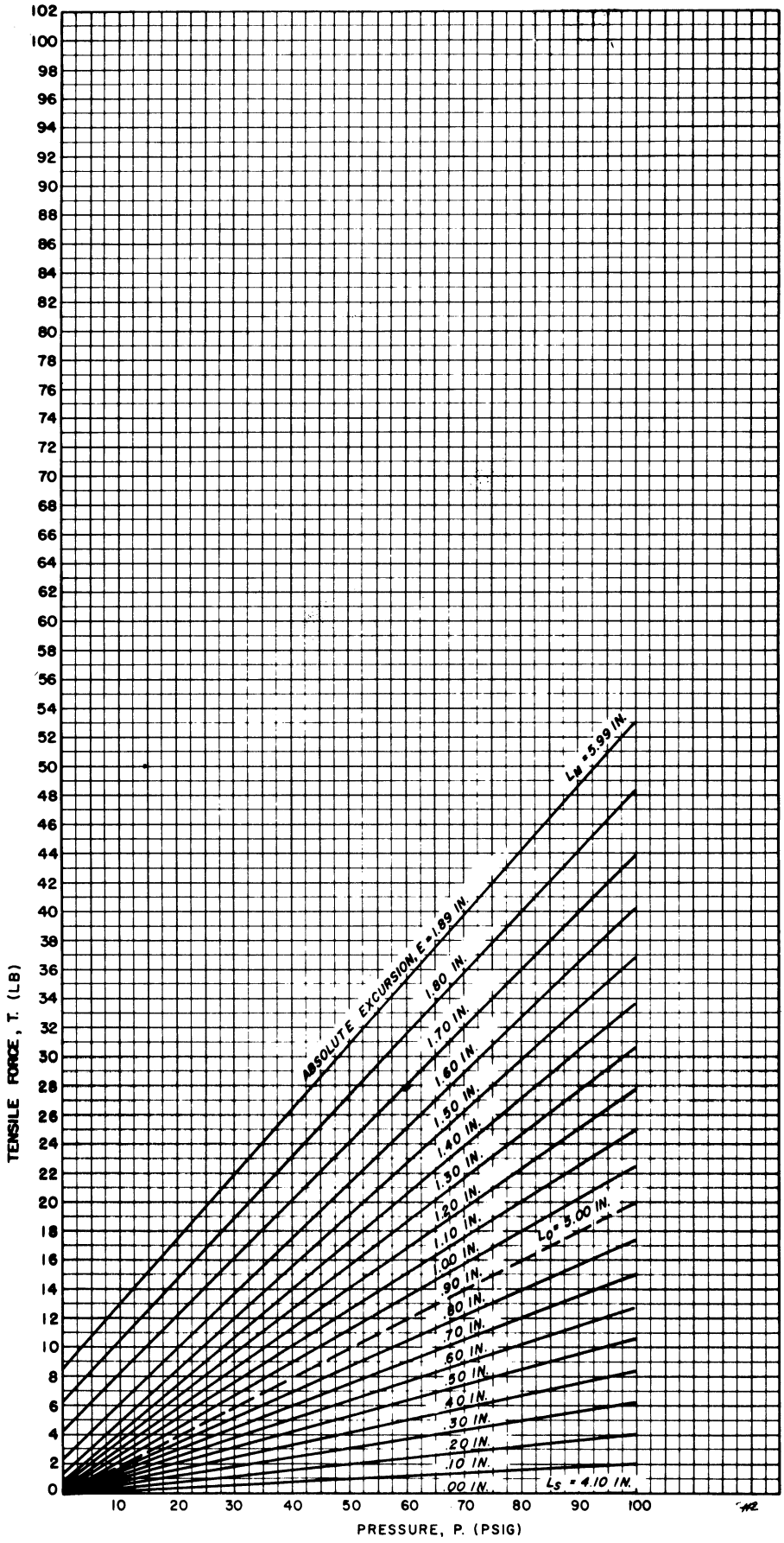

Fig. 32. Isometric tensile-force pressure characteristics as a function of absolute excursion for the W-1 type BFA: L_o = 5.00 in., W = .63 in., D_s = .48 in.

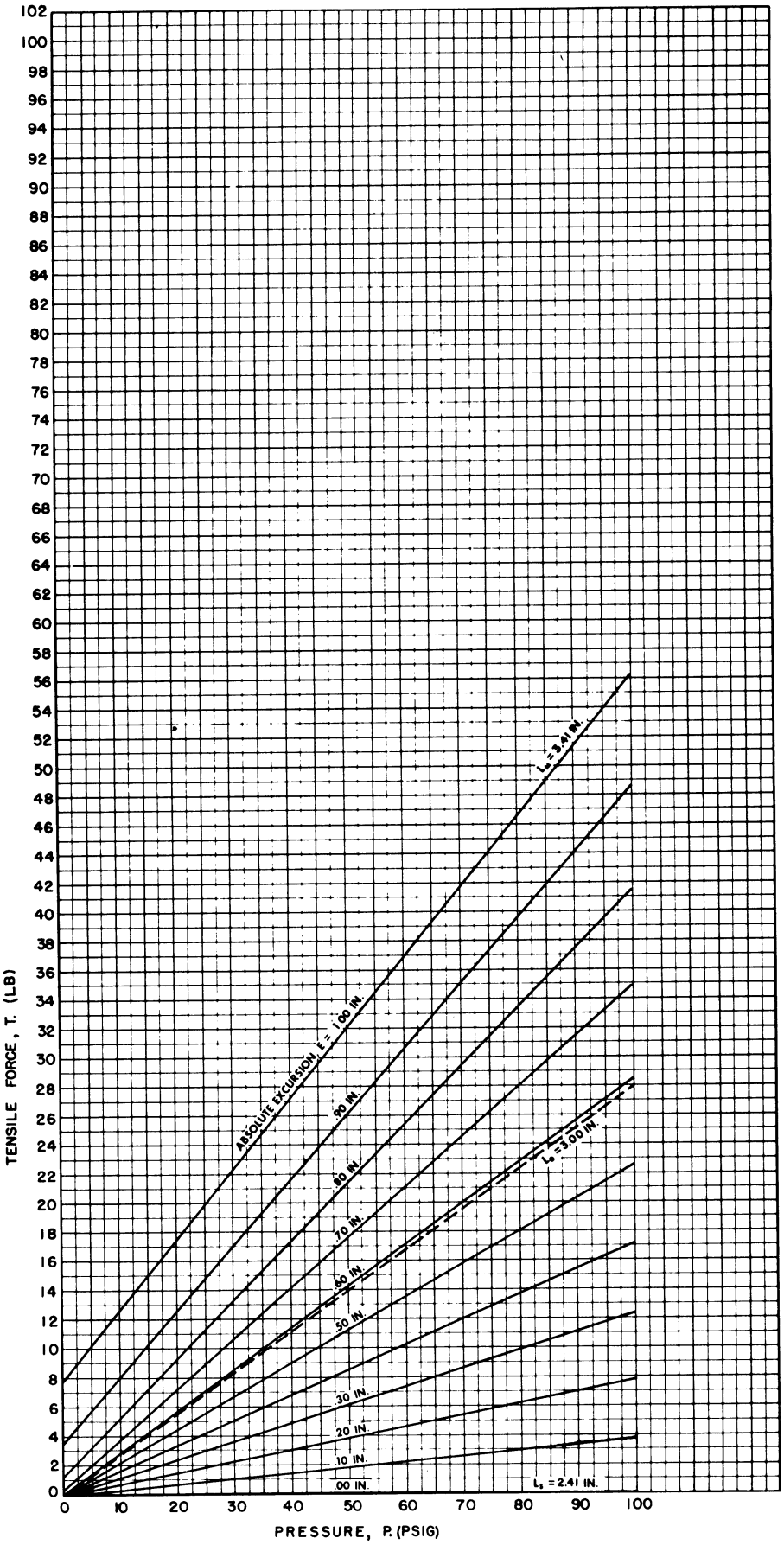

Fig. 33. Isometric tensile force-pressure characteristics as a function of absolute excursion for the W-1 type BFA: L_o = 3.00 in., W = .70 in., D_s = .57 in.

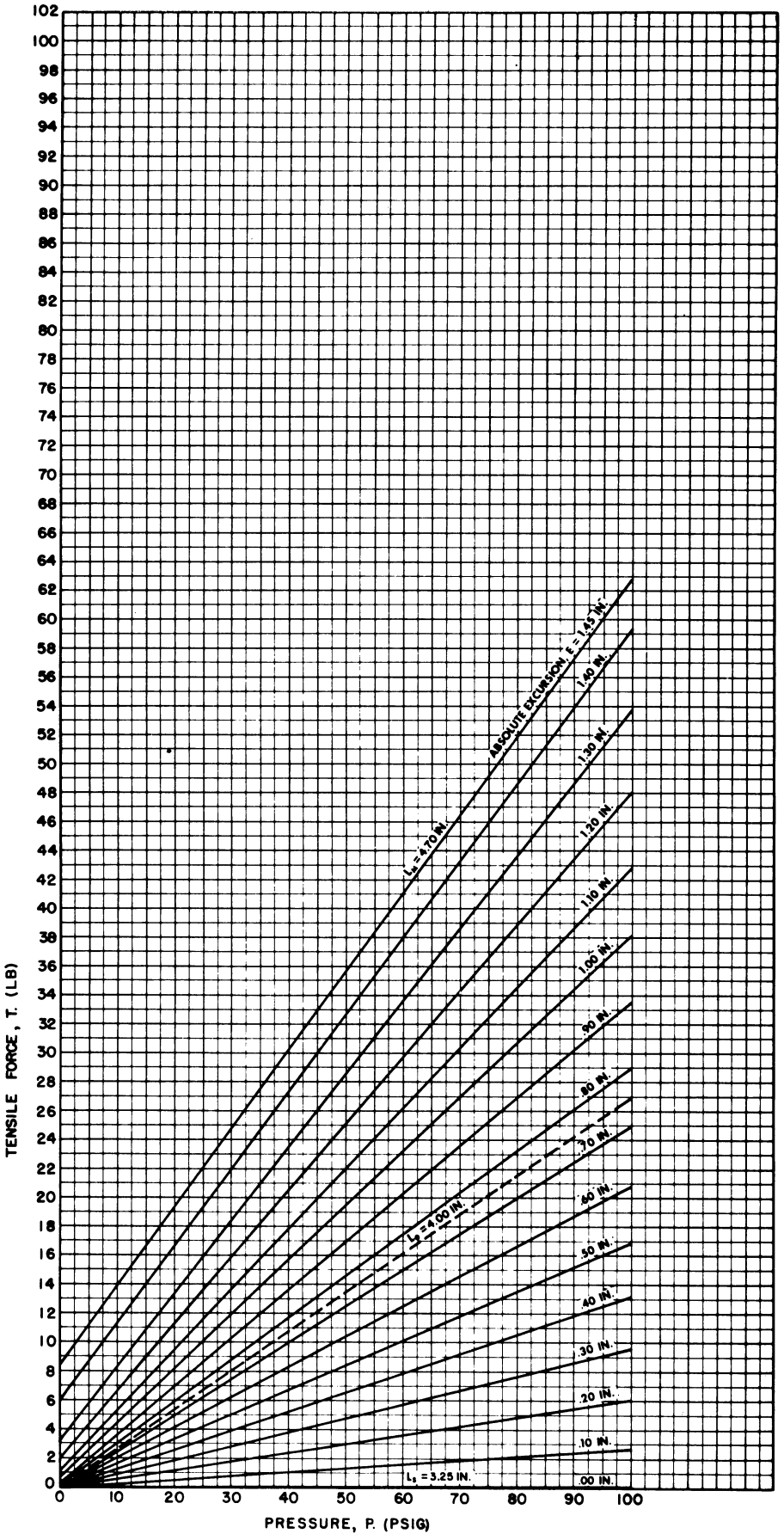

Fig. 34. Isometric tensile-force pressure characteristics as a function of absolute excursion for the W-1 type BFA: L_O = 4.00 in., W = .70 in., D_S = .57 in.

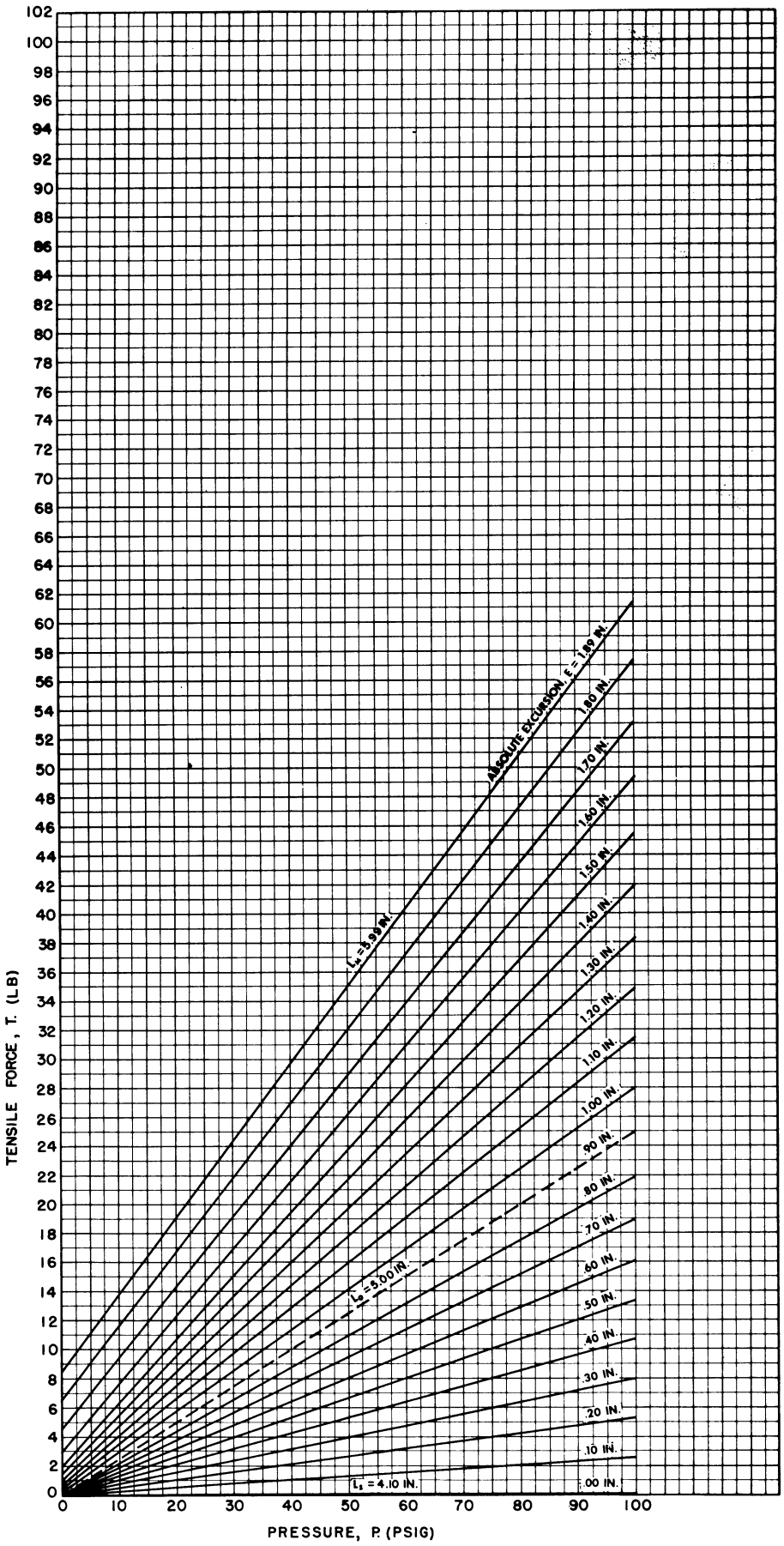

Fig. 35. Isometric tensile force-pressure characteristics as a function of absolute excursion for the W-1 type BFA: L_o = 5.00 in., W = .70 in., D_s = .57 in.

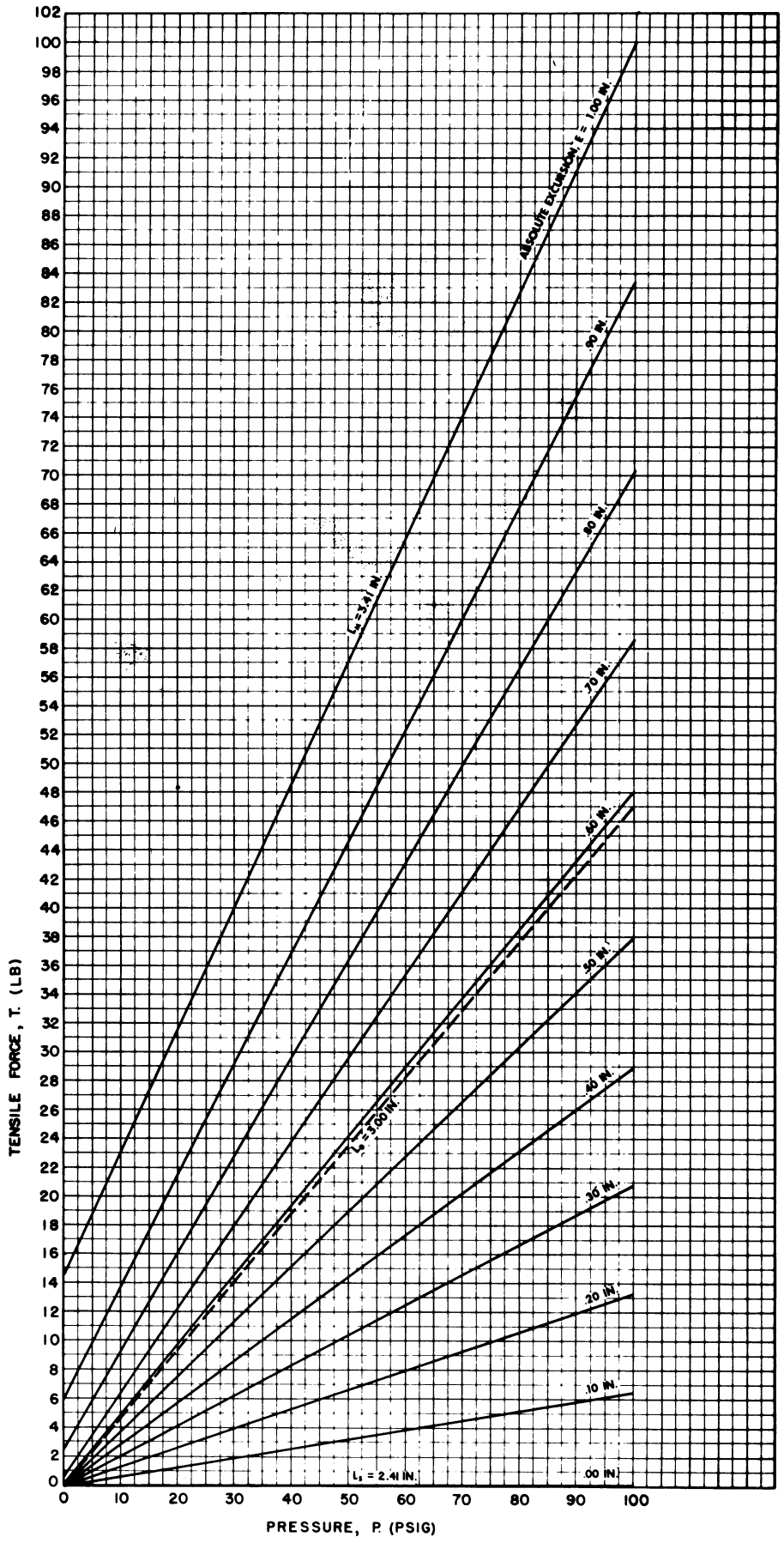

Fig. 36. Isometric tensile force-pressure characteristics as a function of absolute excursion for the W-2 type BFA: L_o = 3.00 in., W = .95 in., D_s = .75 in.

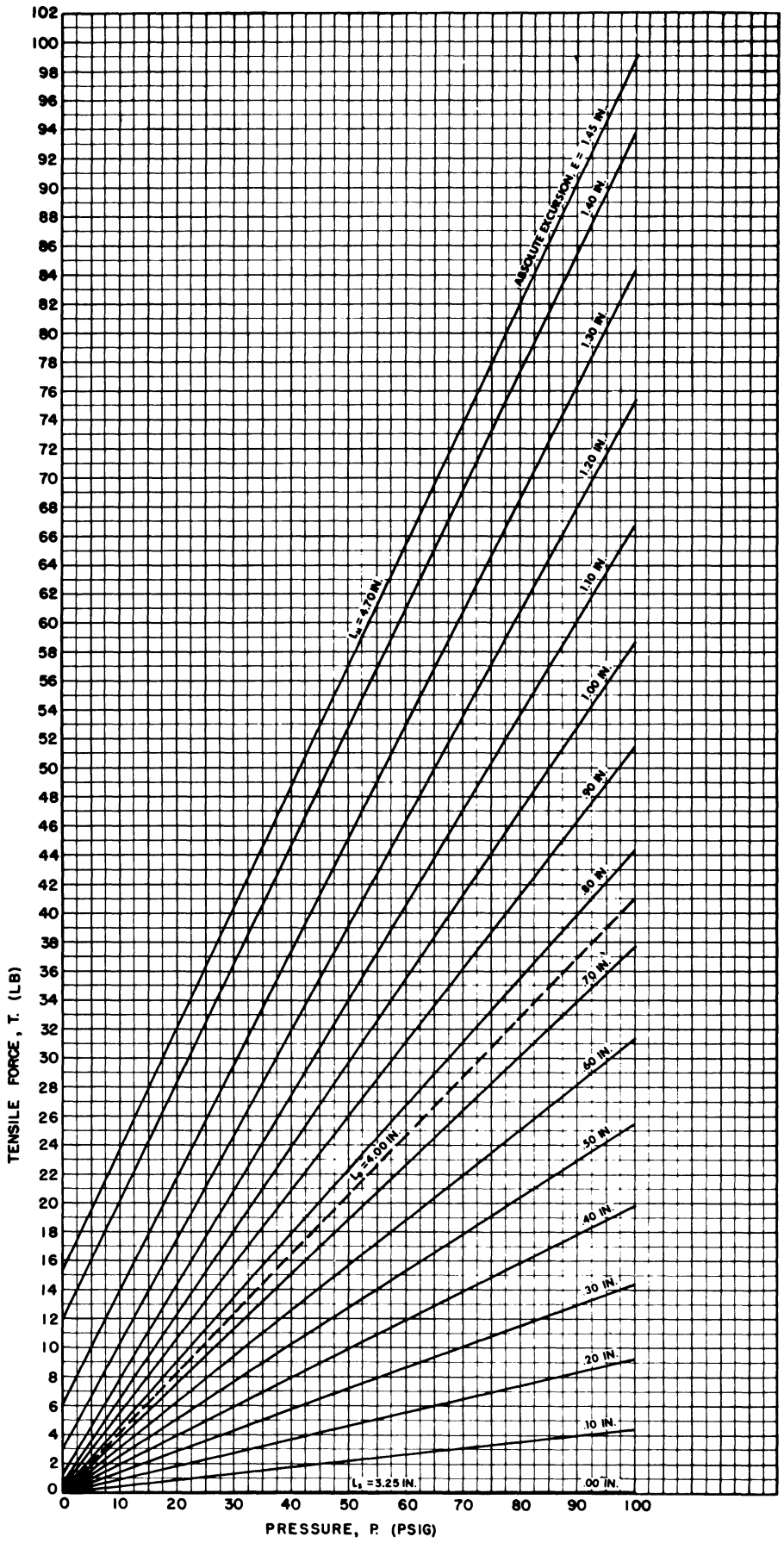

Fig. 37. Isometric tensile force-pressure characteristics as a function of absolute excursion for the W-2 type BFA: L_O = 4.00 in., W = .95 in., D_S = .75 in.

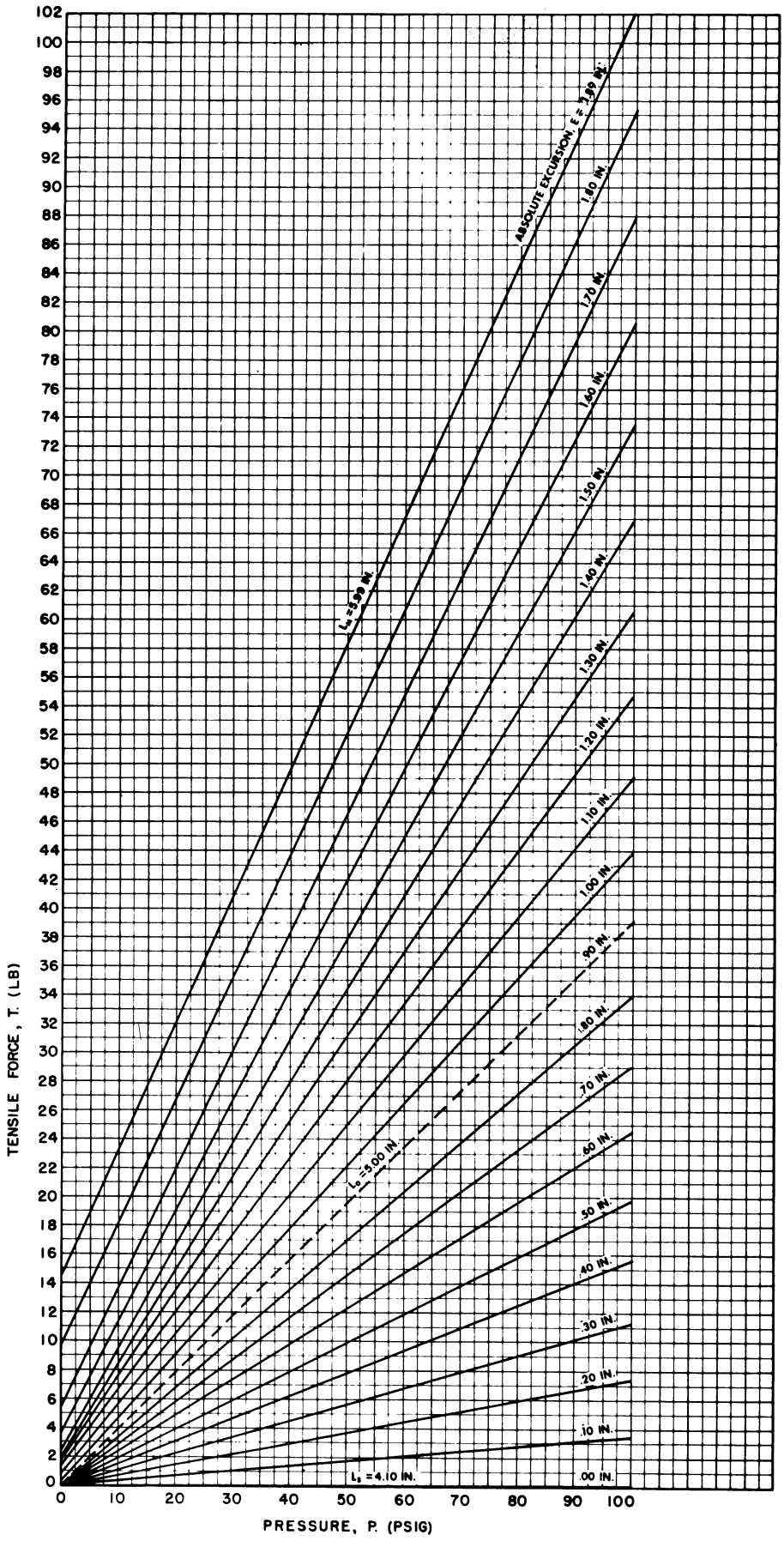

Fig. 38. Isometric tensile force-pressure characteristics as a function of absolute excursion for the W-2 type BFA: L_o = 5.00 in., W = .95 in. D_s = .75 in.

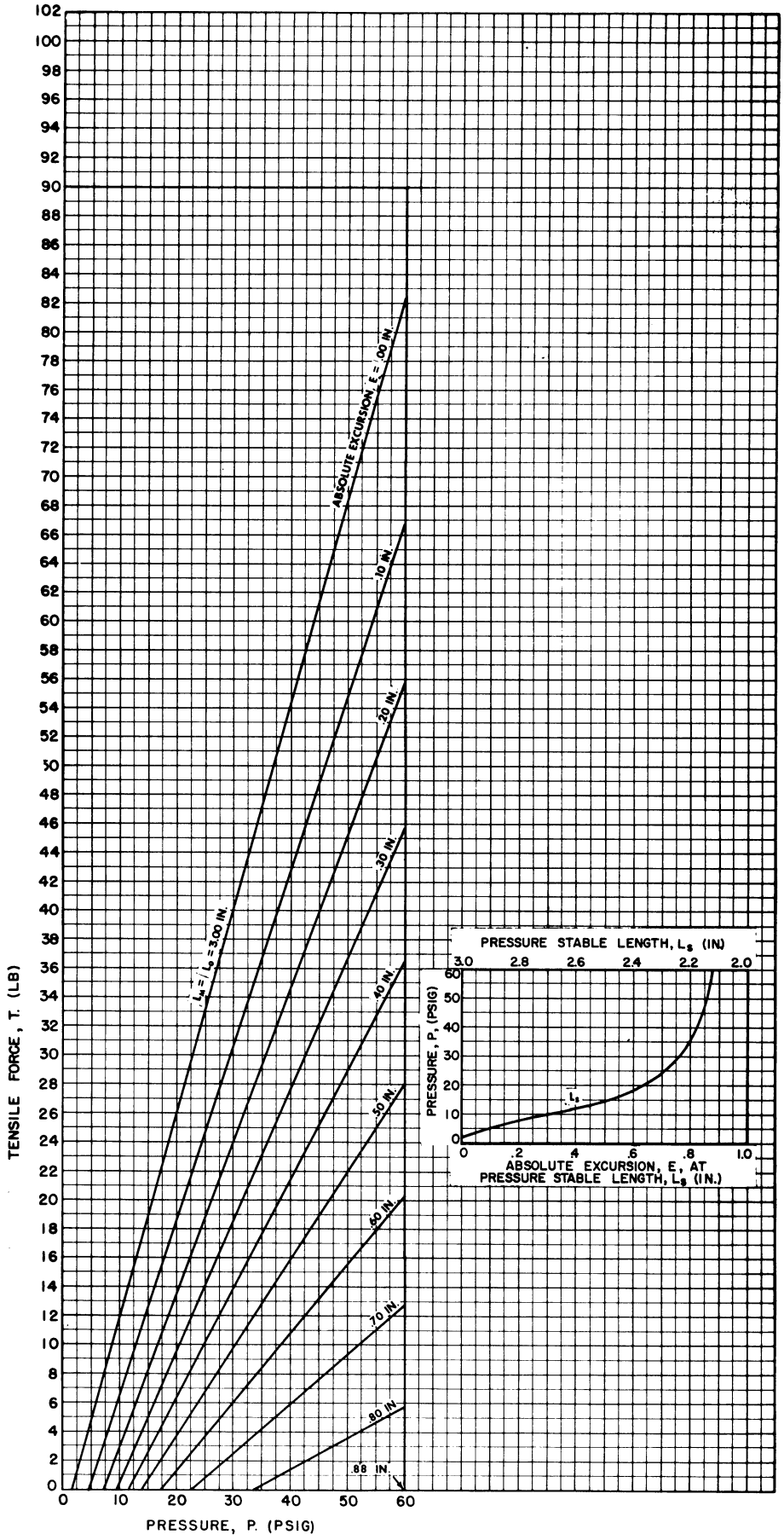

Fig. 39. Isometric tensile force-pressure characteristics as a function of absolute excursion for the W-4 type BFA: L_o = 3.00 in., W = .75 in.

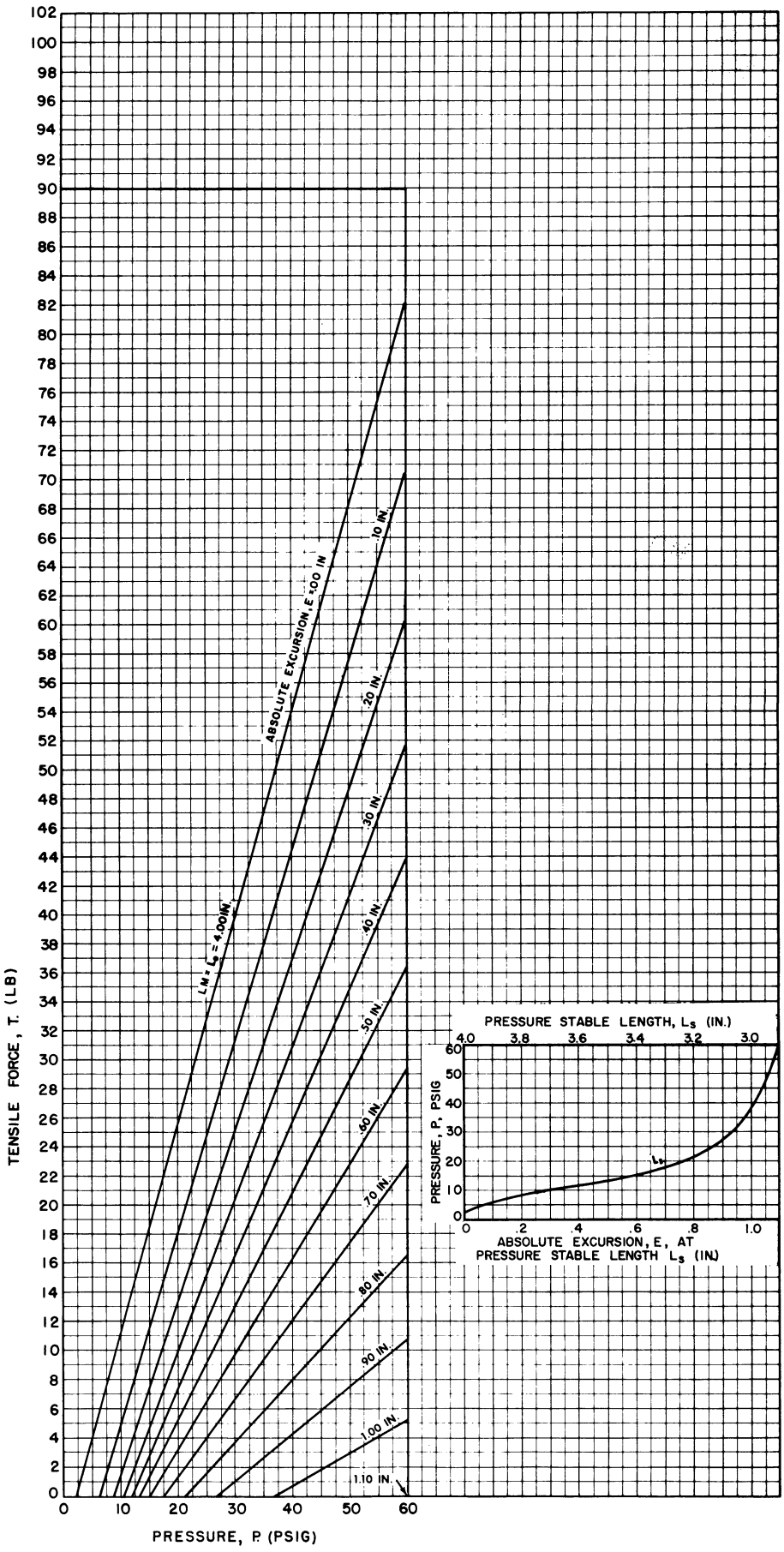

Fig. 40. Isometric tensile force-pressure characteristics as a function of absolute excursion for the W-4 type BFA: L_o = 4.00 in., W = .75 in.

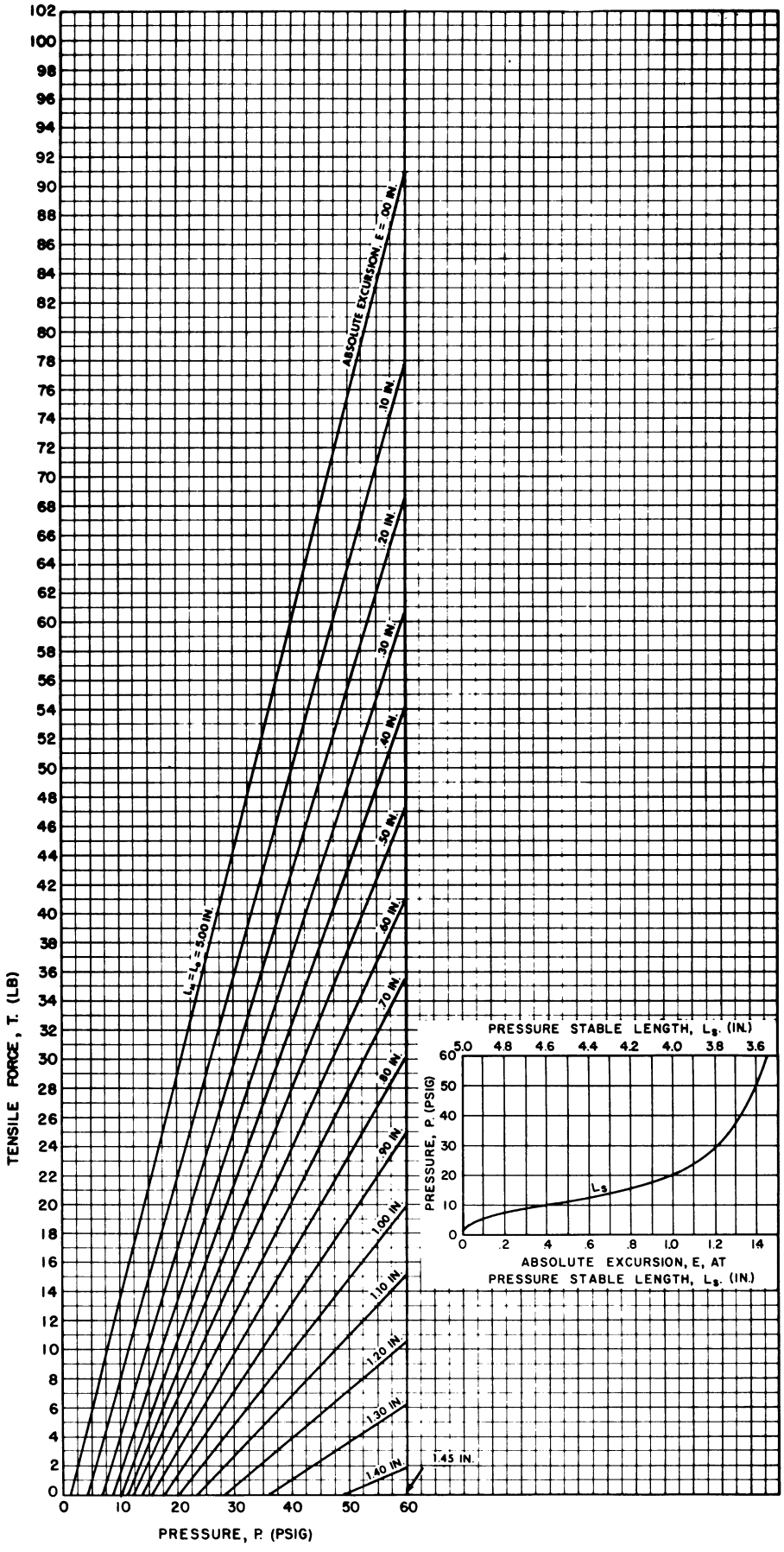

Fig. 41. Isometric tensile force-pressure characteristics as a function of absolute excursion for the W-4 type BFA: L_o = 5.00 in., W = .75 in.

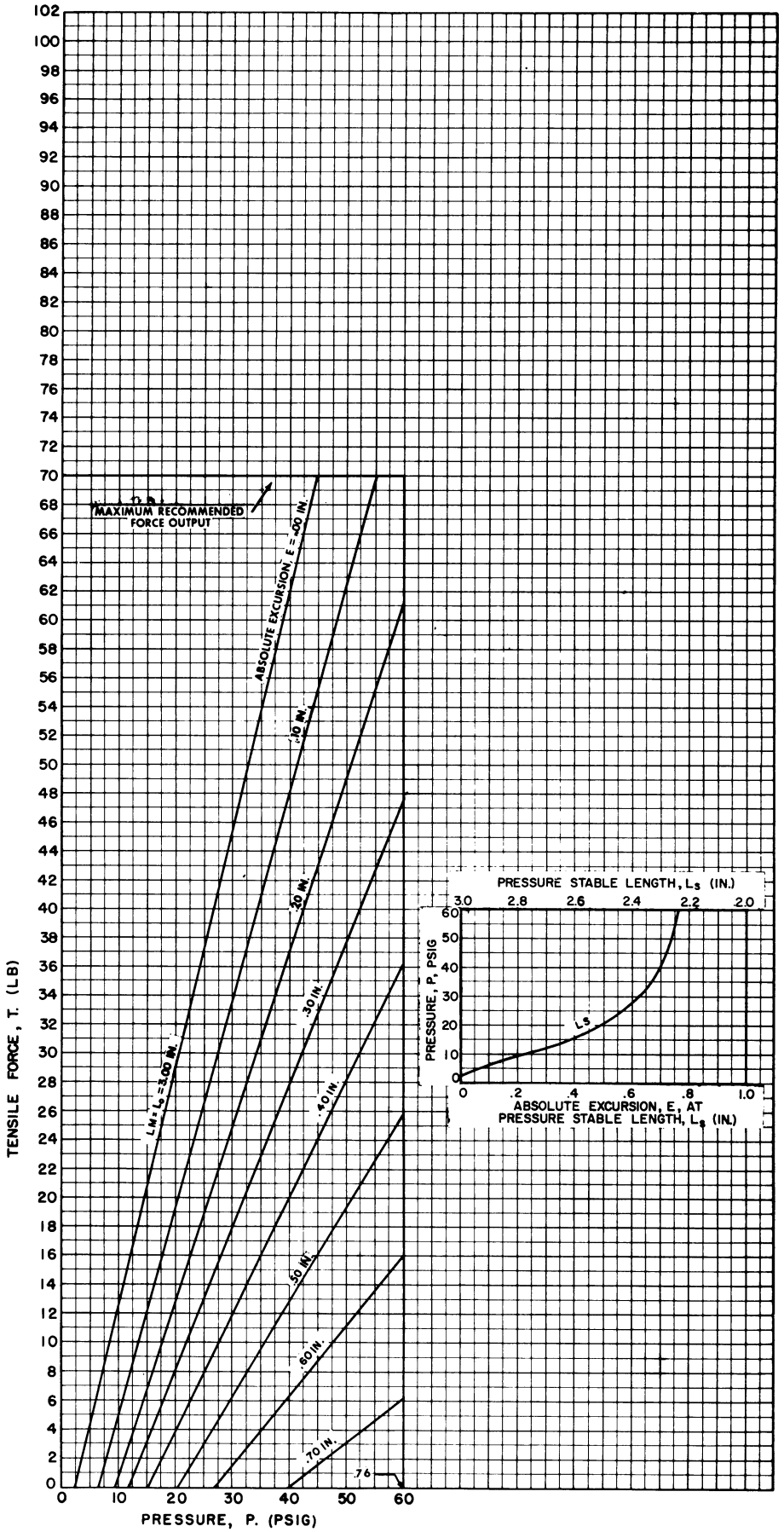

Fig. 42. Isometric tensile force—length characteristics as a function of absolute excursion for the W-3I type BFA: L_o = 3.00 in., W = .95 in.

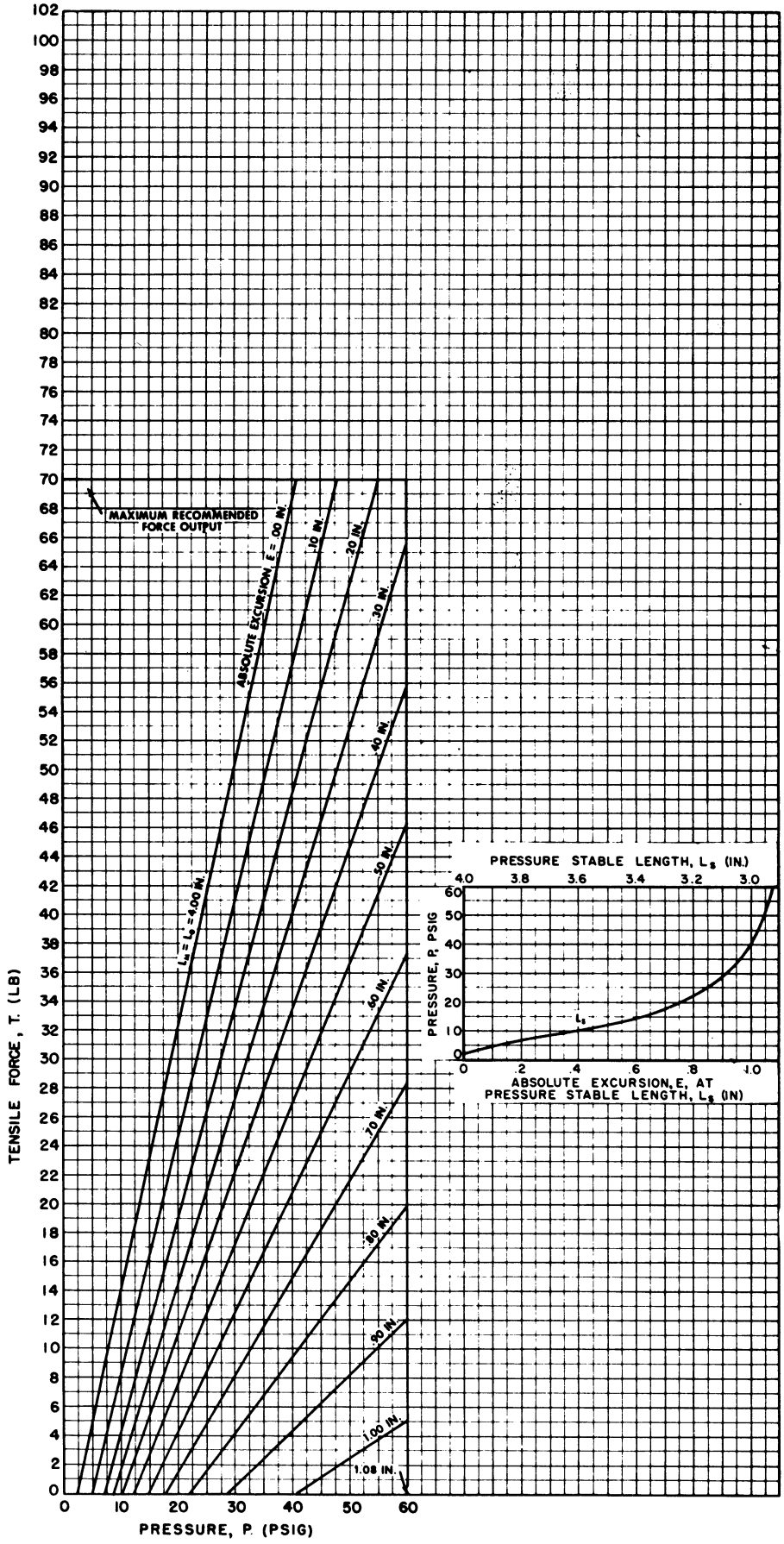

Fig. 43. Isometric tensile force—length characteristics as a function of absolute excursion for the W-3I type BFA: L_o = 4.00 in., W = .95 in.

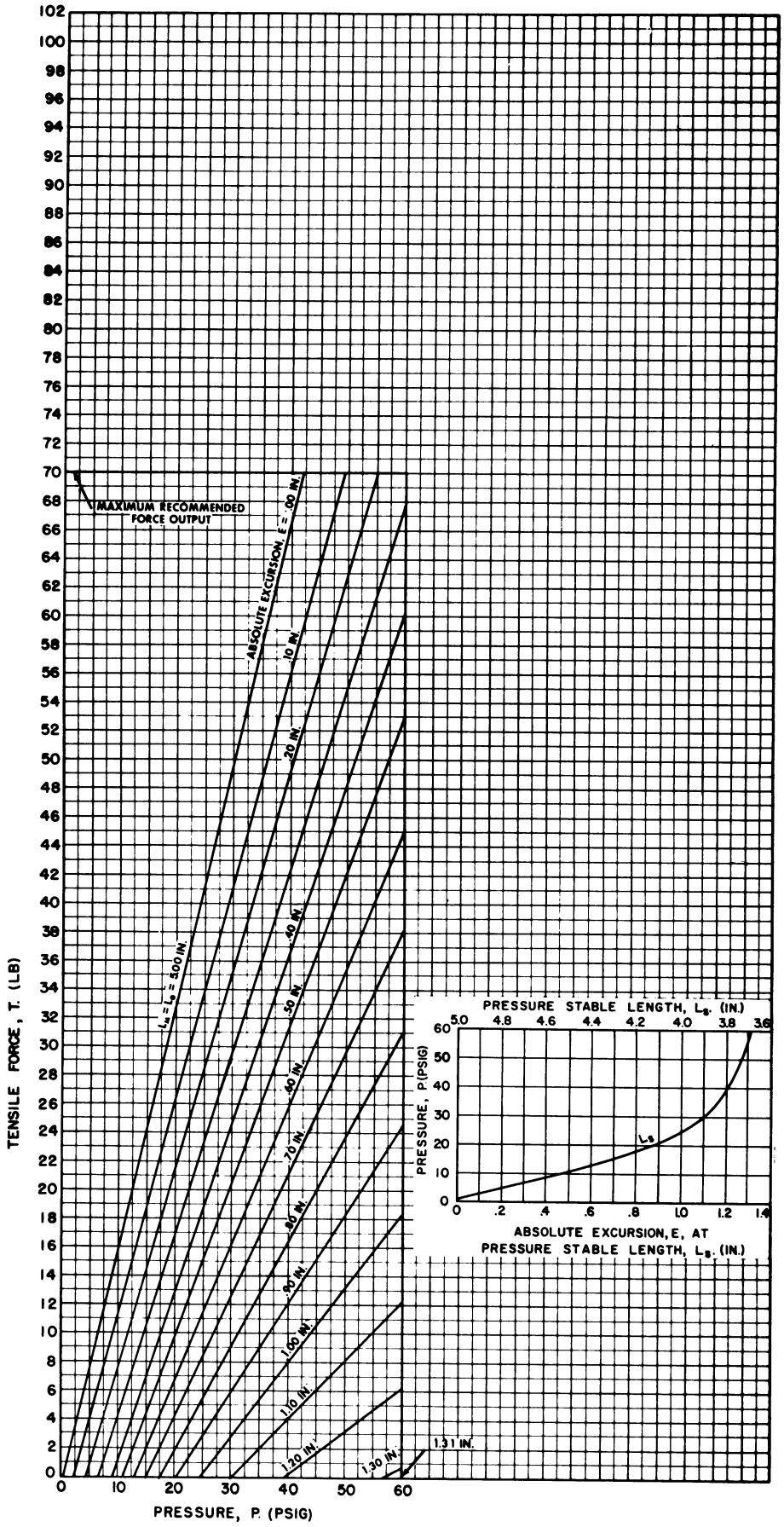

Fig. 44. Isometric tensile force—length characteristics as a function of absolute excursion for the W-3I type BFA: L_o = 5.00 in., W = .95 in.

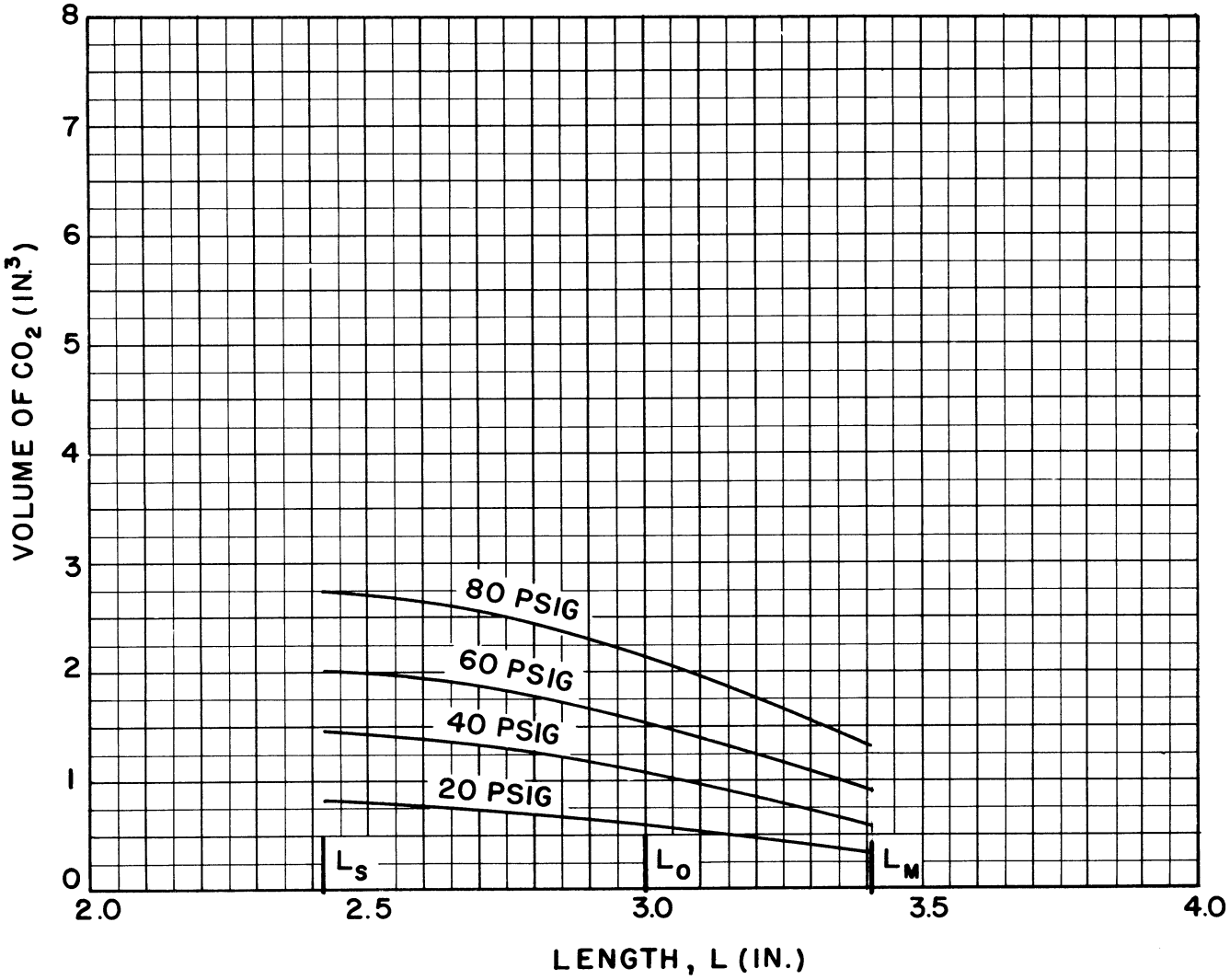

Fig. 45. Gas consumption characteristics on a volume basis as a function of pressure for the W-1 type BFA. Data corrected to standard atmospheric conditions. L_o = 3.00 in., W = .63 in., D_s = .48 in., atmospheric pressure = 14.7 lb/in.^{2}, atmospheric temperature = 77°F.

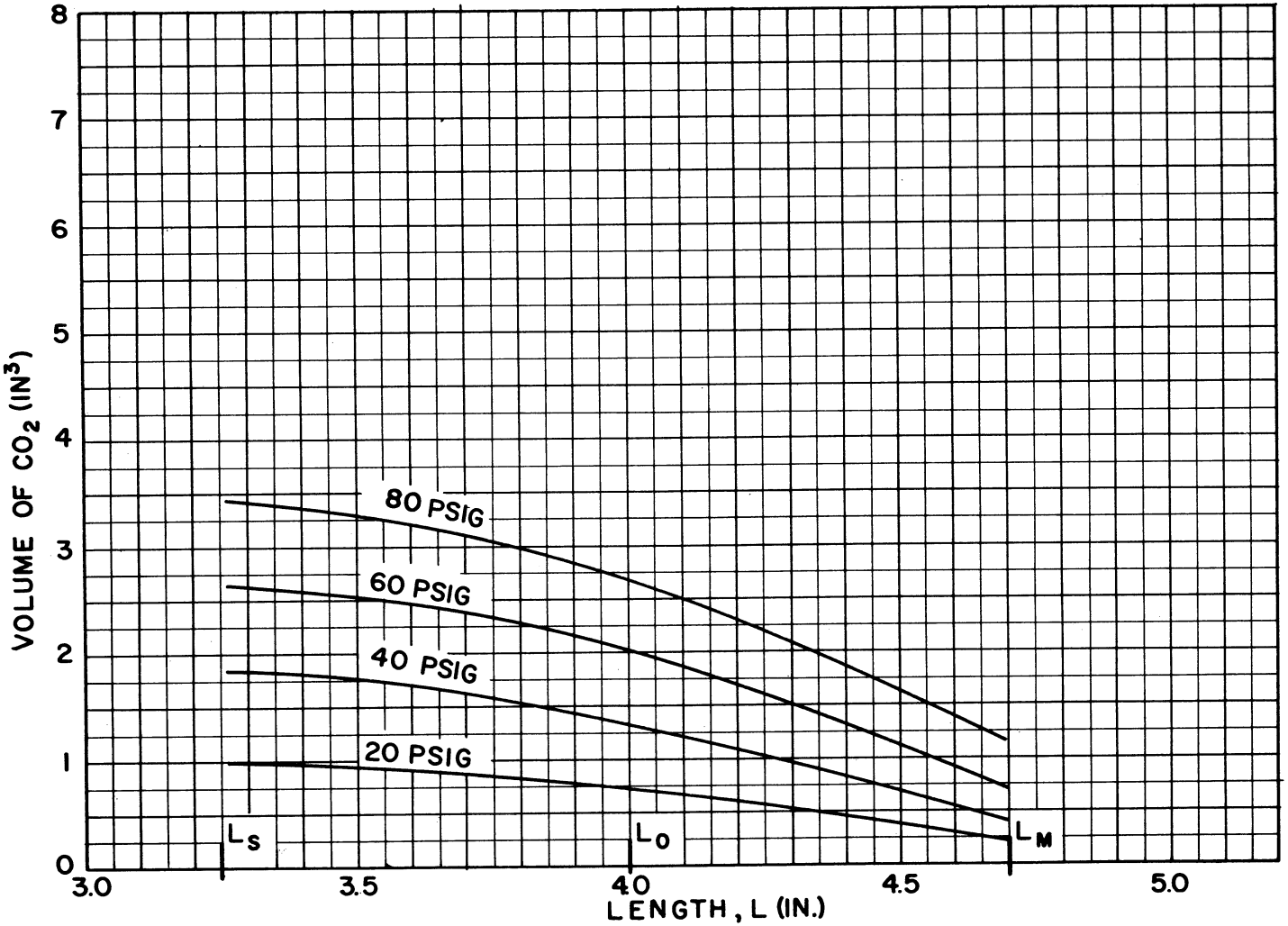

Fig. 46. Gas consumption characteristics on a volume basis as a function of pressure for the W-1 type BFA. Data corrected to standard atmospheric conditions. L_O = 4.00 in., W = .63 in., D_S = .48 in., atmospheric pressure = 14.7 lb/in.^{2}, atmospheric temperature = 77°F.

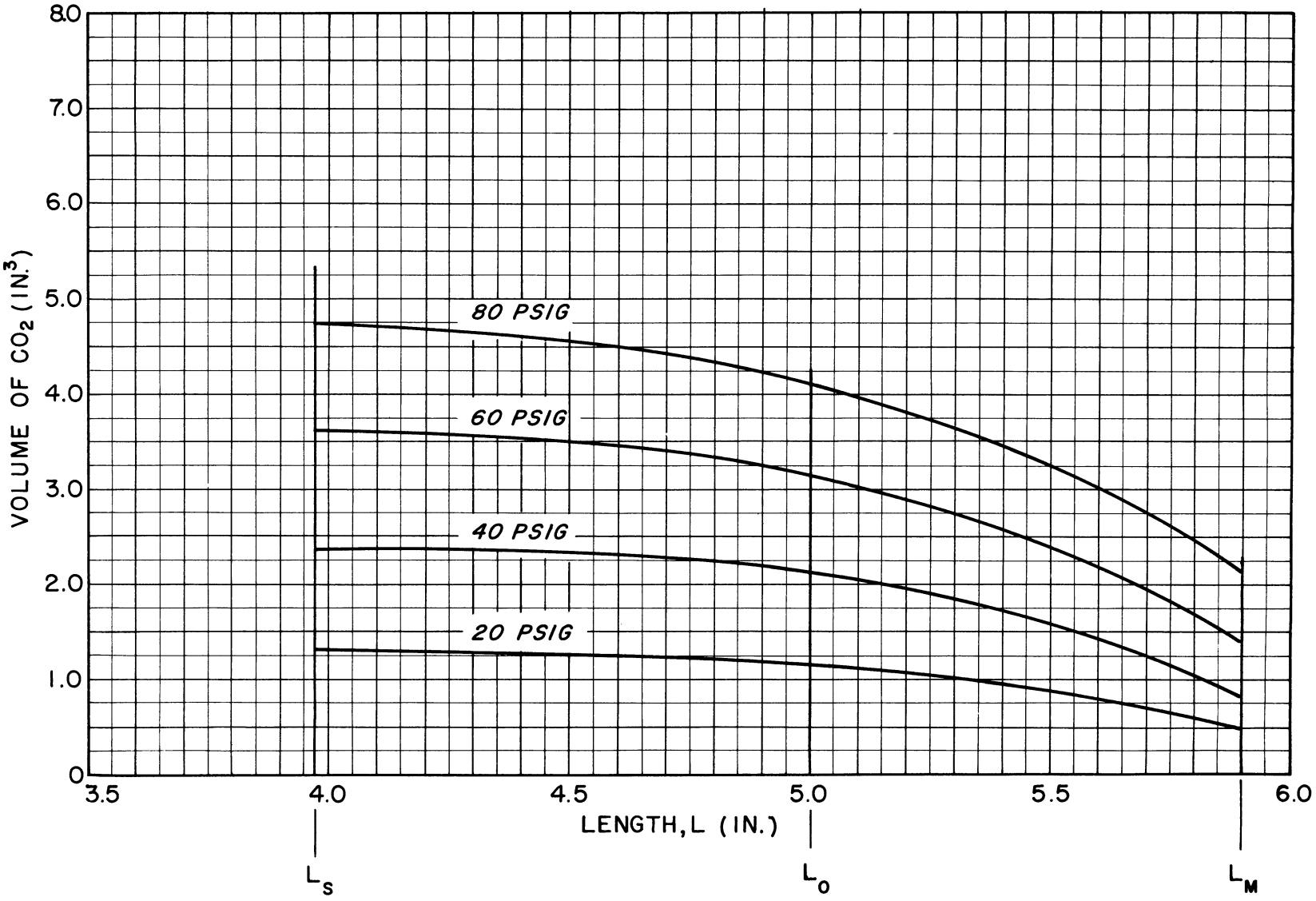

Fig. 47. Gas consumption characteristics on a volume basis as a function of pressure for the W-1 type BFA. Data corrected to standard atmospheric conditions. L_o = 5.00 in., W = .63 in., D_s = .48 in., atmospheric pressure = 14.7 lb/in.^{2}, atmospheric temperature = 77°F.

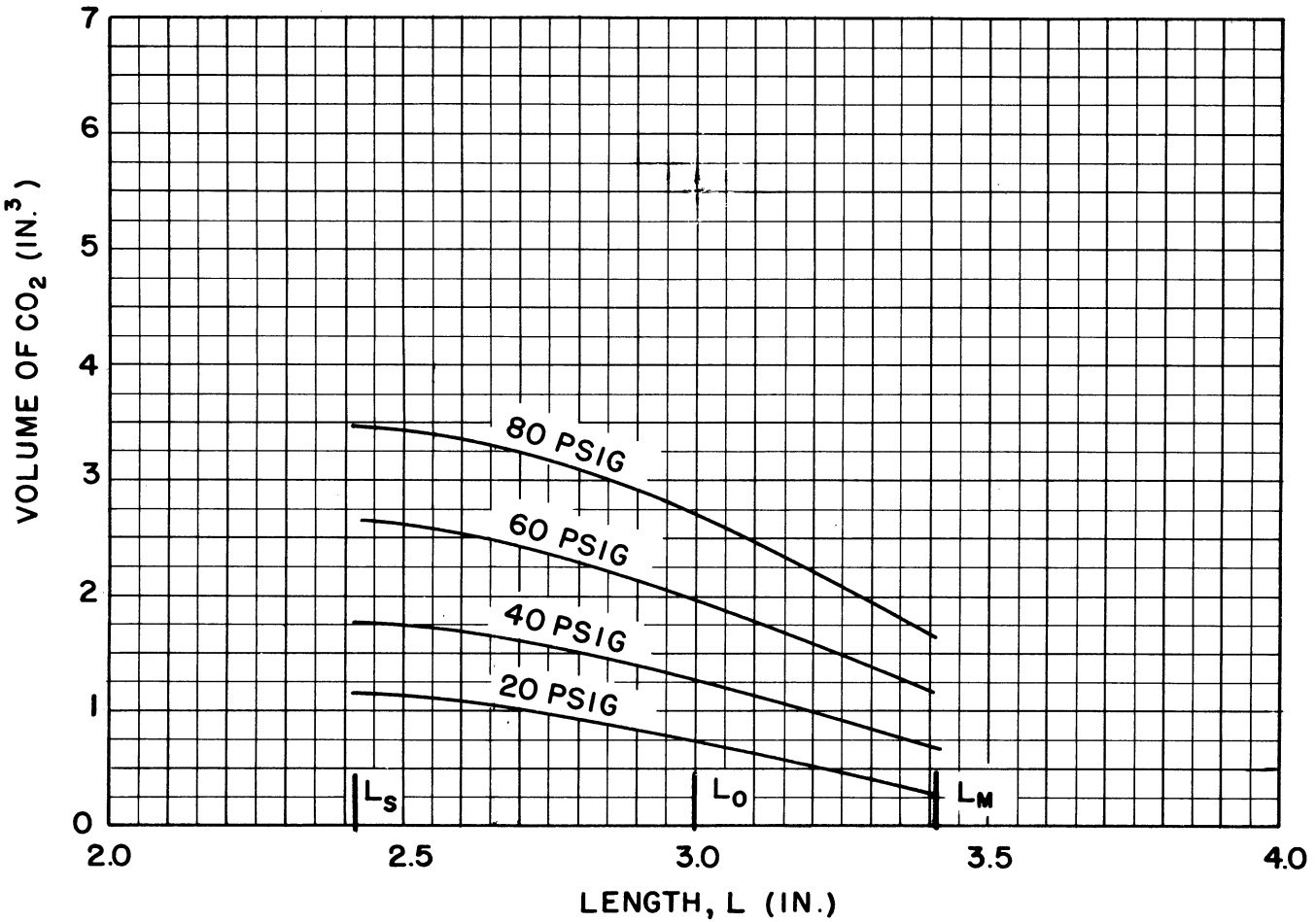

Fig. 48. Gas consumption characteristics on a volume basis as a function of pressure for the W-1 type BFA. Data corrected to standard atmospheric conditions. L_O = 3.00 in., W = .70 in., D_S = .57 in., atmospheric pressure = 14.7 lb/in.^{2}, atmospheric temperature = 77°F.

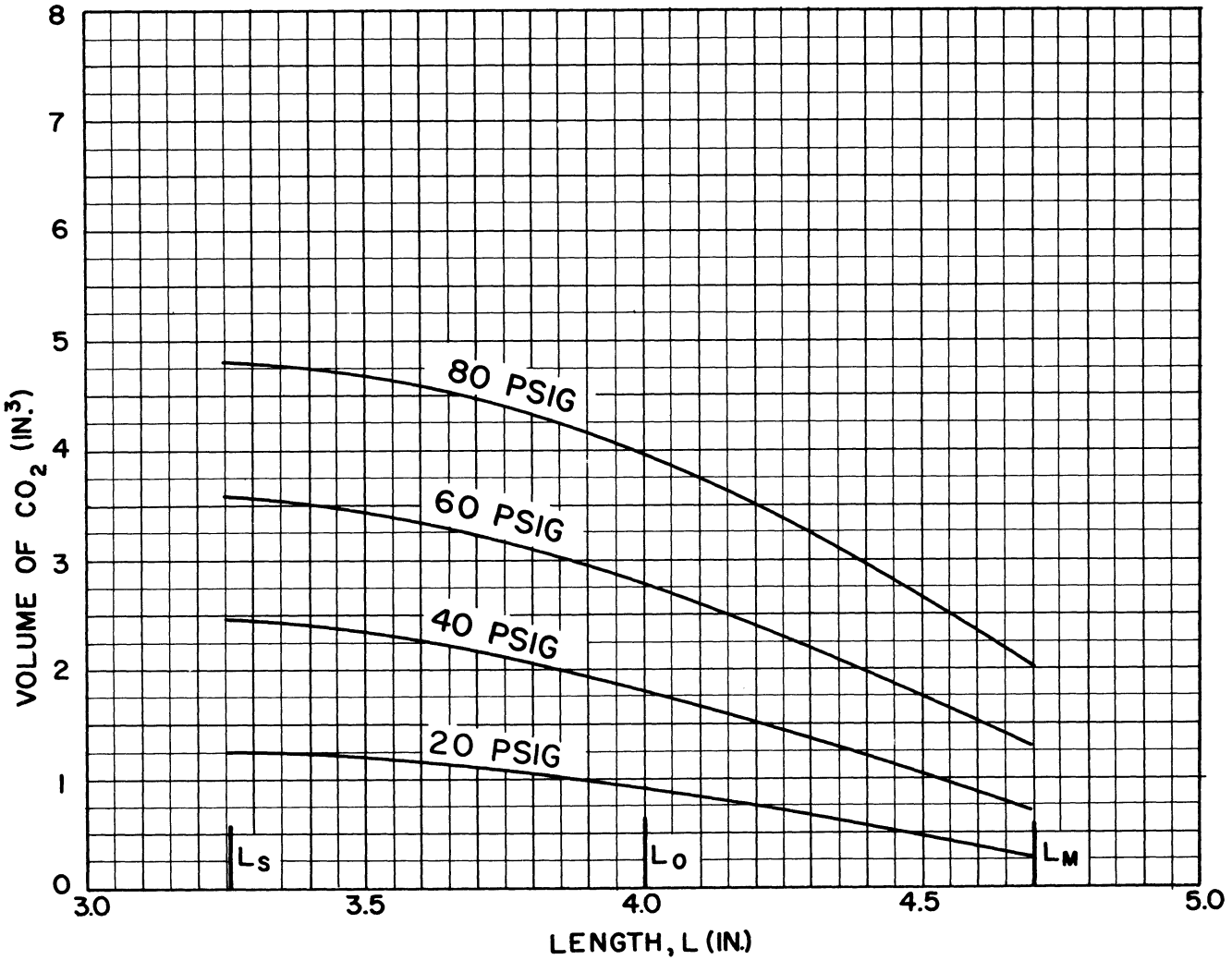

Fig. 49. Gas consumption characteristics on a volume basis as a function of pressure for the W-1 type BFA. Data corrected to standard atmospheric conditions. L_o = 4.00 in., W = .70 in., D_s = .57 in., atmospheric pressure = 14.7 lb/in.^{2}, atmospheric temperature = 77°F.

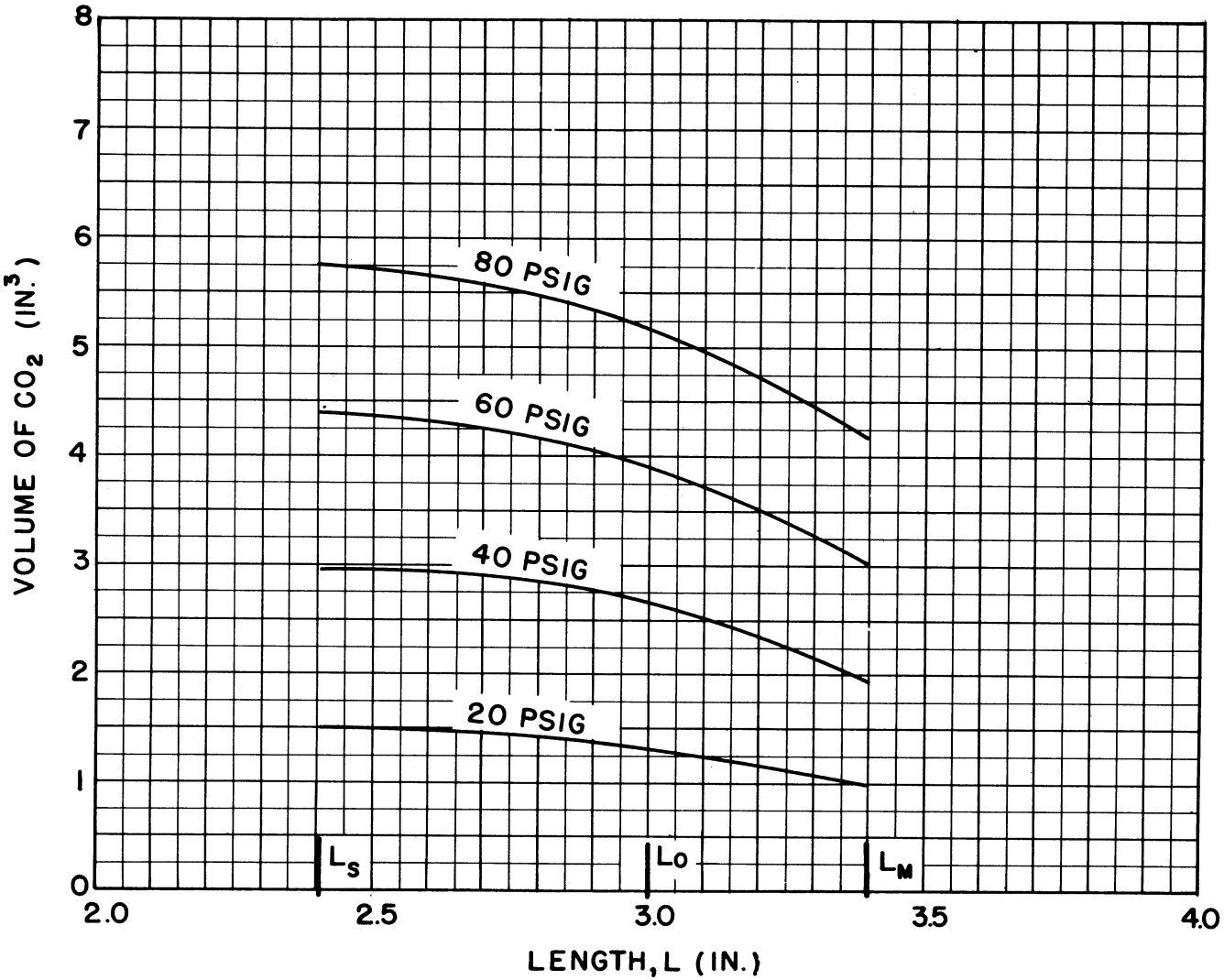

Fig. 50. Gas consumption characteristics on a volume basis as a function of pressure for the W-2 type BFA. Data corrected to standard atmospheric conditions. L_O = 3.00 in., W = .95 in., D_S = .75 in., atmospheric pressure = 14.7 lb/in.^{2}, atmospheric temperature = 77°F.

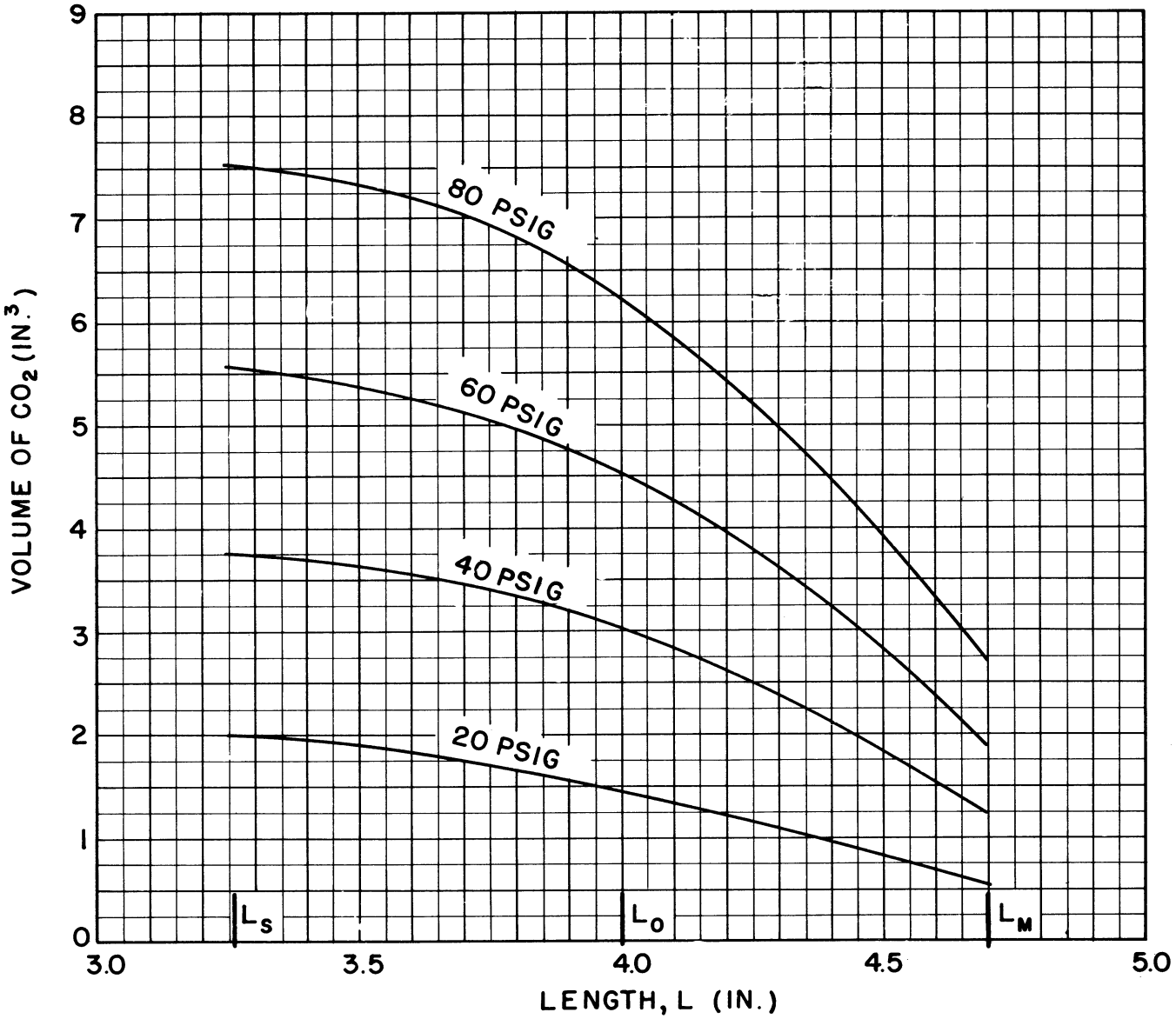

Fig. 51. Gas consumption characteristics on a volume basis as a function of pressure for the W-2 type BFA. Data corrected to standard atmospheric conditions. L_o = 4.00 in., W = .95 in., D_s = .75 in., atmospheric pressure = 14.7 lb/in.^{2}, atmospheric temperature = 77°F.

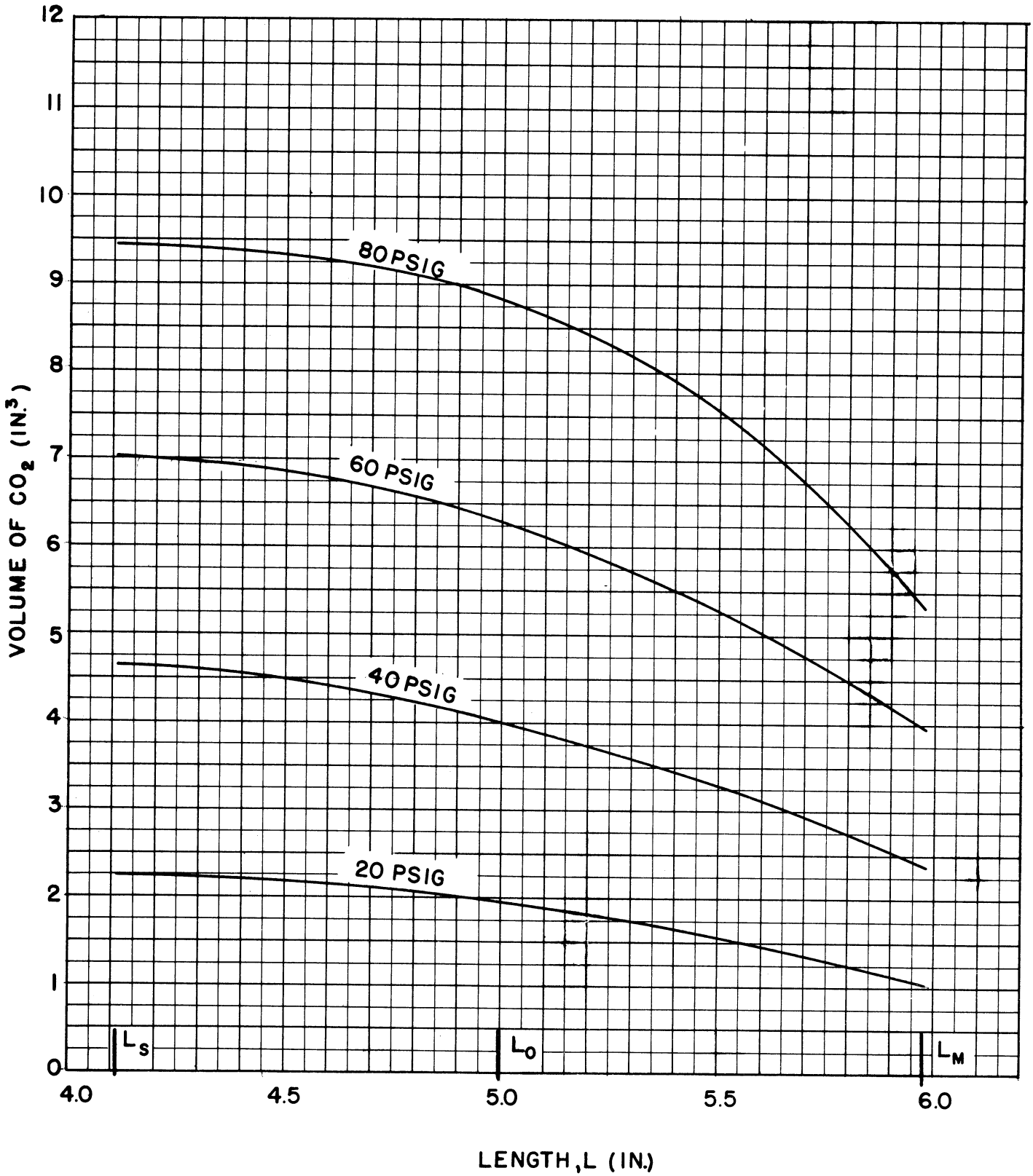

Fig. 52. Gas consumption characteristics on a volume basis as a function of pressure for the W-2 type BFA. Data corrected to standard atmospheric conditions. L_O = 5.00 in., W = .95 in., D_S = .75 in., atomspheric pressure = 14.7 lb/in.^{2}, atmospheric temperature = 77°F.

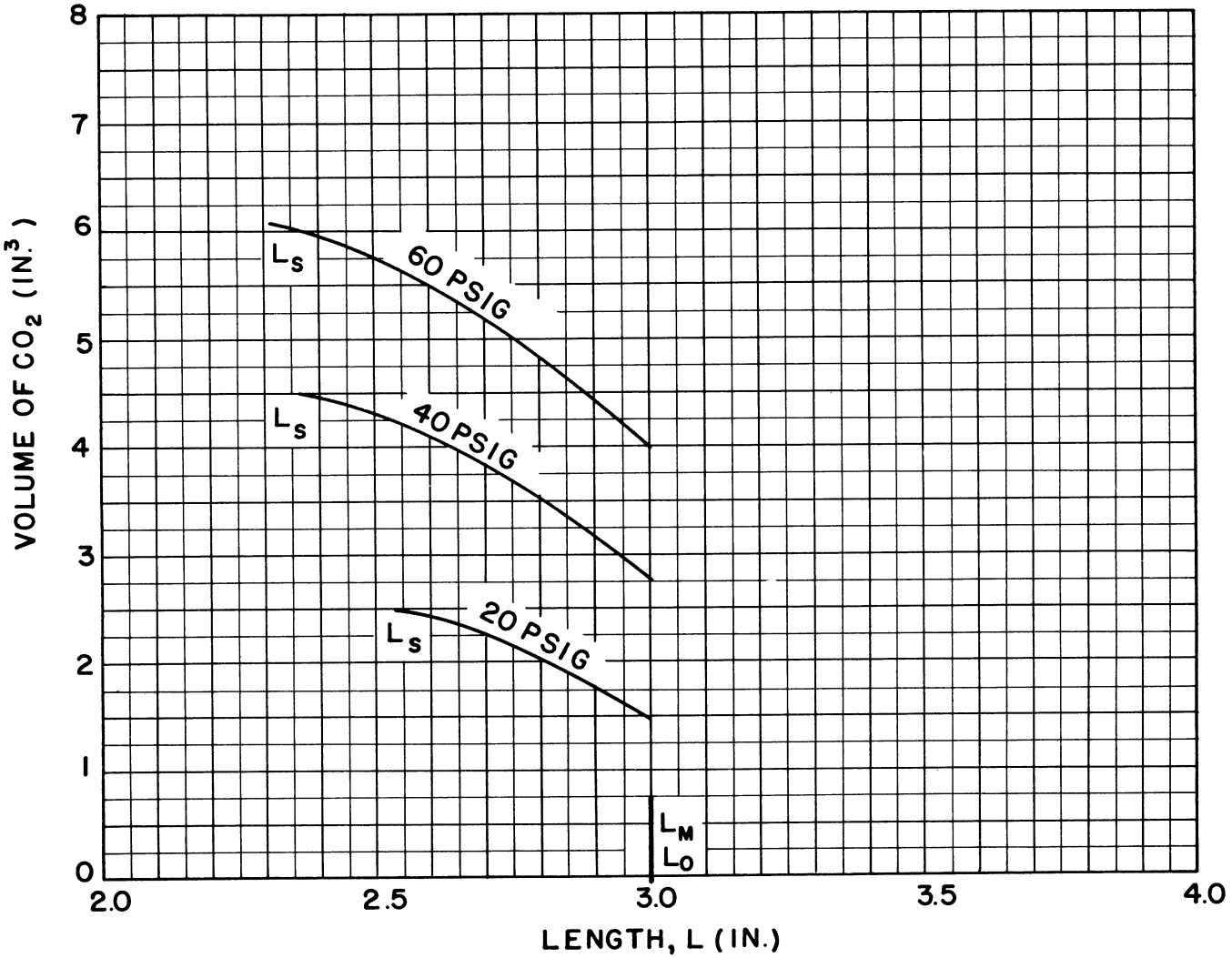

Fig. 53. Gas consumption characteristics on a volume basis as a function of pressure for the W-4 type BFA. Data corrected to standard atmospheric conditions. L_o = 3.00 in., W = .75 in., atmospheric pressure = 14.7 lb/in.^{2}, atmospheric temperature = 77°F.

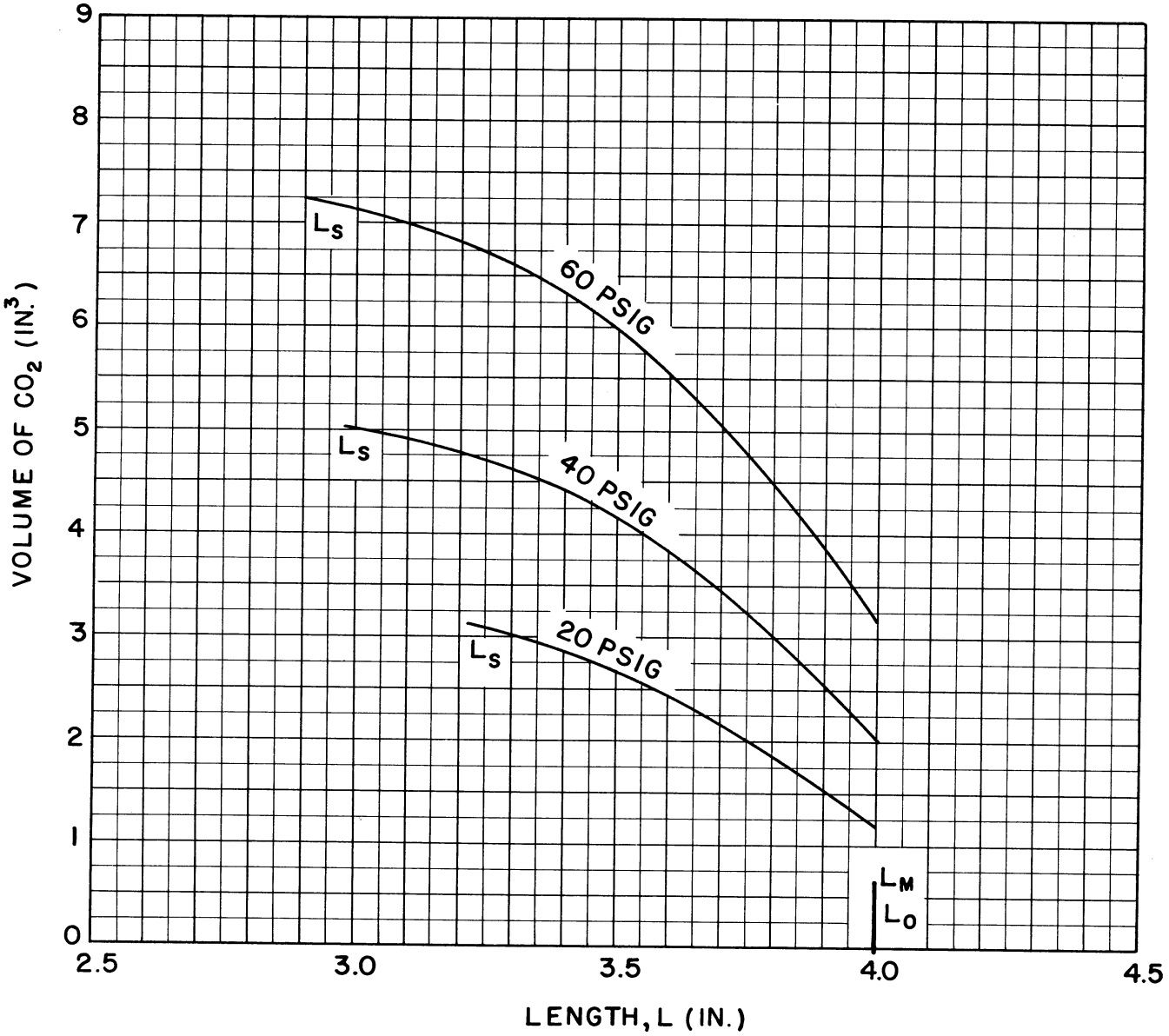

Fig. 54. Gas consumption characteristics on a volume basis as a function of pressure for the W-4 type BFA. Data corrected to standard atmospheric conditions. L_o = 4.00 in., W = .75 in., atmospheric pressure = 14.7 lb/in.^{2}, atmospheric temperature = 77°F.

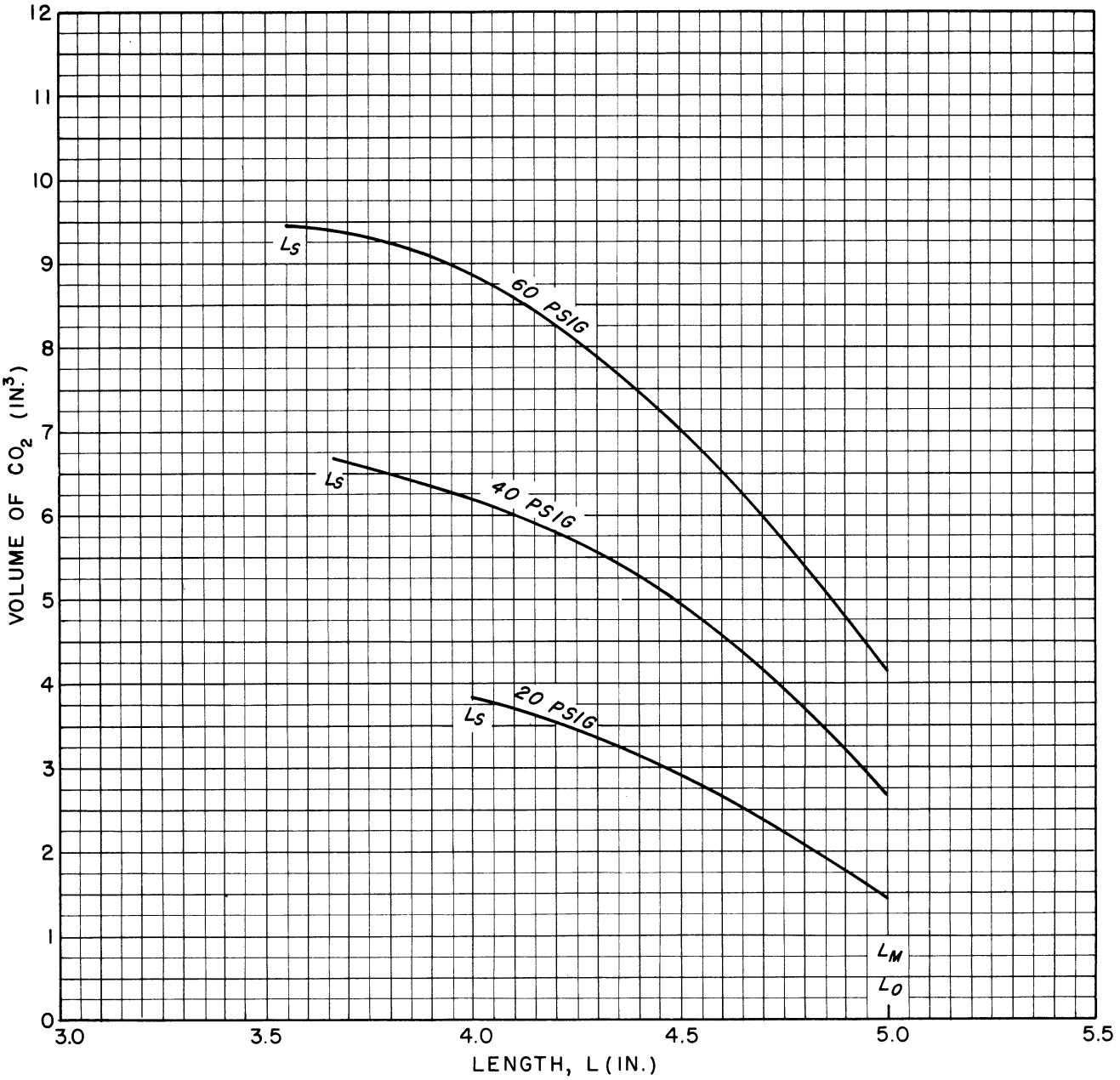

Fig. 55. Gas consumption characteristics on a volume basis as a function of pressure for the W-4 type BFA. Data corrected to standard atmospheric conditions. L_O = 5.00 in., W = .75 in., atmospheric pressure = 14.7 lb/in.^{2}, atmospheric temperature = 77°F.

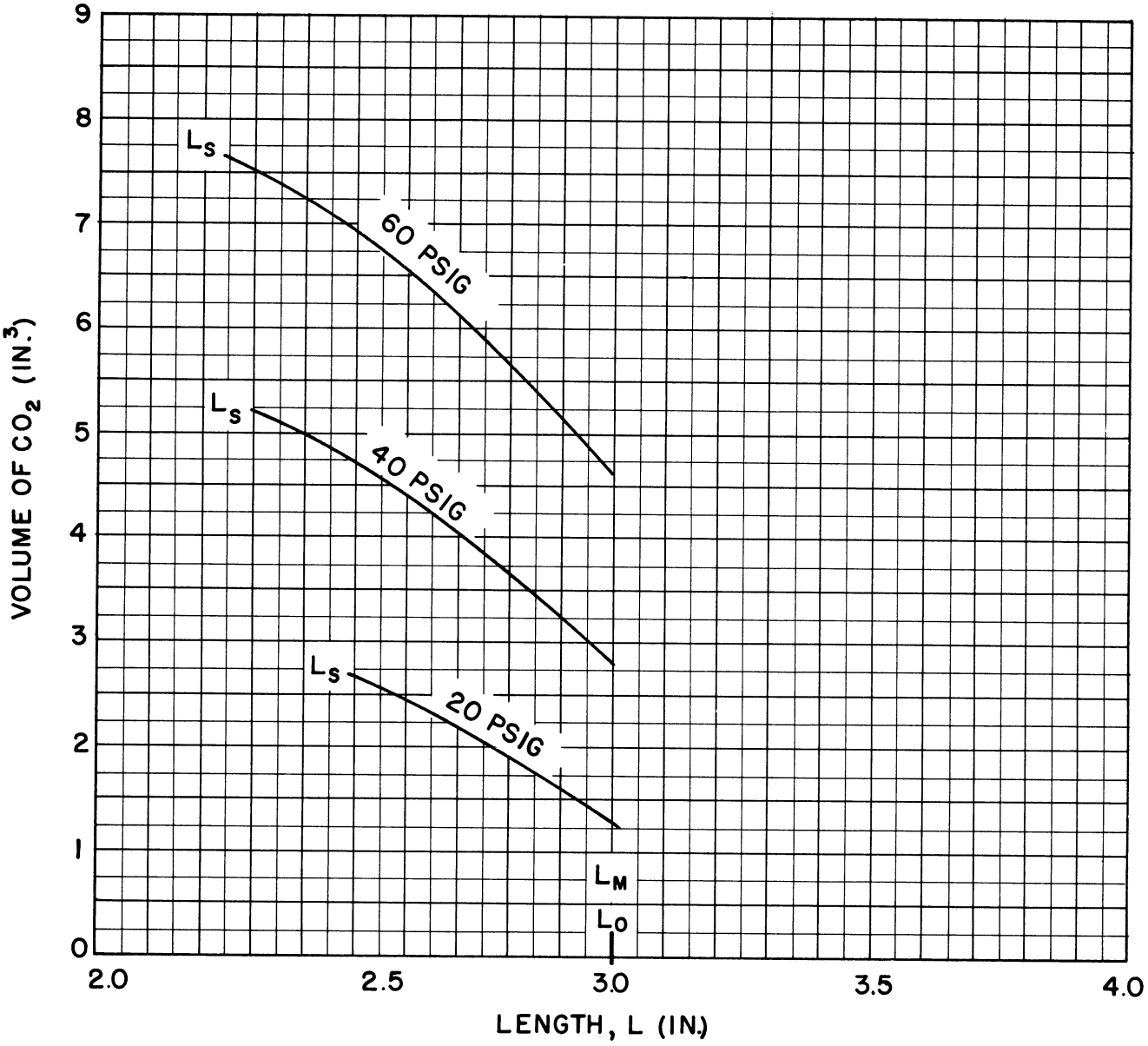

Fig. 56. Gas consumption characteristics on a volume basis as a function of pressure for the W-3I type BFA. Data corrected to standard atmospheric conditions. L_O = 3.00 in., W = .95 in., atmospheric pressure = 14.7 lb/in.^{2}, atmospheric temperature = 77°F.

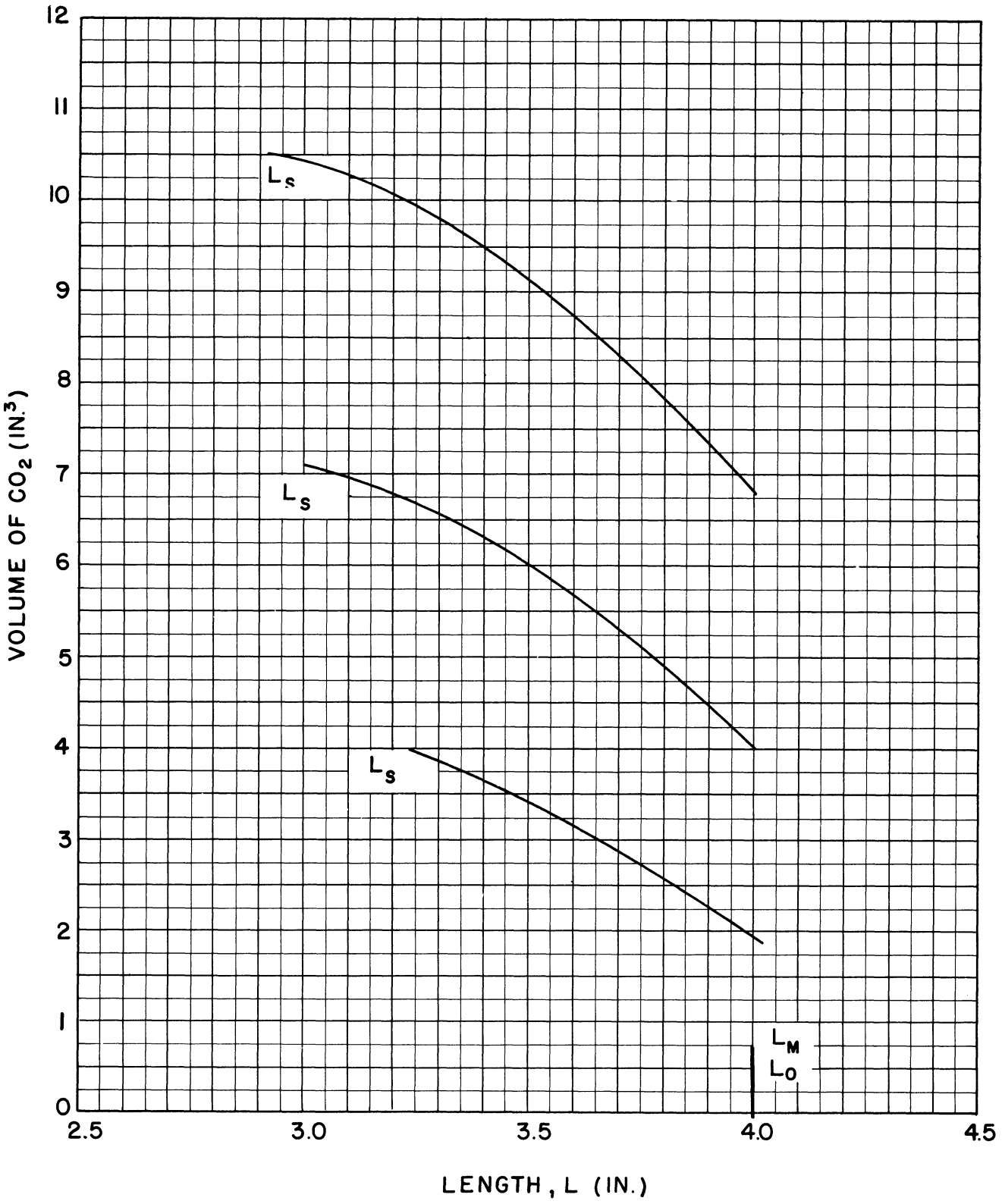

Fig. 57. Gas consumption characteristics on a volume basis as a function of pressure for the W-31 type BFA. Data corrected to standard atmospheric conditions. L_O = 4.00 in., W = .95 in., atomspheric pressure = 14.7 lb/in.^{2}, atmospheric temperature = 77°F.

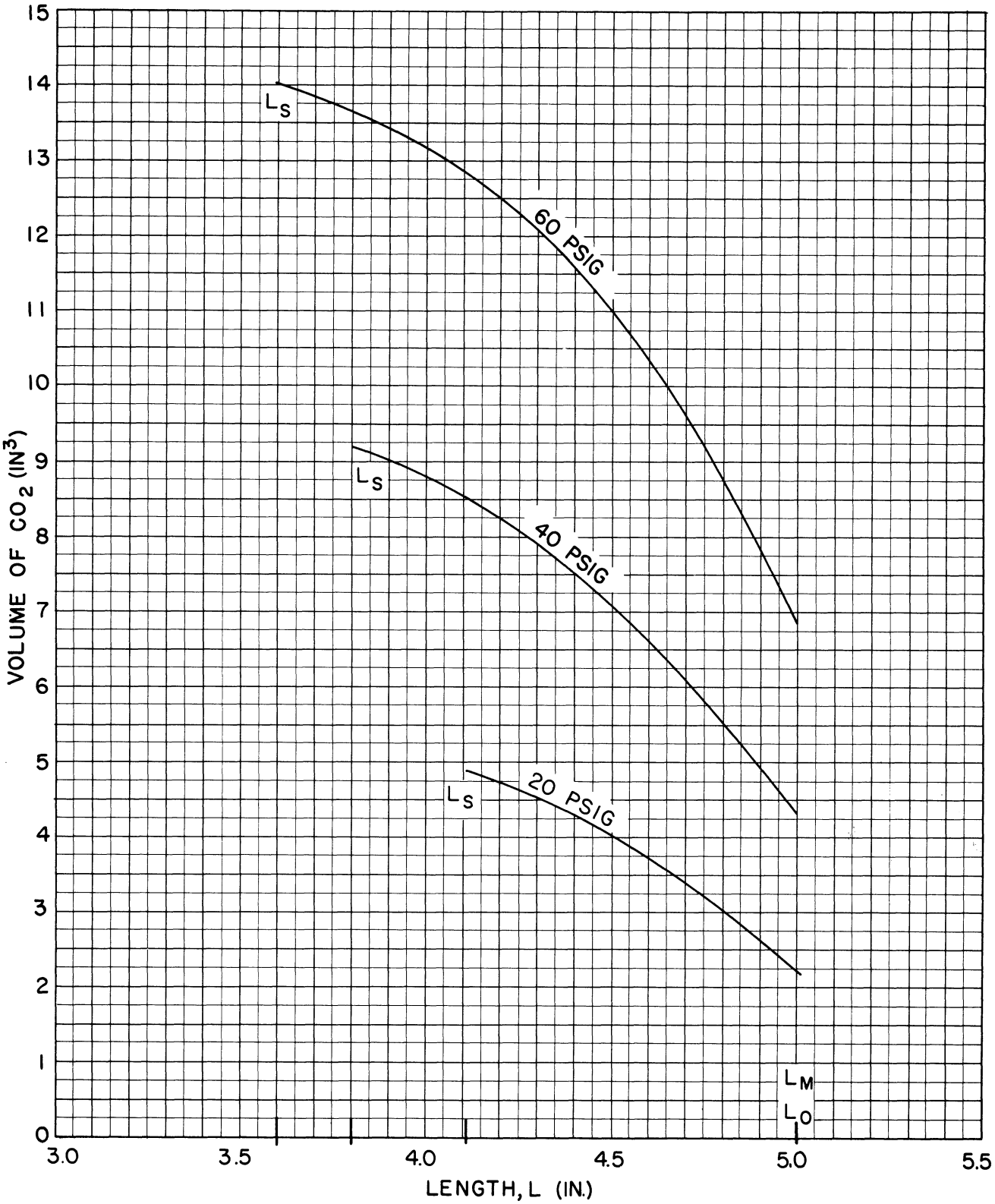

Fig. 58. Gas consumption characteristics on a volume basis as a function of pressure for the W-3I type BFA. Data corrected to standard atmospheric conditions. L_o = 5.00 in., W = .95 in., atmospheric pressure = 14.7 lb/in.^{2}, atmospheric temperature = 77°F.

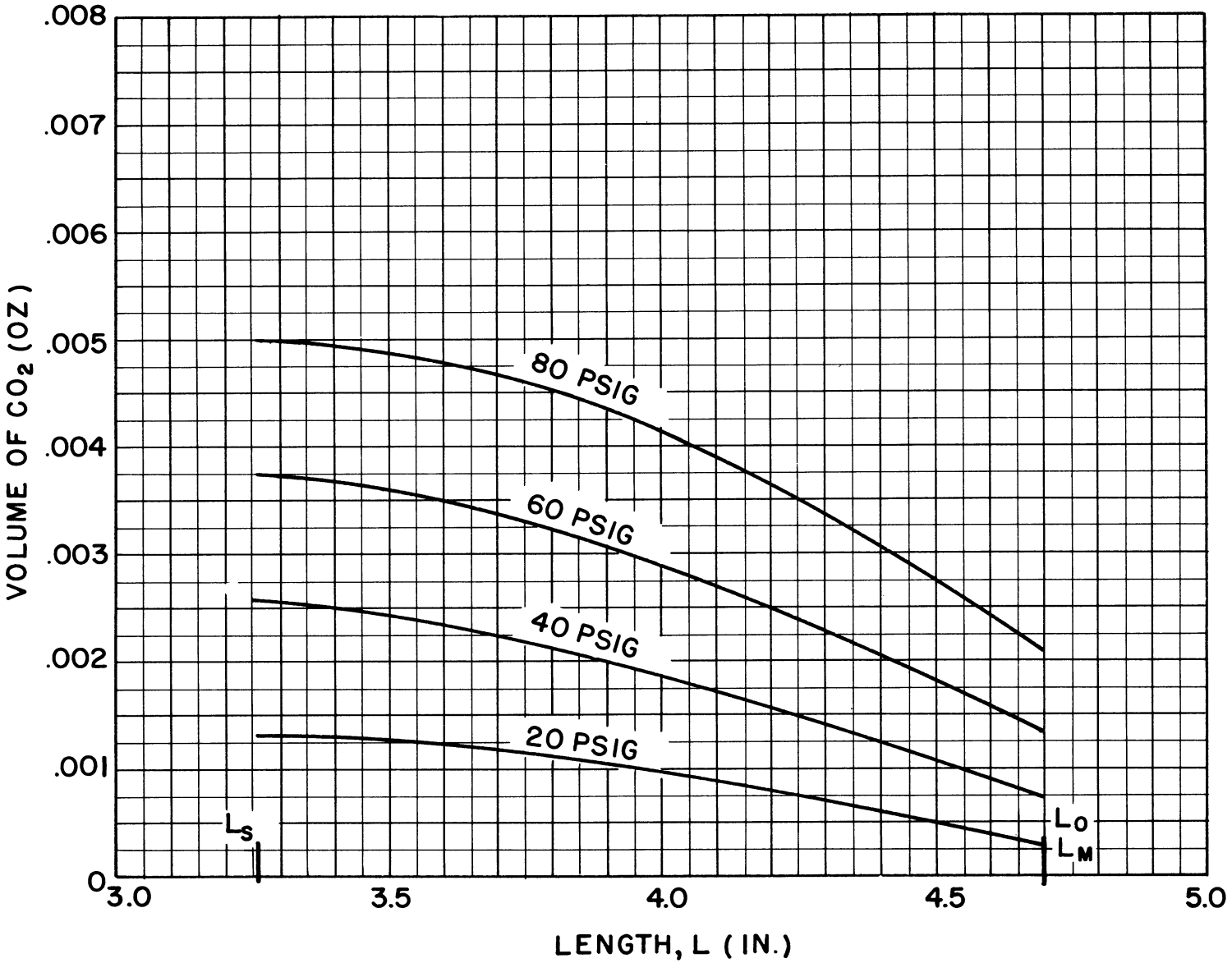

Fig. 59. Gas consumption characteristics on a weight basis as a function of pressure for the W1- type BFA. Data corrected to standard atmospheric conditions. L_o = 4.00 in., W = .70 in., D_s = .58 in., atmospheric pressure = 14.7 lb/in.^{2}, atmospheric temperature = 77°F.

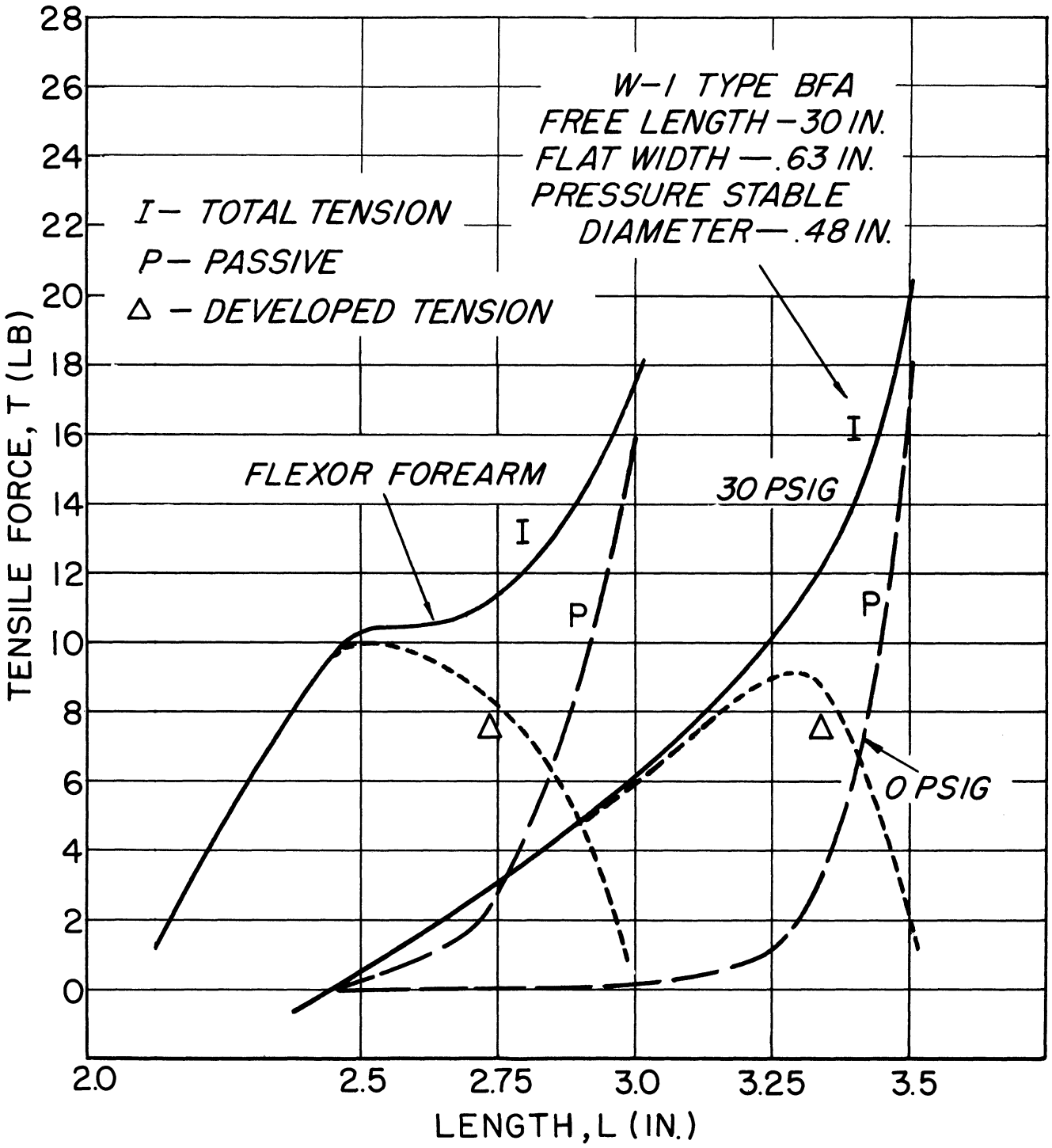

Fig. 60. Comparison between the BFA and flexor muscles of the human forearm.

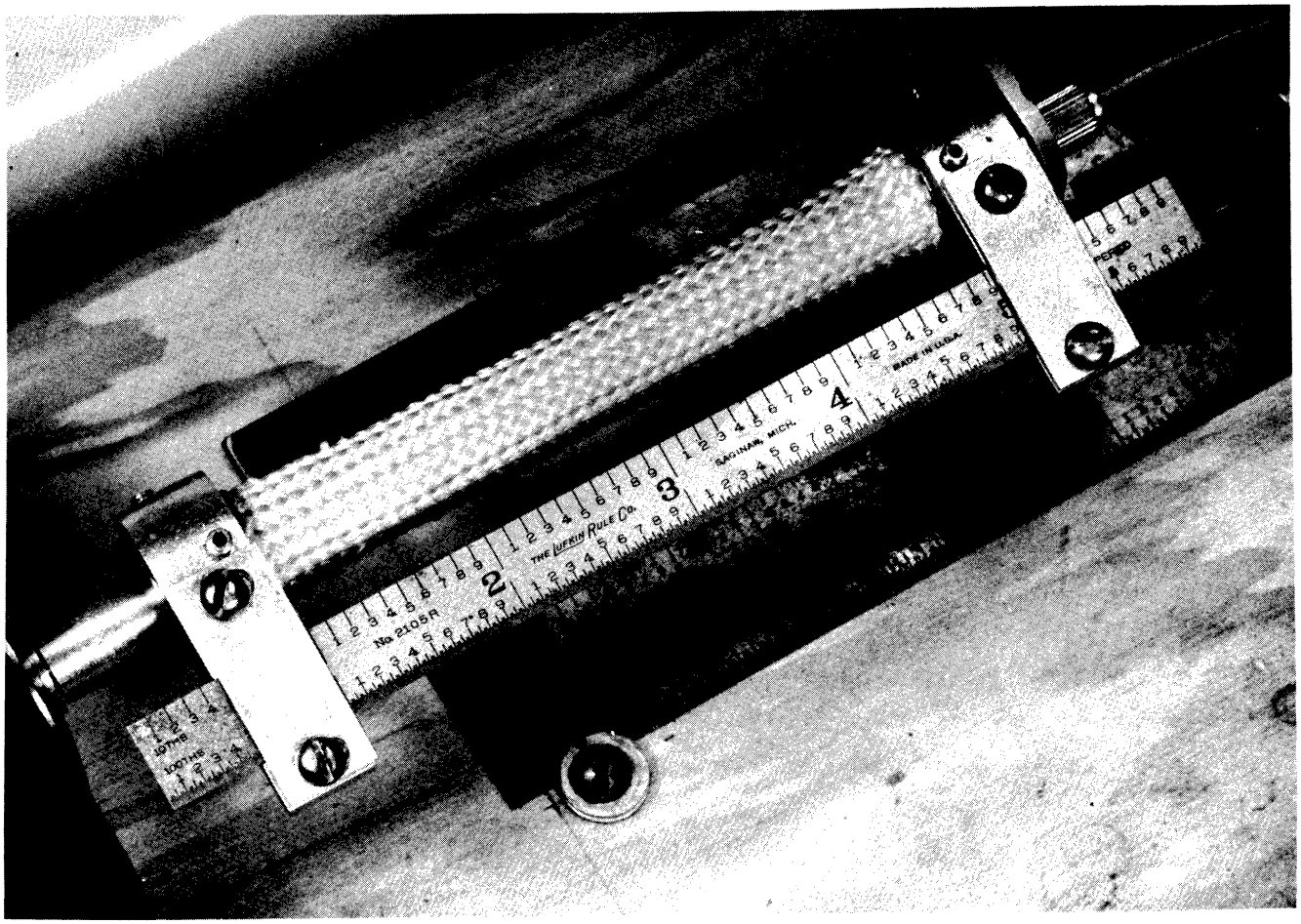

Fig. 61. The W-4 type BFA. Internal pressure at zero psig.

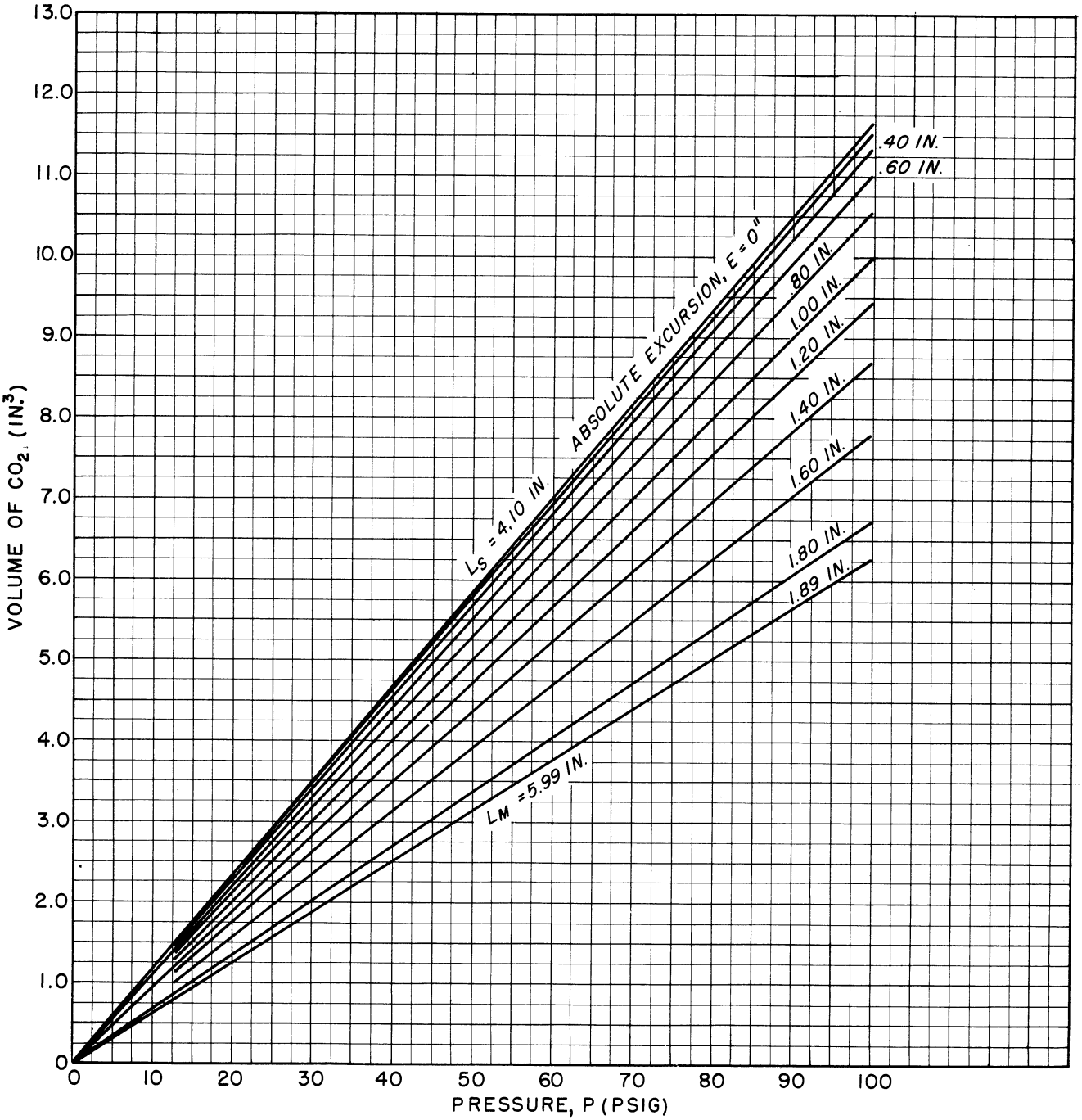

Fig. 62. Gas consumption characteristics on a volume basis as a function of absolute excursion for the W-2 type BFA. Data corrected to standard atmospheric conditions. L_o = 5.00 in., W = .95 in., D_s = .72 in., atmospheric temperature = 70°F, atmospheric pressure = 14.7 lb/in.^{2}.

VI. EVALUATION OF THE EXPERIMENTAL DATA

A. ANALYTICAL ANALYSIS

In view of the similarities between the W-1 and W-2 type actuators, a single empirical relationship between length, pressure, and diameter was investigated using correlation analysis* and normalization** of the experimental data. It was hoped that an equation could be developed which would describe the characteristics of an actuator of any length and diameter for these two types of weave.

The study disclosed that no apparent relationship exists between the different weave types or between the characteristics at different pressures for a given weave type. However, if the normalized curves are averaged and a curve which has values 10% less than this average is plotted (on the basis that overpowering an orthetic device is allowable), two separate relationships can be forced for the W-1 actuators: one covering a range of pressure from 20 to 50 psig, the other, from 50 to 90 psig regardless of free length. In this manner it is possible to express the output of the W-1 actuators by two empirical normalized equations. The same statement holds for the W-2 actuator when considered separately.

Correlation analysis indicates that the equations for the above described curves are of the general form $ax^3 + bx^2 + cx = 0$, where a, b, and c are coefficients which vary with pressure. The coefficient of correlation for this type of equation ranges from .99 at 90 psig to .90 at 20 psig. With curves of this type the process of normalization could be applied in reverse to develop curves similar to those presented in Figs. 13—58. Data from Fig. 10 (which was developed using correlation analysis) could be used to obtain the necessary parameters to denormalize the curves and obtain the characteristics for lengths other than those tested.

In view of the time required to apply the above procedure and the rapid development of the BFA, the above approach was discontinued in favor of obtaining and graphically analyzing data on the W-3, W-4, and W-3I type actuators.

---

*A statistical tool for finding and measuring the relationship between two or more variables.

**A process by which specific variables can be eliminated from analytic equations by dividing the equation by that variable. In graphical analysis this amounts to converting the experimental data to a dimensionless basis by dividing each point on a curve by the variable which is to be eliminated. If two curves are related (i.e., belong to the same family), they will appear as a single curve when both are normalized. In this study the curves were normalized in terms of both the length and force output.

B. GRAPHICAL ANALYSIS

1. Effect of the number of Pics per inch.—As the number of pics per inch decrease for a given strand thickness, the tightness of weave decreases, causing the frictional and binding losses in the braided sheath to decrease, thus increasing the force output. This is shown in Fig. 63 which is a comparison of the four types of actuators represented in Figs. 13—58. The number of pics per inch is a function of both the weave tightness and the free length helix angle as can be seen from the geometry of the braided sheath.

2. Effect of strand thickness.—The geometry of the actuator indicates that its excursion is limited by the thickness of the strands for a given number of pics per inch (i.e., for strands which will not compress and for a given number of pics per inch, as the thickness of the strands increase the pressure stable helix angle (θ_s) increases while the helix angle at the maximum working length of the actuator (θ_m) decreases). This means that the total excursion decreases.

3. Effect of strand compressibility.—The yarn type of fiber is more compressible than the twisted type. The effect of this factor can tend to nullify that of strand thickness. Thus it is possible for two weaves of the same tightness and pics per inch to give different excursions if one is composed of yarn and the other of twisted strands.

4. Effect of flat width (W).—The flat width is a measure of the free-length cross-sectional area of the actuator. The greater the flat width, the greater the force output. This effect is readily seen in Fig. 63 for the W-1 and W-2 types of actuator. No attempt has been made to establish a usable graphical or analytical relationship between actuators of various diameters.

5. Effect of free-length helix angle (θ_o).—The theoretical derivation of the force output (see Appendix B) has shown that for an ideal actuator the maximum working length (L_m) approaches a maximum value as the helix angle approaches zero degrees and the pressure stable length (L_s) approaches a minimum value as θ approaches 54°44'. In practice these limits cannot be achieved due to the finite thickness of the strands. Thus it is apparent that L_m and L_s and therefore θ_m and θ_s are functions of the thickness of the strands and the number of pics per inch.

By varying the free-length helix angle (θ_o) from θ_s to θ_m (i.e., from 54°44' to 0°) the zero-pressure curve can be positioned to intersect the zero tensile force axis at any length from L_s to L_m. An actuator with θ_o close to zero degrees will have a shorter excursion from L_m to L_o than from L_o to L_s. Conversely, an actuator with θ_o close to 54°44' will have shorter excursion from L_o to L_s than from L_m to L_o. These points are illustrated in Fig. 64 where it is seen that the loose-weave W-3 actuator with a free-length helix angle of 25° has an excursion from L_m to L_o of only .17 in. as opposed to the

.37 in. of the W-2 actuator with a free-length helix angle of 40°. On the other hand, the W-2 actuator has an excursion of only .58 in. from L_o to L_s as opposed to the .93 in. of the W-3 actuator. This comparison is made on a relative basis since only two different weave types are compared. Study of Fig. 63 tends to corroborate statements made concerning the pics per inch, strand thickness, and strand compressibility.

Shifting of the zero-pressure force curve along the zero force axis due to a change in θ_o will affect the total force curve since it is the sum of the developed force due to the internal pressure acting on the actuator and the zero pressure curve. The effect is shown in Fig. 65. Note that the zero-pressure curves all yield approximately the same force output at the maximum working length (L_m), because the zero-pressure curve is the sum of two forces, the elasticity of the rubber inner tube and binding of the strands. Near the free length (L_o) the elasticity of the inner tube is the prime component, while at (L_m) binding of the strands is the primary component.

6. Effect of thickness of the elastic inner tube.—On the basis of the preceding discussion, increasing the thickness of the rubber inner tube will increase the over-all magnitude of the zero-pressure curve and thus the total force curve. In practice, this effect is generally negligible for small increases in thickness. The effect is shown in Fig. 66.

7. Effect of free length (L_o).—For an actuator of the same free-length helix angle (θ_o) and free-length diameter (D_o), increasing the length increases the absolute excursion but not the force output. This is illustrated in Fig. 67 which shows a linear relationship between increases in excursion for a constant-force output. Prediction of the total force curves for the 3.5-, 4.5-, 5.5-, 6-, 6.5-, and 7-in. free lengths was possible using Fig. 11 and the linear relationships established between the experimentally tested lengths of 3, 4, and 5 in.

No attempt was made to establish a similar relationship for the W-4 and W-3I actuators; however, there is no reason to expect that such a relationship does not exist.

Figure 65 appears to contradict the above statements since changes in θ_o will change L_o as shown. In this case the change is due purely to geometry of the braided sheath since the same absolute excursion can be maintained by keeping the straight length L_h of the strands the same as θ_o is changed.

8. Effect of repeated use.—Life tests have been conducted by continuously cycling the various actuators to 50 psig under the action of a 25-lb dead weight. Results indicate that the W-1, W-2, and W-4 actuators have a useful life in excess of 100,000 cycles. The useful life of the W-3I actuator, however, is only between 6,000 and 10,000 cycles. Failure of this actuator

occurred due to separation of the impregnated braided sheath and the metal end elements.*

Although the W-1, W-2, and W-4 actuators have essentially the same useful life, the yarn-type strands used in the W-4 actuator have proven less durable than the twisted type of the W-1 and W-2 actuators. This type of strand tends to form small loops of nylon fibers along its length, giving the actuator a fuzzy appearance after approximately 1,000 to 2,000 cycles of operation. From the viewpoint of orthetic applications this fact, although minor, would be somewhat detrimental both to durability of the device and its cosmetic appearance. This effect was not observed in the twisted strands regardless of the number of cycles of operation.

Repeated cycling also decreases the force output of the various type actuators. Figure 68 shows this effect for a W-1 actuator. The decrease in force shown is typical for the other actuators excluding the W-3I type. The solid curve was obtained during the first 1,000 cycles of operation and the dashed curve from 2,000 to 3,000 cycles of operation. This effect is attributed to cold flow of the nylon under heavy loads which in this case occurred intermittently as the actuator was cycled. The phenomenon of creep (lengthening due to cold flow) is illustrated in Fig. 69 which was obtained by loading a W-1, .65-in.-flat-width, 5-in.-long actuator to a load of 60 lb at zero internal pressure, locking its ends in position and observing the decrease in force as a function of time.

9. Effect of ambient temperature.—Environmental tests have indicated that the force output of the actuators decrease as the temperature increases. Figure 70 shows this effect as the temperature is changed from 70°F to 90°F. The effect is attributed to the change in elasticity of nylon with temperature. No attempt was made to control humidity during the test.

10. Accuracy of the data.—The standard error of estimate[8] of the graphical data in this report is typically less than ± 10% of the indicated value. This increases somewhat in the case of the force-versus-excursion curves when the BFA approaches its fully contracted state because plotting and instrument reading errors become proportionately greater as the force output approaches zero. Studies were not conducted to determine what standard deviation from the curves should be expected if a number of similar BFA's are compared. It would probably be safe to assume, however, that most BFA's would fall within ± 15% of the indicated values.

*These tests were conducted at the Rancho Los Amigos Hospital in Downey, California.

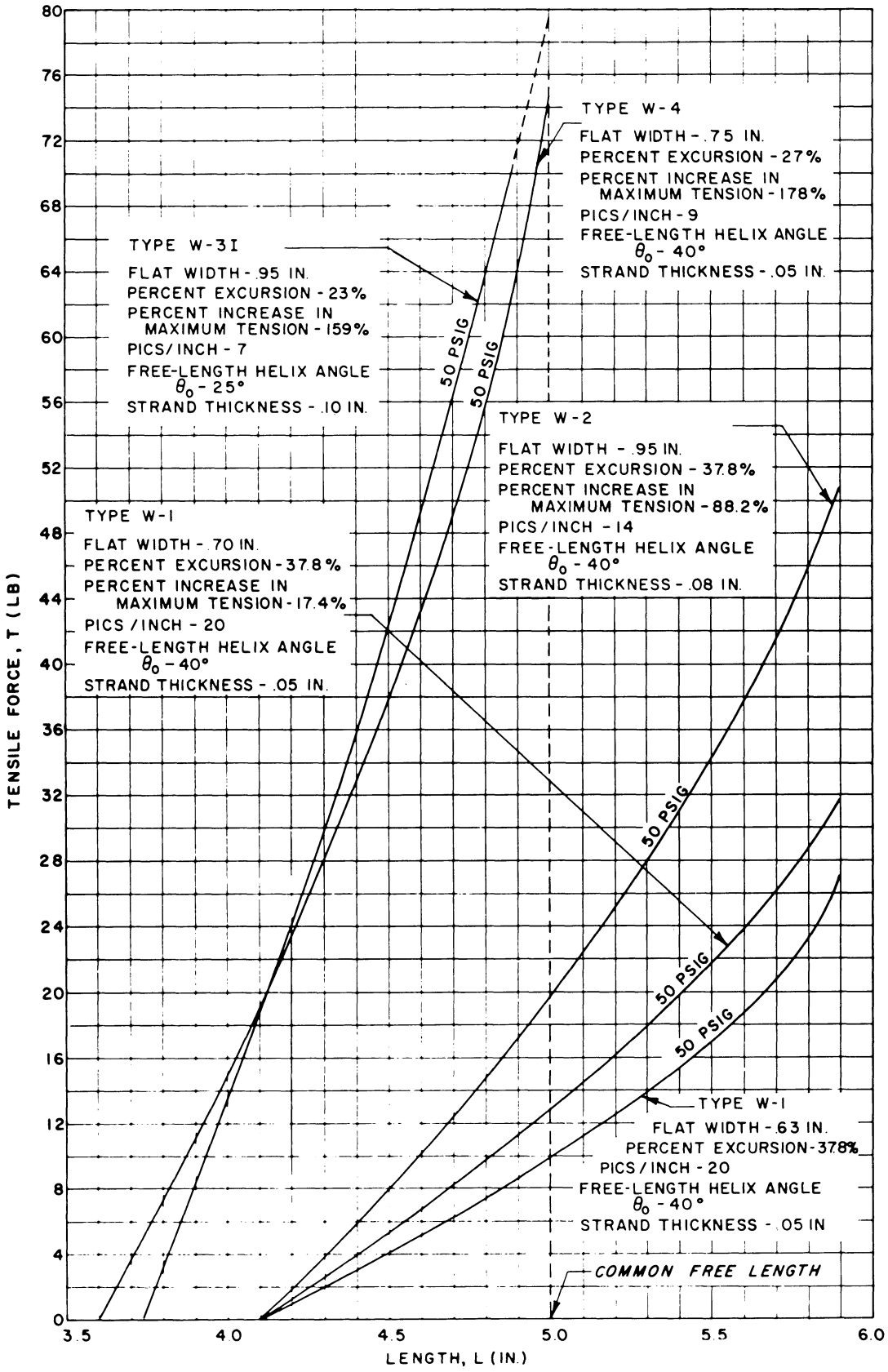

Fig. 63. Comparison of the various type actuators for a common free length and pressure. Note: 1. Percent excursion based on free length. 2. Percent increase in maximum tension based on maximum excursion of the W-1, .63 flat width BFA.

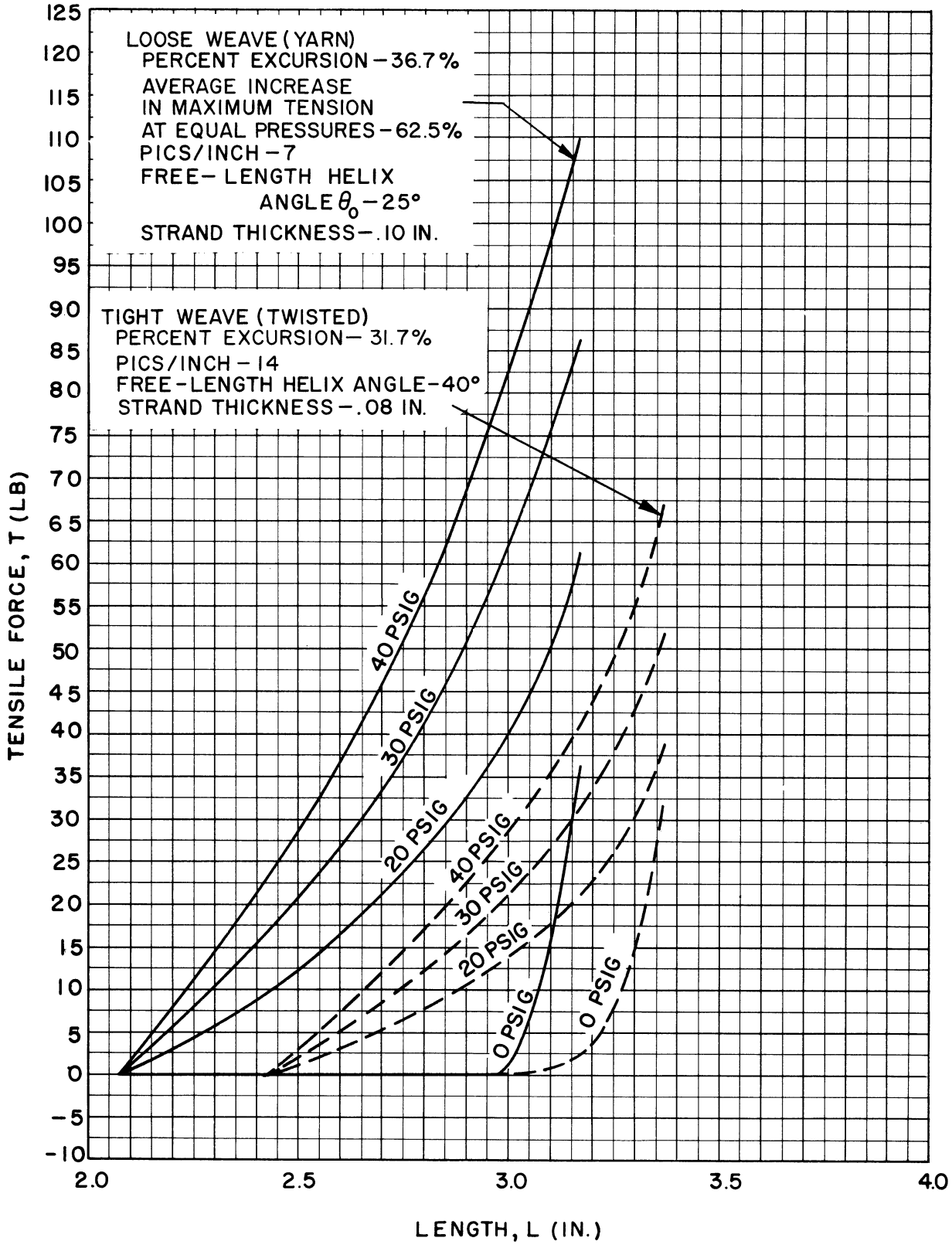

Fig. 64. Effect of strand thickness and free length helix angle on the isometric tensile force—length characteristics of the BFA. Common free length = 3.0 in., common flat width = 1.2 in. Pressure stable diameters: tight weave = 1.0 in., loose weave = 1.7 in. Weave types: tight weave = W-2, loose weave = W-3.

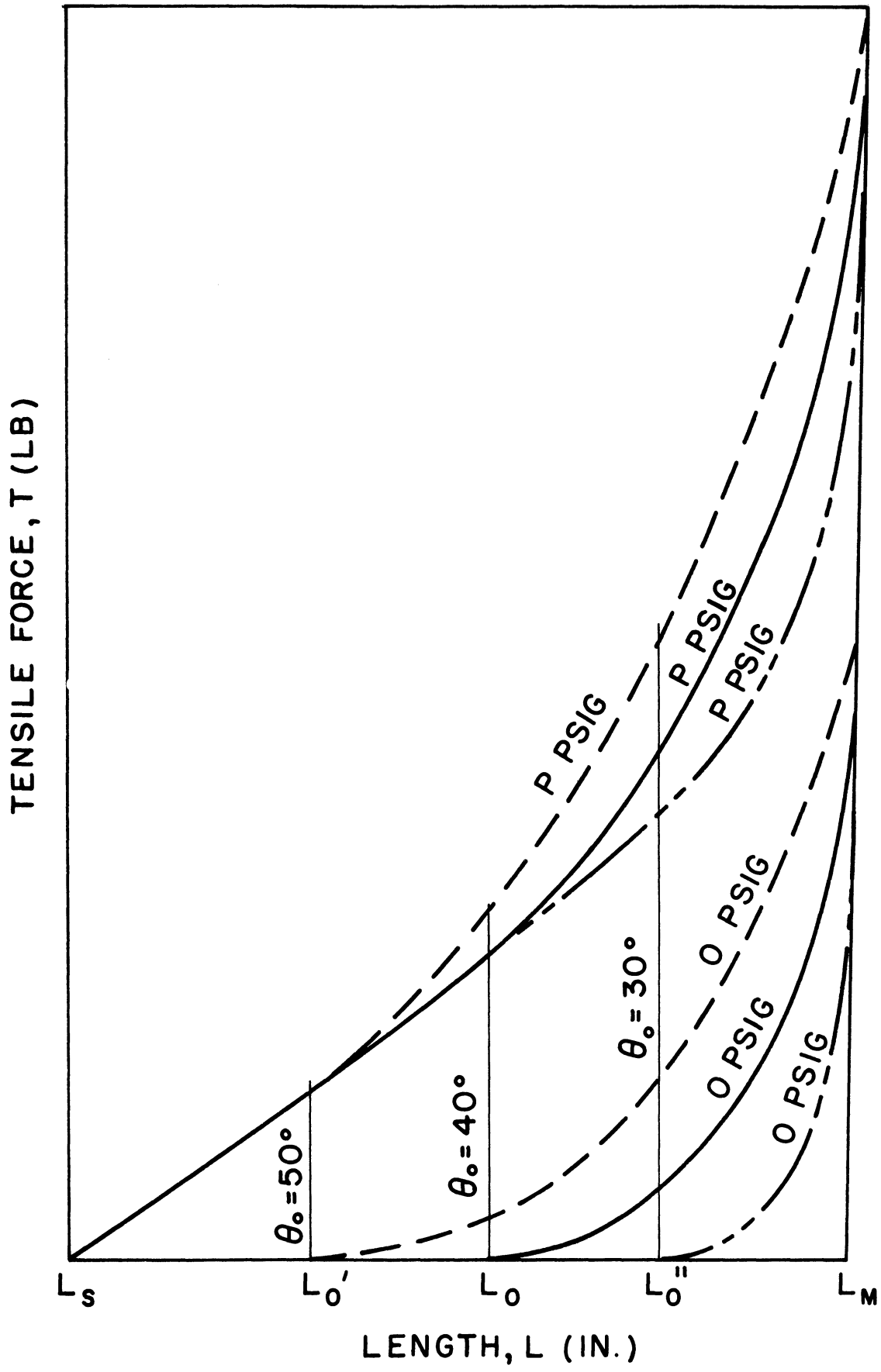

Fig. 65. Effect of changing the free length helix angle on the total force output of the BFA. Diagram not to scale.

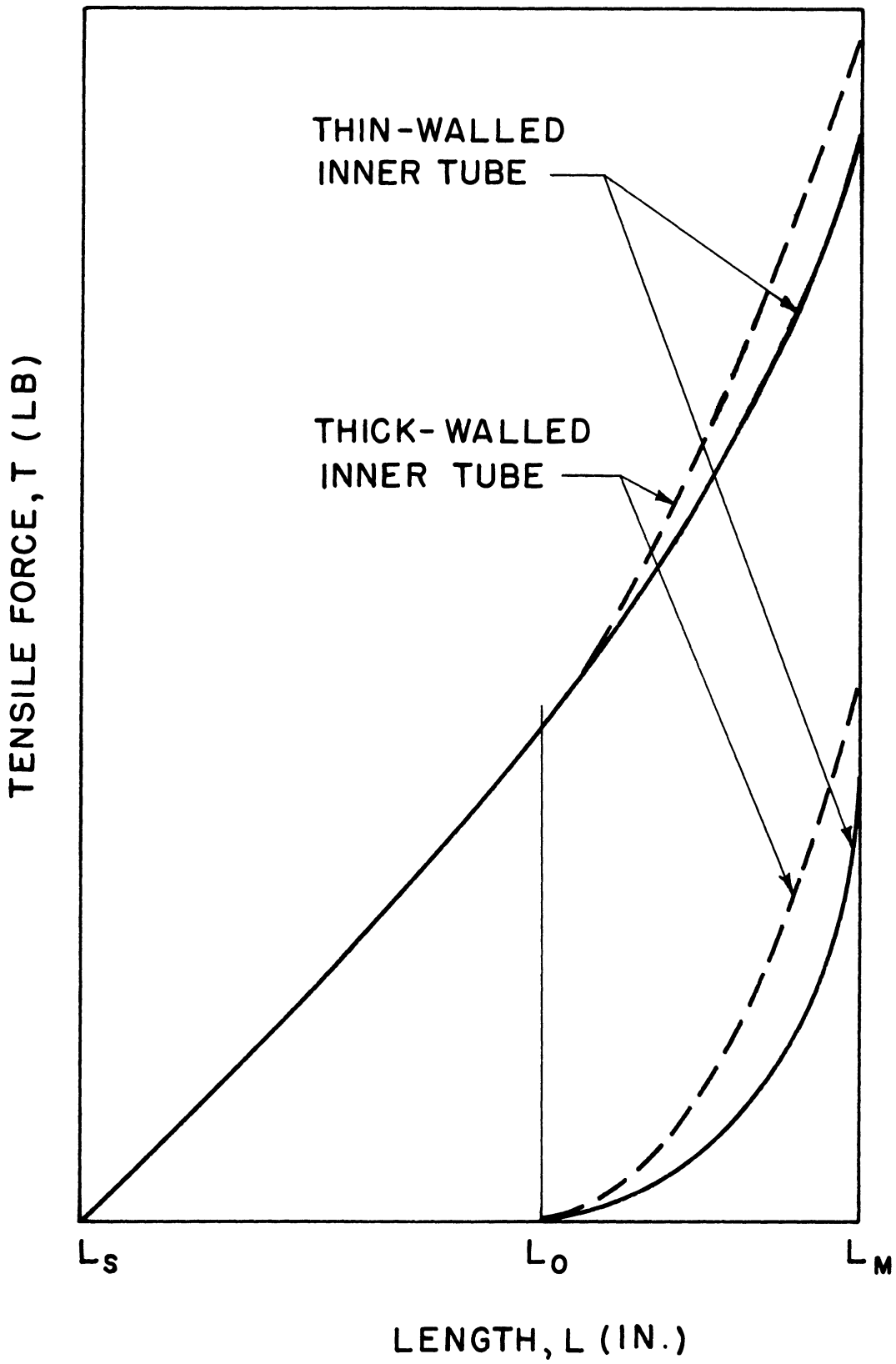

Fig. 66. Effect of increasing the wall thickness of the elastic inner tube on the total force output. Diagram not to scale.

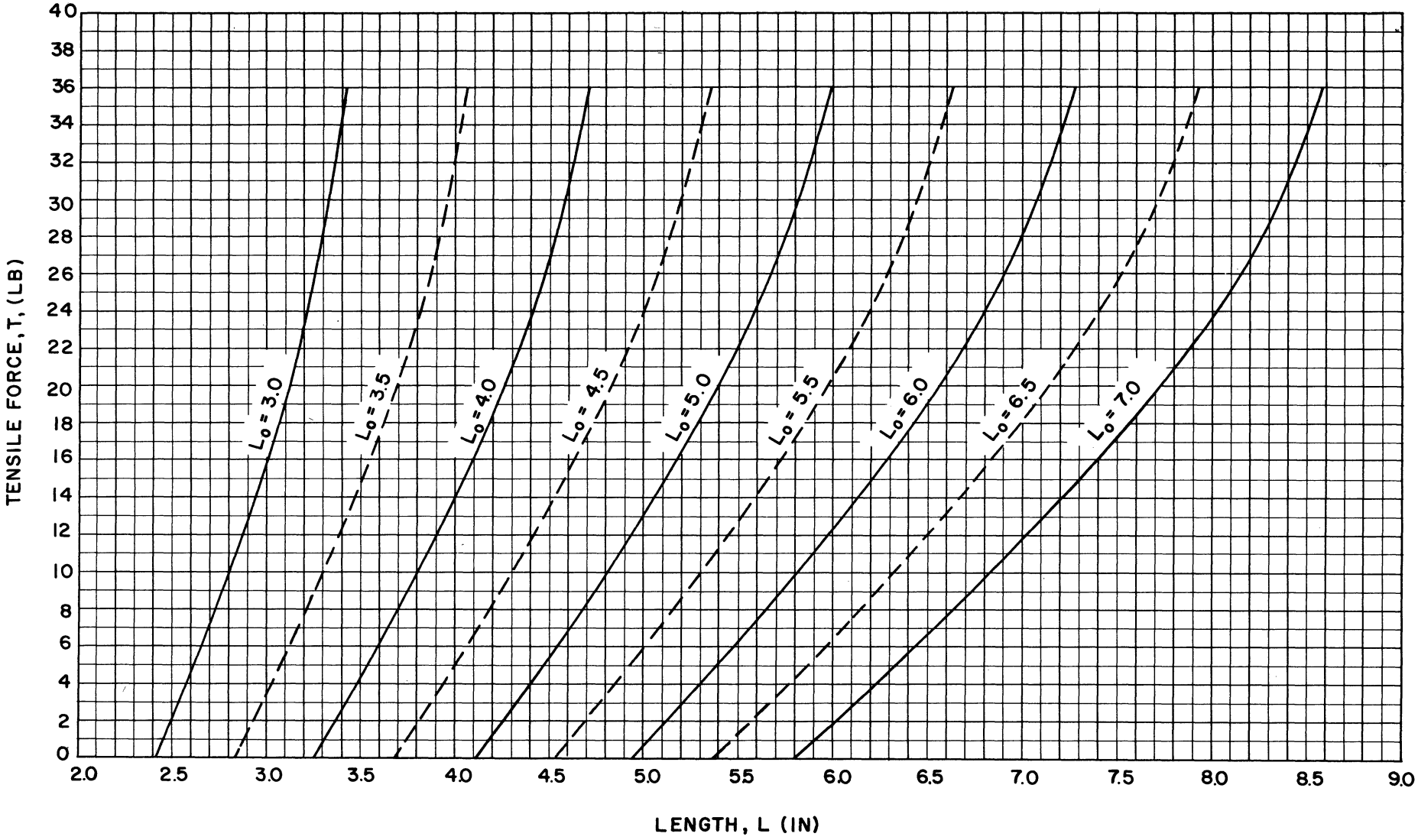

Fig. 67. Effect of increasing the free length of the W-1 type BFA at constant internal pressure: W = .70 in., P = 50 psig.

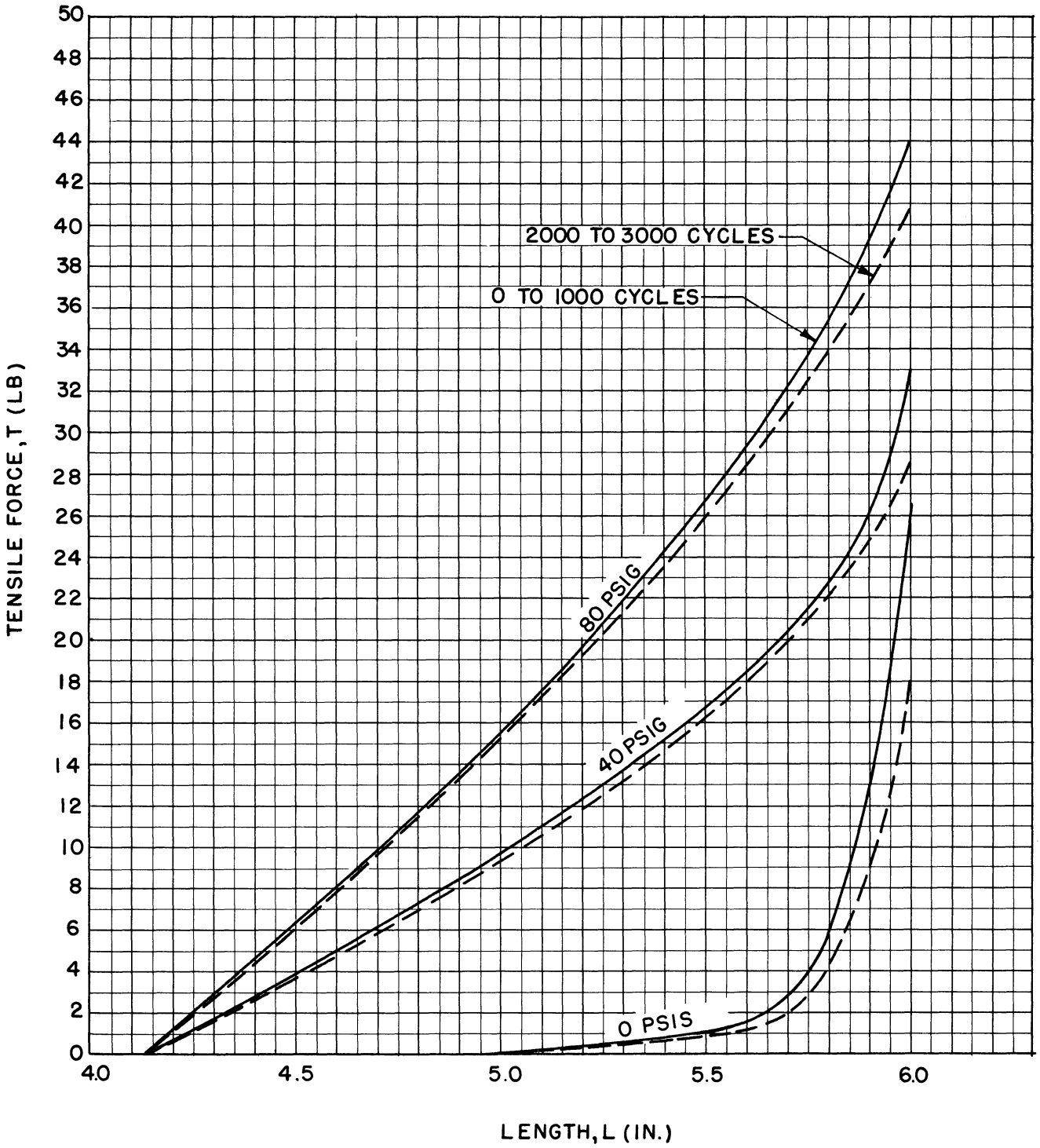

Fig. 68. Effect of repeated use on the isometric tensile force—length characteristics of the W-1 type BFA: L_o = 5.00 in., W = .63 in., D_s = .50 in.

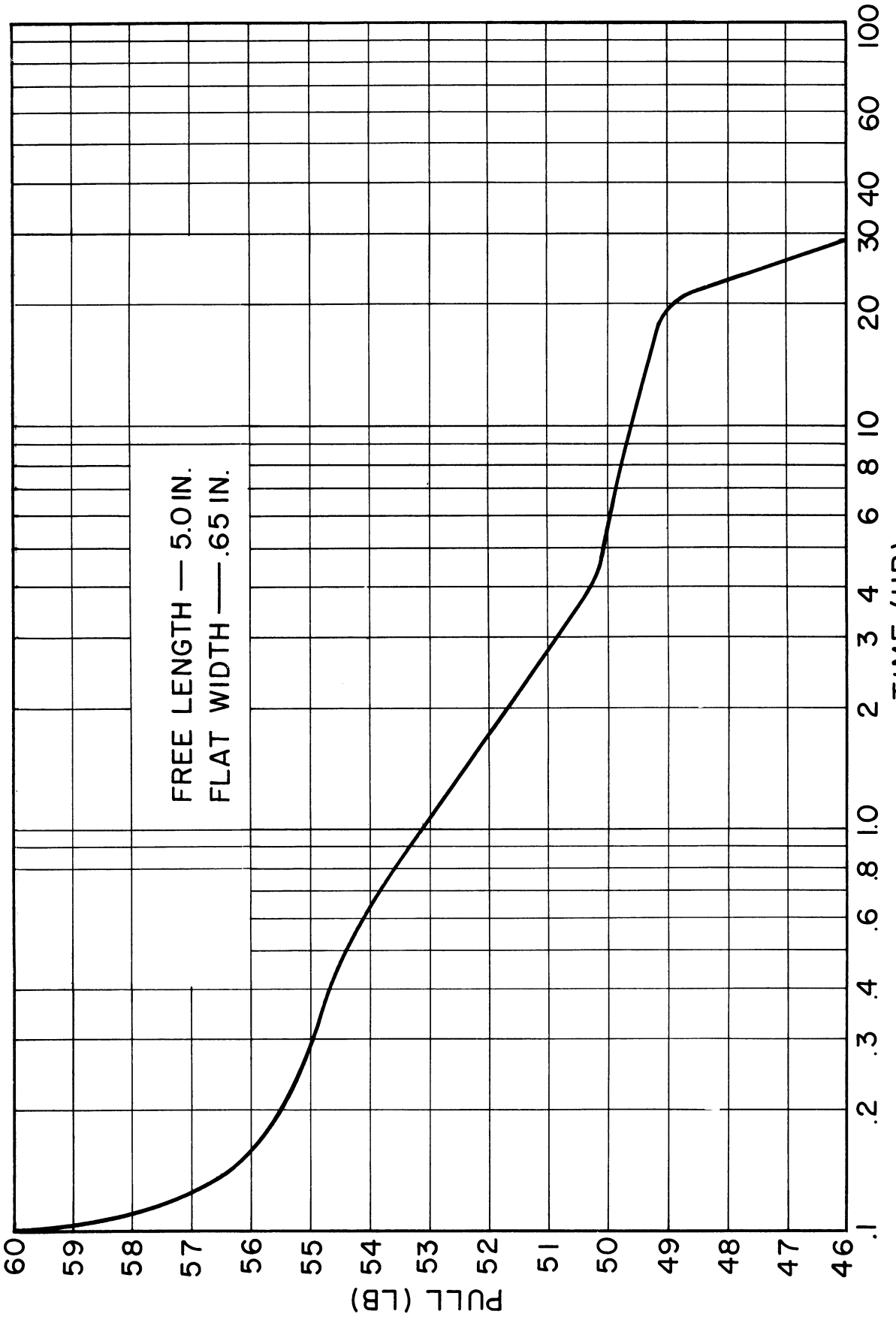

Fig. 69. Zero-pressure creep characteristics of the BFA.

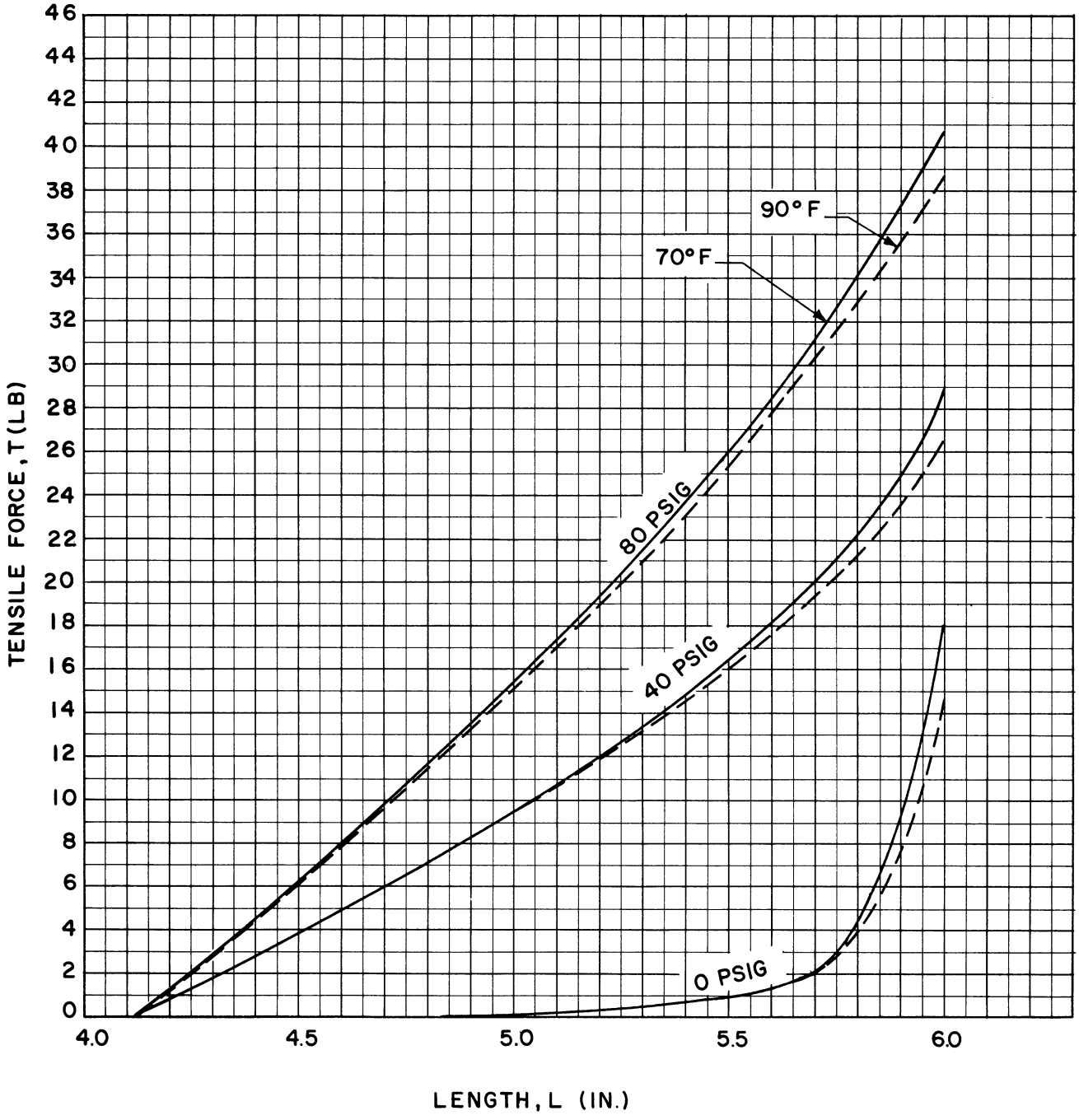

Fig. 70. Effect of ambient temperature on the isometric tensile force—length characteristics of the W-1 type BFA: L_o = 5.00 in., W = .63 in., D_s = .50 in.

VII. RECOMMENDATIONS FOR CONTINUED INVESTIGATION

A. IMPROVE THE END ELEMENT DESIGN

Tests have indicated that the cone-type ends used on the W-1 and W-2 actuators have greater holding power than the cylindrical crimped type used on the W-3I and W-4 actuators. As previously stated, due to lack of holding power of the end elements, the W-3I and W-4 actuators could not be elongated beyond their free length (L_o), thus rendering their passive stretch or zero-pressure force output unusable (although it occurred only over a short excursion beyond L_o). For the same reason the W-3I device was also limited to a maximum tensile force output of 70 lb. On the other hand, the cylindrical crimped ends have the advantage of low cost and simplicity in comparison to the cone type.

The lack of effectiveness of these ends is due to polyethylene grommet separating the male and female elements. It is felt that eliminating this grommet and redesigning the male element as shown in Fig. 71 will increase the holding power of these ends to equal that of the cone type.

B. DECREASE GAS CONSUMPTION

The gas-consumption characteristics indicate that a finite absolute volume within the actuator must be filled with gas before it can begin to do work (i.e., before it begins to exert a tension and contract). This volume (defined by the walls of the actuator) occurs at the maximum working length (L_m); however, the relative volume of gas occupying this absolute volume varies with the internal pressure due to compressibility of the gas. The relationship and magnitude of this relative (or "dead") volume to the total gas consumed as a function of pressure is indicated in Fig. 72 for a W-2 type, 5-in.-long actuator. At 20 psig the relative volume (or volume of gas which does no work each time the device is filled and completely exhausted) corresponds to that defined by point "a" (i.e., 1.8 $in.^3$). Similarly, volumes corresponding to points b, c, and d would be wasted at 40, 60, and 80 psig, respectively.

By eliminating this "dead" volume a considerable savings in gas consumption could be attained. One way of accomplishing this is to insert a solid plug composed of a light material to fill the space. Figure 73 illustrates the allowable size and effect of an aluminum plug which was built into the end element of a W-2 actuator. Comparing the curves of Figs. 72 and 73, which are for the same size of actuator, it is seen that the plug reduces the gas consumption per pressure by approximately 25% over that of an actuator without a plug.

The size of a solid plug is limited by the diameter of the actuator at the maximum working length (L_m) and the pressure stable length (L_s). These size limitations could be eliminated by inserting a pliable plug which would change shape as the actuator contracts. Such a plug could be constructed with a volume equal to the physical volume within the actuator at the maximum working length (L_m).

The design of one type of plug to accomplish this is shown in Fig. 74. It is reasonable to assume that a 30 to 50% savings in gas consumption per pressure could be obtained by use of such a device. Construction and evaluation of this proposal is left for future investigation.

C. EXPAND AND FURTHER EVALUATE THE LENGTH TENSION AND GAS-CONSUMPTION RELATIONSHIPS FOR PRACTICAL ORTHETIC USE

Methods of expanding the data of this report to include actuators of different lengths and diameters other than those tested have been discussed on pages 21 and 83 . However, such expansion of the data will leave orthetic designers with a large quantity of information difficult to use unless they have considerable experience in its application. To obtain a qualitative evaluation of the various actuators tested, it is recommended that efficiency curves be developed and evaluated from the data of this report. Such curves should give the efficiency as a function of excursion (change of length), thus allowing selection of one actuator over another where doubt exists.

Since this report was first drafted, further reports of investigations dealing with the latter two suggestions have been reported. The question of gas-consumption and efficiency has been discussed in The University of Michigan Orthetics Research Project Technical Report 04468-2-T entitled "Gas Liquid Pressure Transmitter" by Robert Juvinall. An analysis covering the same subject appears in a University of California Los Angeles Biotechnology Laboratory Report No. 60-84 in the article entitled "Braided Pneumatic Actuators, Preliminary Analysis, and Some Test Results," by Paskusz, Gwynne, and Lyman.

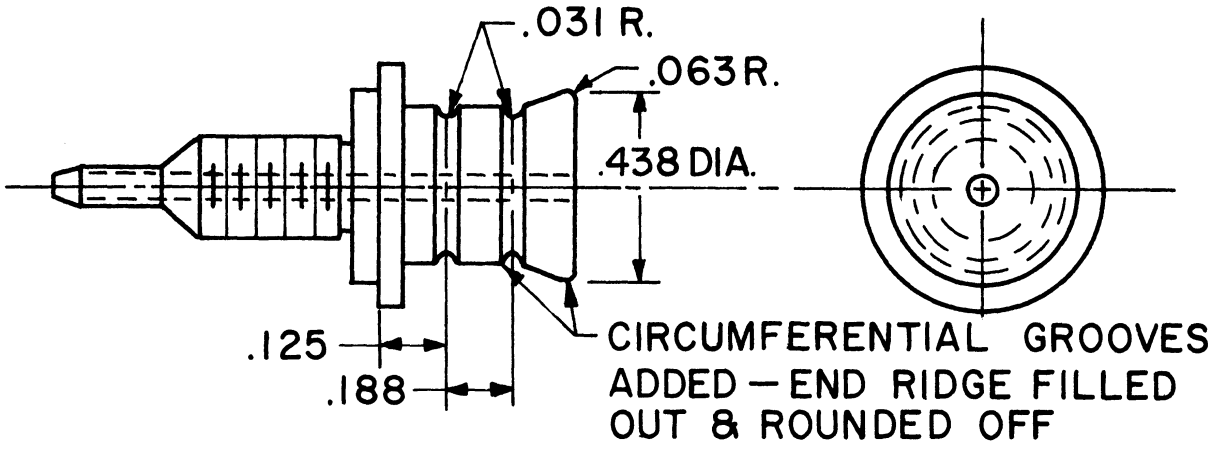

(a) Significant dimensional changes (see Appendix C, Fig. C-3 for dimensions not shown).

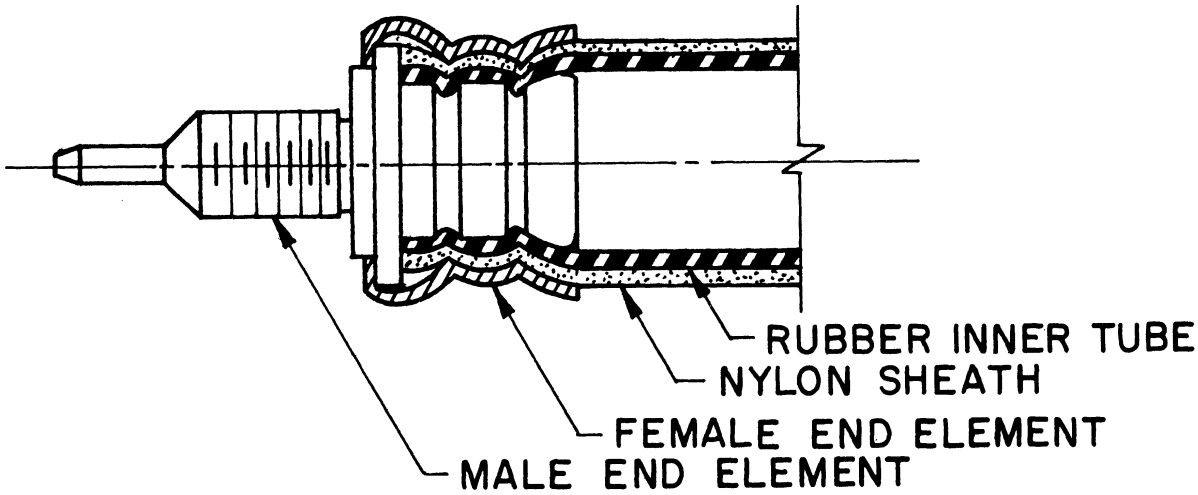

(b) Assembled section showing embedding of the rubber inner tube and braided sheath into the circumferential groves.

Fig. 71. Improved design of the male element for the cylindrical crimped end assembly. Blind end male element not shown.

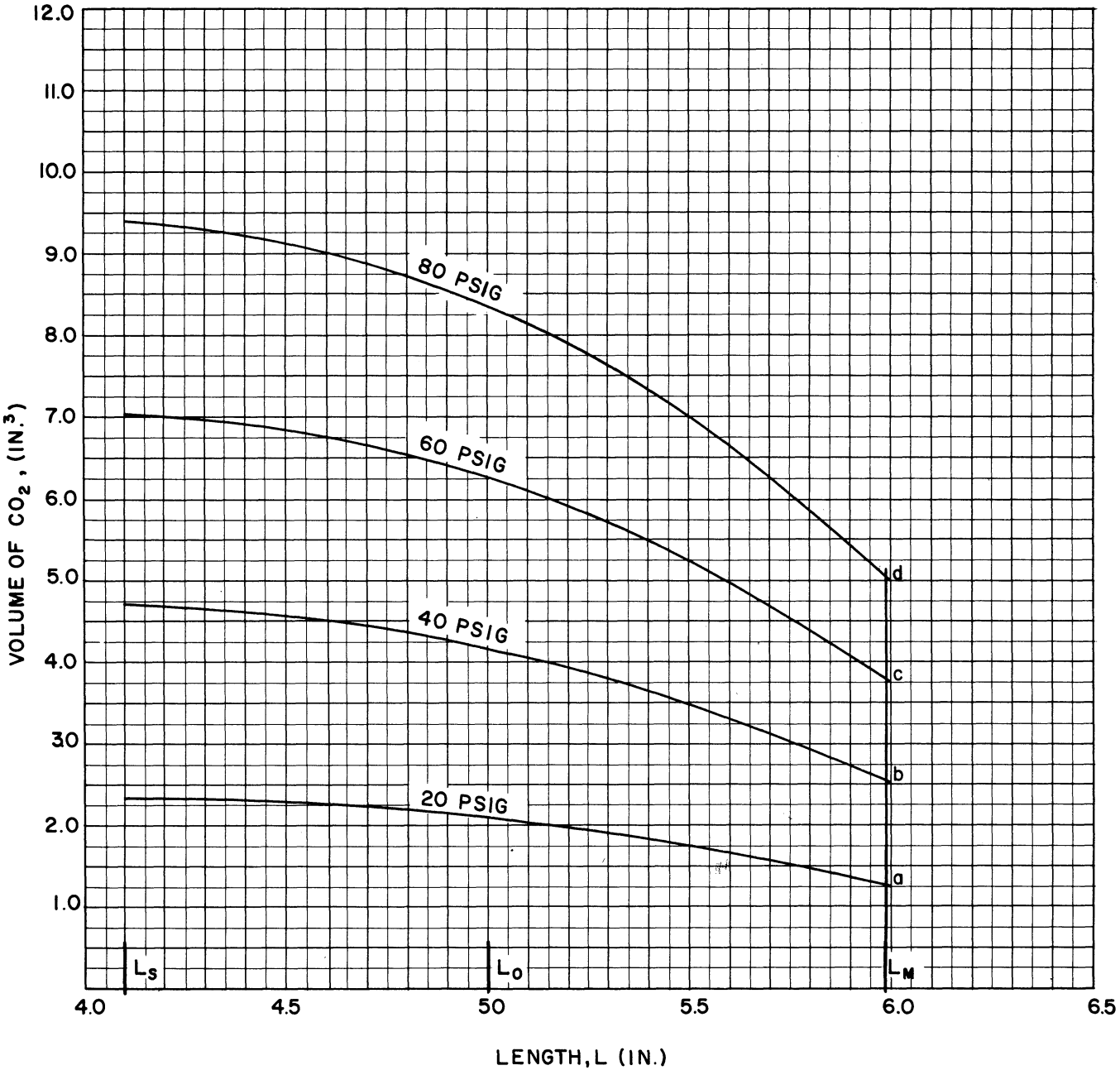

Fig. 72. Gas consumption characteristics on a volume basis as a function of internal working pressure for the W-2 type BFA. The volumes identified by points a, b, c, and d correspond to the volume of gas which does no work each time the actuator is filled and exhausted at 20, 40, 60, and 80 psig, respectively. Data corrected to standard atmospheric conditions. L_O = 5.00 in., W = .95 in., D_S = .75 in., atmospheric pressure = 14.7 lb/in.^{2}, atmospheric temperature = 77°F.

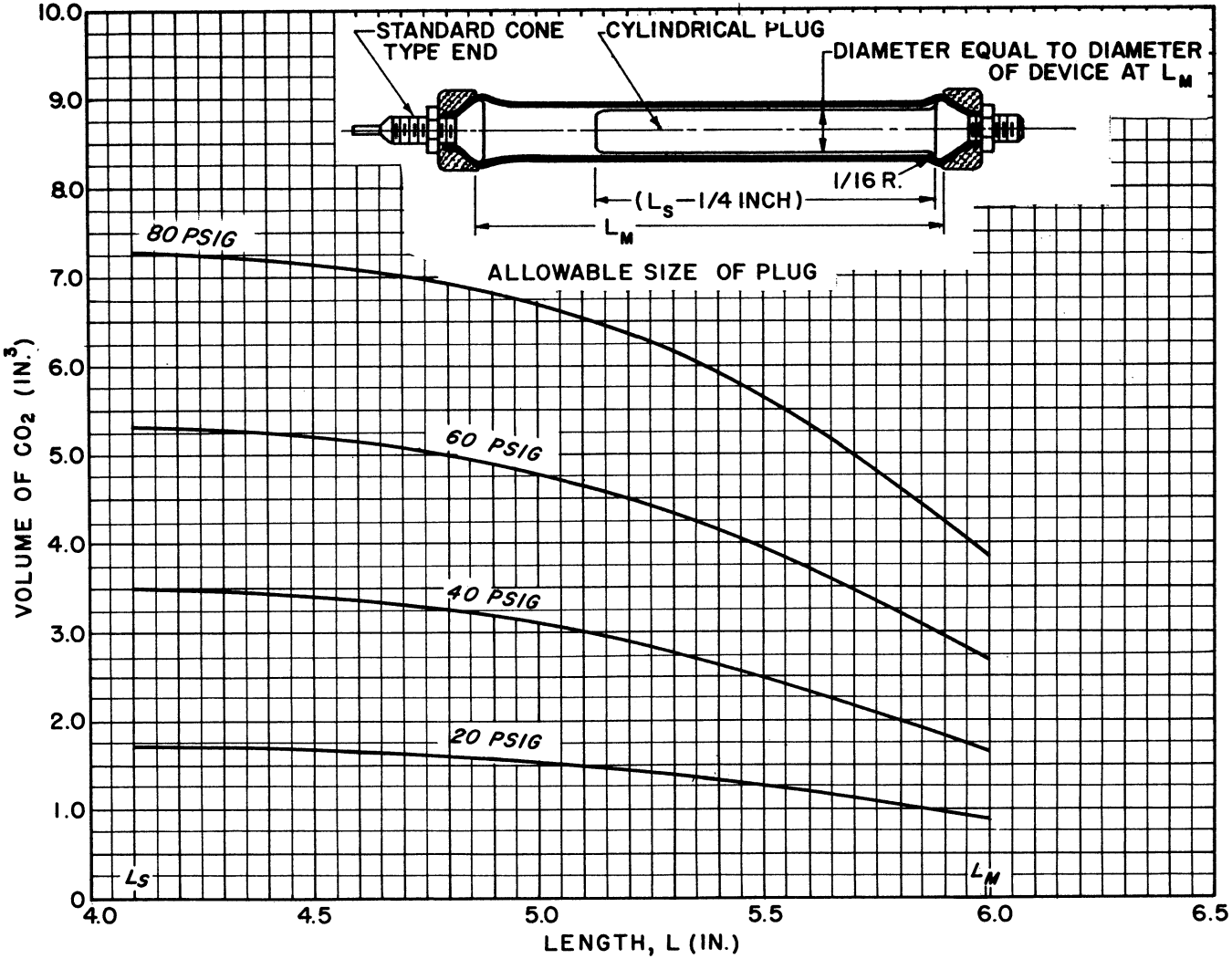

Fig. 73. Gas consumption characteristics on a volume basis as a function of internal pressure for the modified W-2 type BFA. Data corrected to standard atmospheric conditions. L_o = 5.00 in., W = .95 in., D_S = .75 in., atmospheric pressure = 14.7 lb/in.^{2}, atmospheric temperature = 77°F.

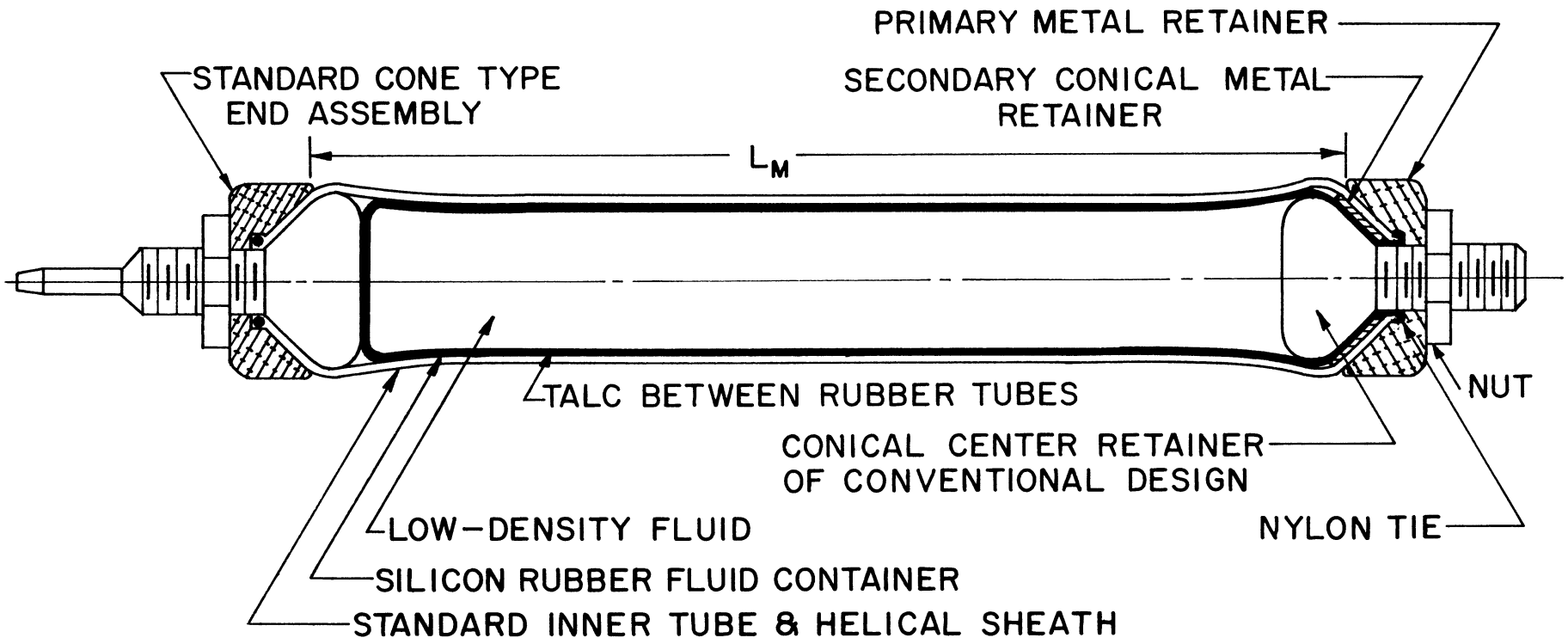

Fig. 74. Construction of one type of pliable plug intended to reduce gas consumption of the BFA. The fluid should be of low density and nontoxic. The fluid container should be made of a relatively inert elastic material such as silastic S-9711 (manufactured by Dow Corning Corp.). The talc is intended to reduce sticking and friction between the two elastic tubes.

APPENDIX A

EXPERIMENTAL TECHNIQUES

ISOMETRIC TENSILE FORCE—LENGTH CHARACTERISTICS

A dynamometer consisting of a Hunter force gage and an adjustable slider mechanism was constructed to measure the force output of the BFA. The complete test setup (Fig. A-1) consisted of a standard BFA pressure-reducing valve and gas-control valve connected in series with a pressure gage and the BFA, which were in turn mounted between the force gage and slider assembly. Details of the setup are shown in Fig. A-2. A length gage (Fig. A-3), connected to the ends of the BFA, was constructed to give direct measurement of length. Ranges of the force, pressure and length gages were, respectively: 0 to 90 lb, 0 to 100 psig, and 0 to 6 or 12 in. (depending on the length of the scale used). Accuracies of these instruments were respectively 1/2 lb, 1 psig, and 0.01 in.

Tests were conducted by filling the BFA with gas and allowing it to reach the pressure stable length (L_s) while the slider and its positioning bracket were allowed to move freely. The positioning bracket was then clamped at successive positions 0.10 in. apart starting from L_s and ranging to the maximum working length (L_m). The slider assembly (see Fig. A-2) was constructed so that the slider moved freely until it engaged a stop on the positioning bracket. Thus the power device was allowed to contract freely from the free length (L_o) until it was restrained at a given length dictated by the location of the positioning bracket. During a given run the pressure was held constant by appropriate adjustment of the pressure-reducing valve (prior to the run) while the length was varied. At each length the tension was recorded. In elongating a device beyond its free length (L_o), a force was developed due to resistance of the passive elastic elements (inner tube and braided sheath). This force was recorded at each increment of length before filling the actuator with gas. The data were then plotted.

The characteristics obtained in this manner are referred to as "isometric" in that the power device was pressurized without shortening, thus generating a tension but doing no work. A similar type of force system in human muscle is involved in trying to crush a nut between the teeth.

GAS-CONSUMPTION CHARACTERISTICS

Gas-consumption data were obtained using the setup shown schematically in Fig. A-4. The same instruments as described on the preceding pages were used to monitor pressure and length except that the small gas cylinder was replaced by a large one. Gas line valve No. 1 was used to close off the portion of the

system in front of the BFA (i.e., the pressure gage, gas-supply and pressure-reducing valves, gas cylinder and related supply lines). Gas line valve No. 2 was then used to bleed rapidly the gas from the BFA to the bellows-type Sanborn Spirometer which measured the volume in cubic inches. An oscilloscope was used to increase the sensitivity of the spirometer. The gas measuring system was calibrated to read from 0 to 20 $in.^3$ with an accuracy of 1/2 $in.^3$

Tests were conducted in the same manner as for the tensile force characteristics except that at each successive length increment the gas was bled into the spirometer and then to the atmosphere. The data were corrected to standard atmospheric conditions and plotted.

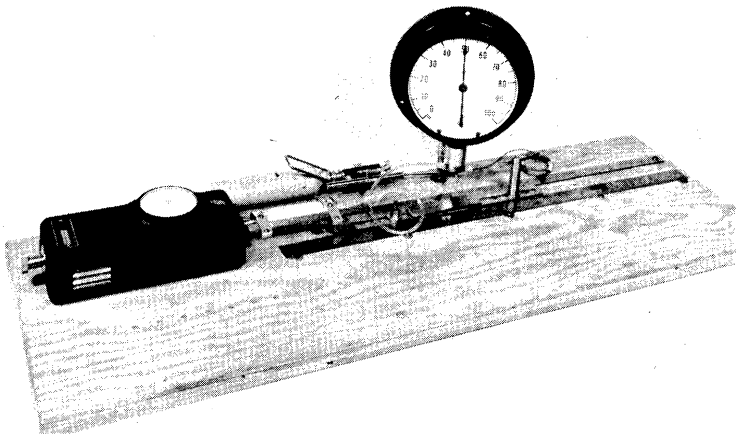

(a) Overall view.

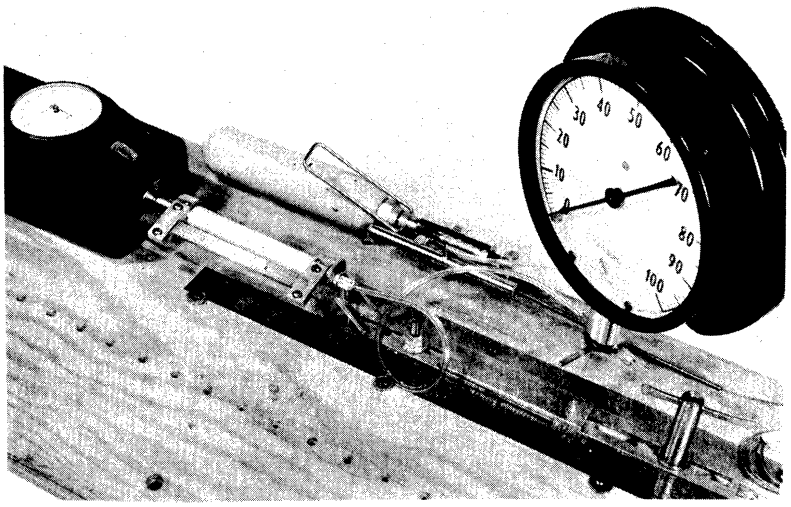

(b) Front closeup.

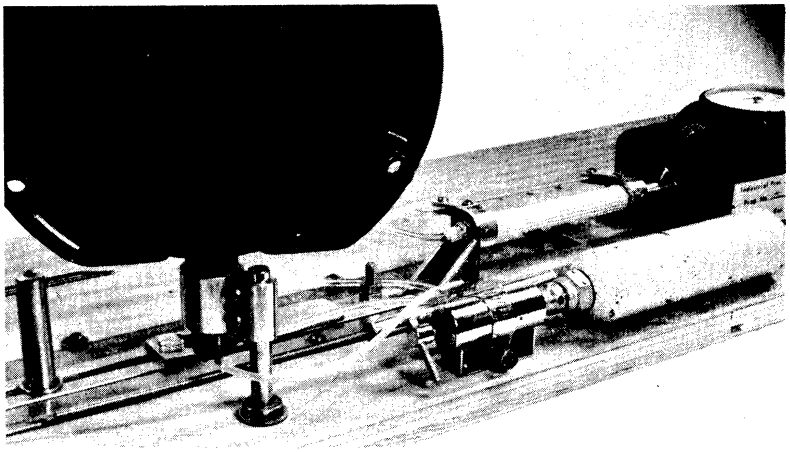

(c) Rear closeup.

Fig. A-1. Test setup used to obtain the isometric tensile force—length characteristics.

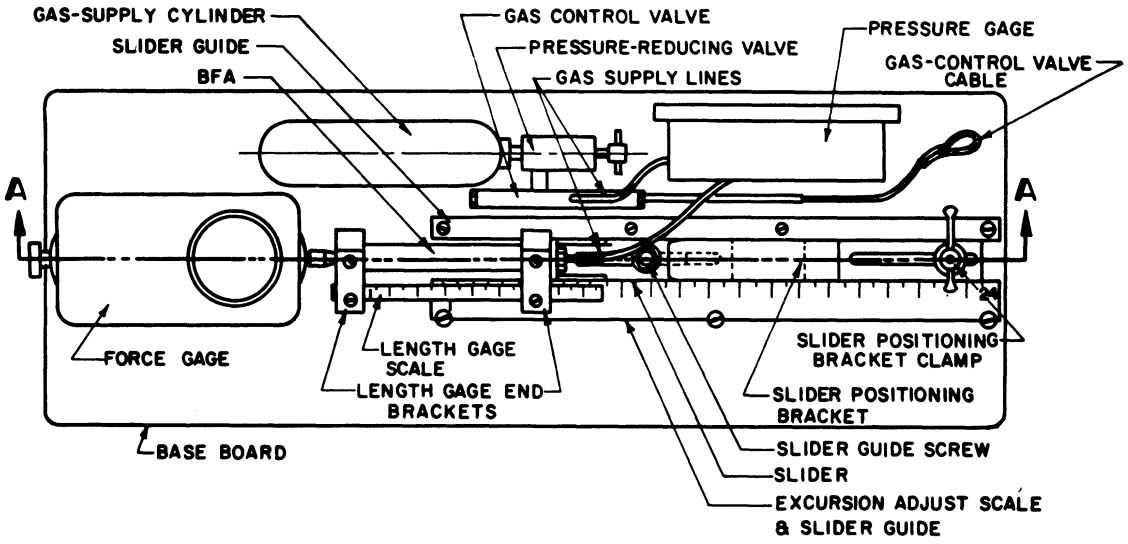

PLAN VIEW

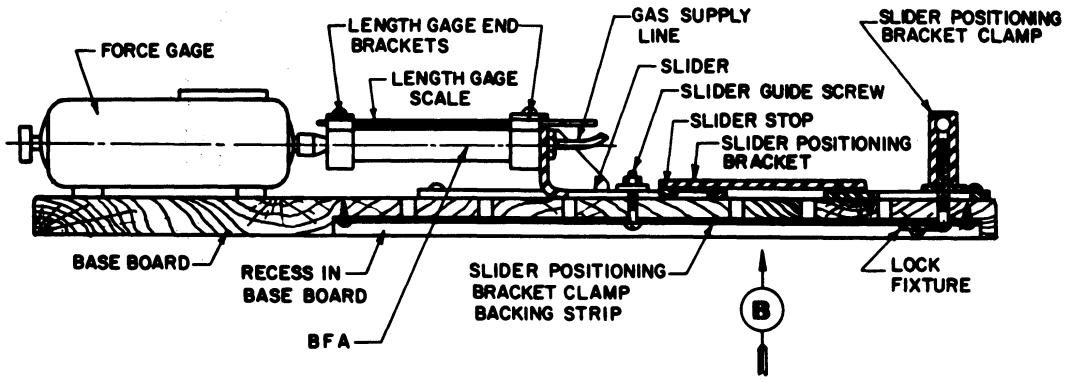

SECTION A-A

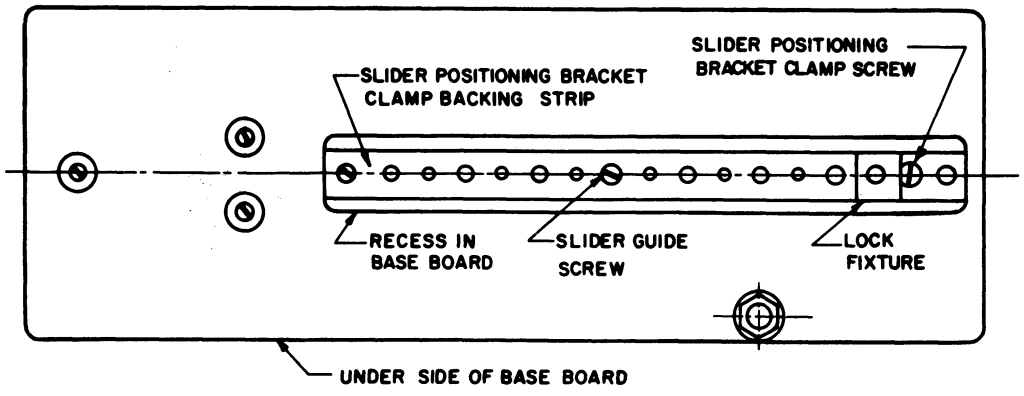

VIEW IN DIRECTION OF ARROW B

Fig. A-2. Plan view and details illustrating the various components of the test setup used to obtain the isometric tensile force—length characteristics.

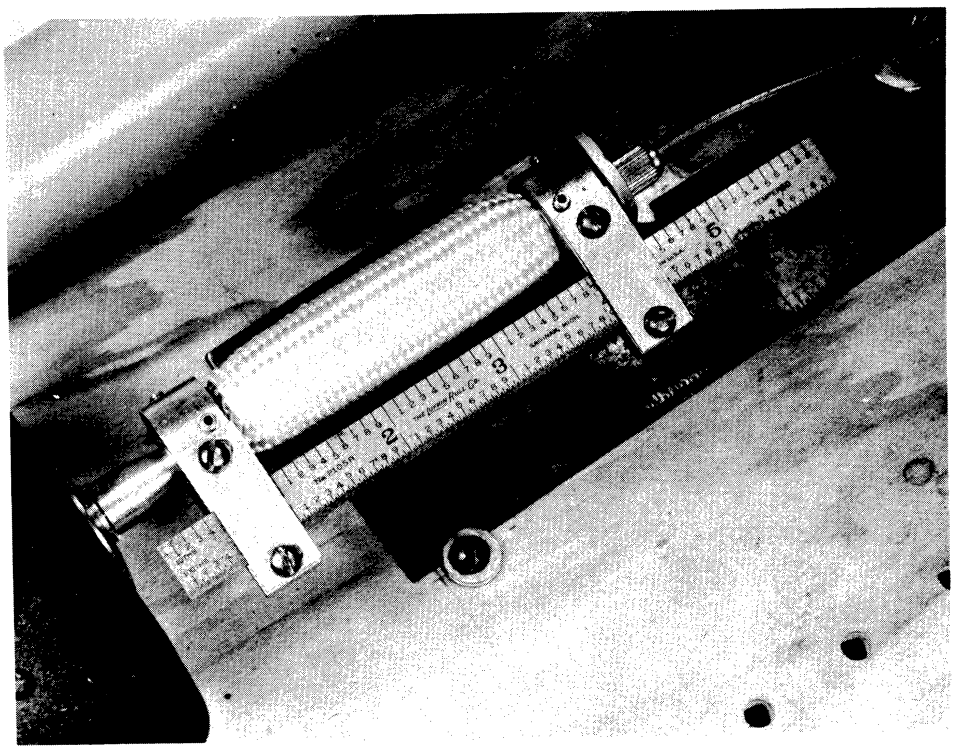

(a) Actuator at maximum working length (L_m).

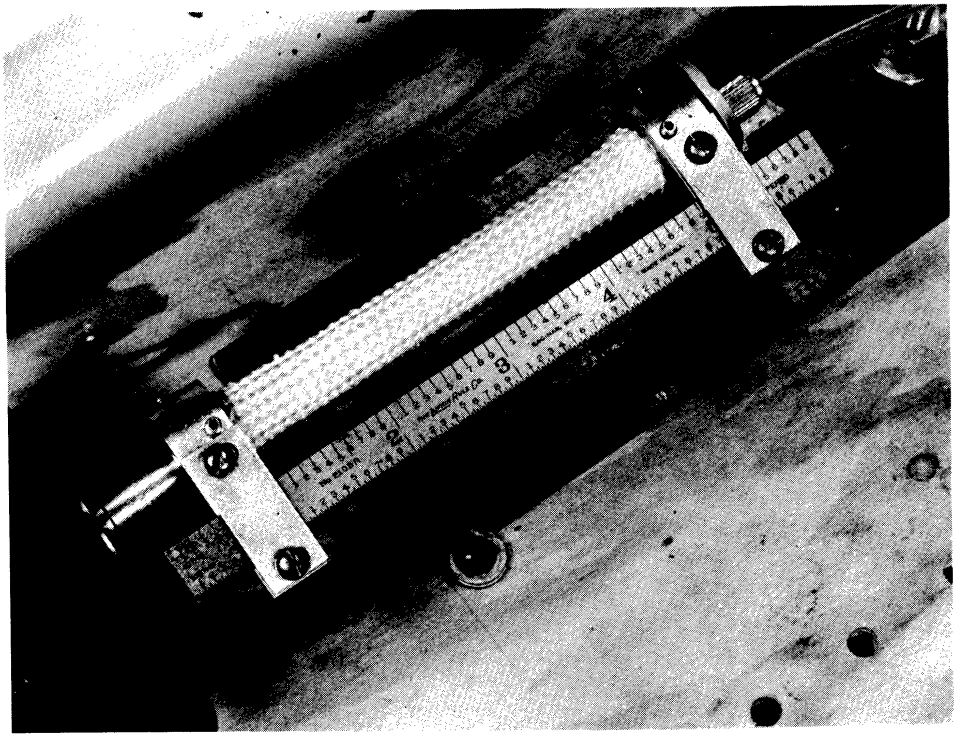

(b) Actuator at pressure stable length (L_s).

Fig. A-3. Gage used to measure the edge to edge length of the BFA. The end brackets, which hold the scale, fit over the ends of the actuator and are held in place by four equally spaced pointed set screws. The actuator shown is the W-4 type.

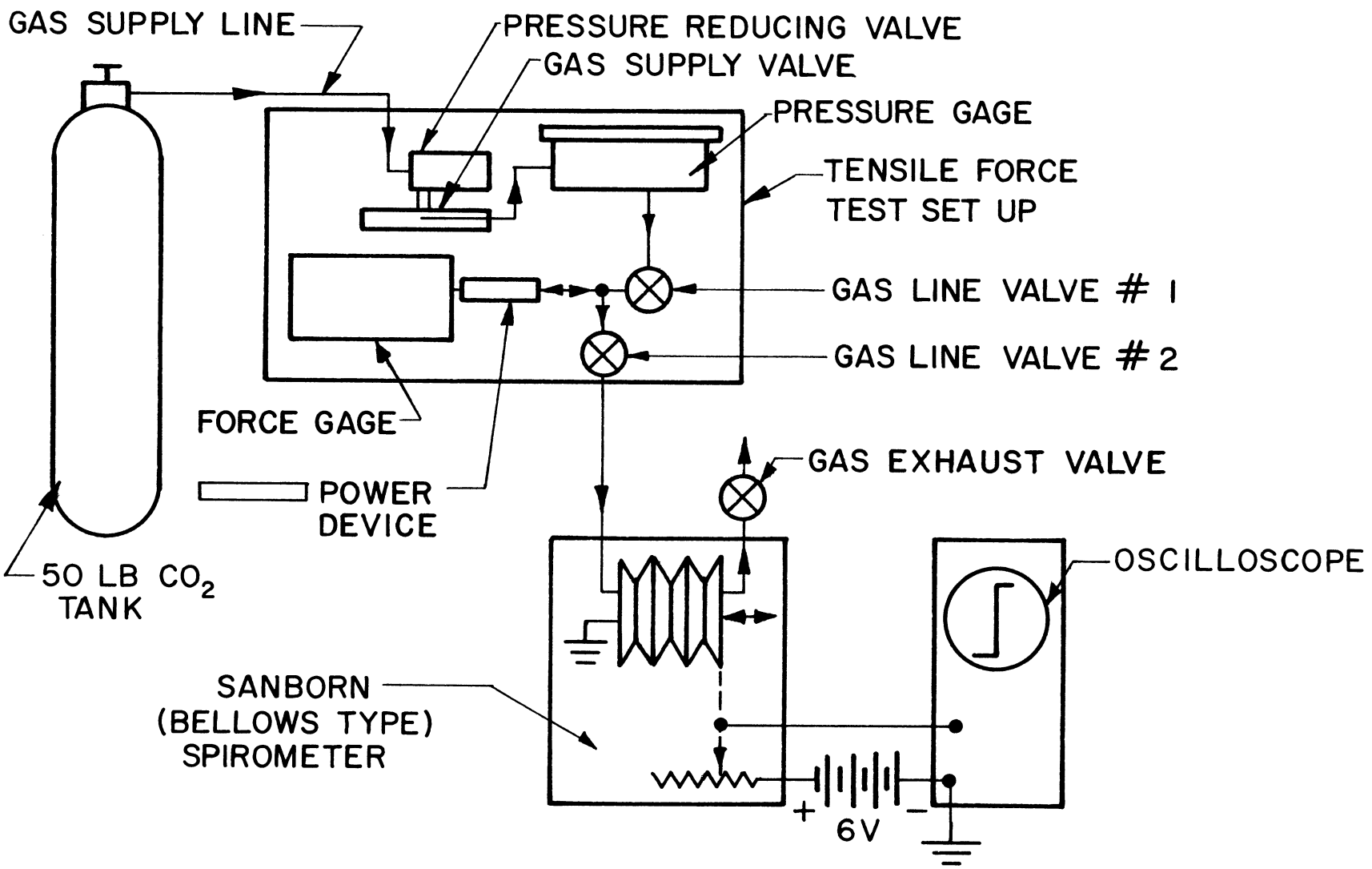

Fig. A-4. Schematic of the test setup for obtaining gas consumption data. The isometric tensile force—length test setup is as previously described except for the addition of line values 1 and 2. Arrows on the gas lines indicate direction of flow.

APPENDIX B

THE THEORETICAL TENSILE FORCE LENGTH EQUATION DERIVATION

The general equation for the tensile force generated by a braided (helical) sheath with an elastic inner tube when inflated by an internal pressure can be written as

T =	Total axial component of the tension in the braided sheath	+	Axial retractive force of the elastic inner tube	-	Force of the pressure acting on the ends of the tube	
						- Frictional forces

or

$$T = t_t + t_r - t_p - t_f \qquad (1)$$

Each term of this equation can be analyzed separately. The following expressions exist due to the geometrical relationship of the elements of the sheath as represented in Fig. B-1.

$$L_h = \pi Dn \qquad (2)$$

$$L = L_h \cos \Theta \qquad (3)$$

$$d = D \sin \Theta \qquad (4)$$

L_h, L, and d are, respectively, the straight length of a single strand of material in the braided sheath, the length of the actuator at any value of Θ, and the diameter of the actuator at any value of Θ. D is an ideal parameter defined as the maximum diameter of the actuator when the helix (braid) is fully compressed or when Θ approaches 90° and n is the number of turns made by strand L_h.

Consider the braided sheath and elastic inner tube as an integral unit forming a thin-walled cylinder. The relationship for the circumferential force (F) (sometimes called hoop tension) exerted on any longitudinal element of

length (L) in this idealized cylinder (as shown in the half cylinder of Fig. B-2a) due to a uniform internal pressure of intensity (P) can be developed in the following manner. Let Fig. B-2b represent the cross section of such a cylinder acted on by internal pressure and Fig. B-2c represent the distribution of the fluid pressure exerted by the fluid in the upper half of the semi-cylindrical wall and upon the fluid or gas occupying the lower half of the cylinder. Since the upper half of the cylinder is loaded the same in both Figs. B-2b and B-2c, the force (F) acting across the wall element (L) at A must be the same in both cases. If the thickness of the cylinder wall is neglected and the upper and lower parts of the cylinder in Fig. B-2c are shown separately as in Fig. B-2d, the force (F) is readily calculated from the conditions for static equilibrium of the lower part.

$$2F = P \text{ (projected area)} = P\,(Ld)$$

and therefore

$$F = \frac{PLd}{2} \tag{5}$$

If the elastic inner tube and braided sheath are now considered as separate idealized thin-walled cylinders one inside the other, it is apparent that

$$F = F' + F'' \tag{6}$$

where F' is the circumferential force (hoop tension) in the elastic inner tube and F'' is the circumferential force in the braided sheath.

The circumferential force (F') is the retractive force created by virtue of circumferential expansion of the inner tube caused by action of a portion of the internal pressure P.* Defining k_e as the elastic constant in pounds

---

*The internal pressure (P) referred to in Fig. B-2 may be considered as composed of two partial pressures (P') and (P'') (i.e., P = P'+P''). If P' and P'' are applied to the elastic inner tube and the braided sheath, respectively, and if the conditions for static equilibrium are applied to the thin-walled cylinders formed by these units, it is apparent that

$$F' = \frac{P' Ld}{2}$$

$$F'' = \frac{P'' Ld}{2}$$

These expressions are identically equal to the expressions for F' and F'' of Eqs. (7) and (8) derived in the text.

per square inch of tube surface area increase and assuming this parameter to be equal in both the axial and circumferential directions, it is apprent that

$$F' = k_e L\pi(d - d_o); \ (d - d_o) > 0 \qquad (7)$$

where d_o is the mean unelongated diameter of the elastic inner tube (i.e., when P = 0). The restriction that the quantity $(d-d_o)$ must be greater than zero is imposed on this equation since the elastic inner tube must be elongated circumferentially to exert a force of the type under discussion.

The force created by the remaining portion of the pressure P acting on the walls of the idealized thin-walled cylinder formed by the braided sheath is balanced by a restraining circumferential tension (F") in the strands of the sheath. The force relationship for a single strand is shown in Fig. B-3. In this diagram m is the number of strands in the braided sheath. There are m/2 strands spiralling in each direction to prevent a relative twisting of the end elements with respect to each other. From this diagram it can be seen that

$$F'' = mn \ (F \sin \Theta) \qquad (8)$$

Substituting Eqs. (5), (7), and (8) into Eq. (6) and simplifying yields

$$F = \frac{L}{2mn \sin \Theta} \ [Pd - 2\pi k_e \ (d - d_o)] \qquad (9)$$

Also from Fig. B-3, the first term (t_t) of Eq. (1) is

$$t_t = m \ (F \cos \Theta) \qquad (10)$$

Substituting Eq. (9) into this expression eliminates m.

$$t_t = \frac{L \cos \Theta}{2n \sin \Theta} \ [Pd - 2\pi k_e \ (d - d_o)]; \ (d - d_o) > 0 \qquad (11)$$

Now considering the elongation of the elastic inner tube in the axial direction, the second term (t_r) of Eq. (1) is

$$t_r = k_e \pi d \ (L - L_o); \ (L - L_o) > 0 \qquad (12)$$

where L_o is the unelongated length of the elastic inner tube (i.e., when P = 0). The restriction that the quantity $(L-L_o)$ must be greater than zero is imposed on this equation since the elastic inner tube must be elongated to exert a force.

The third term (t_p) in Eq. (1) is the force of the internal pressure (P) acting on the ends of the actuator. This force tends to decrease the tensile force output of the actuator and has the form.

$$t_p = \frac{P\pi d^2}{4} \qquad (13)$$

The frictional forces also tend to decrease the output of the actuator. These forces are created by the effects of friction between the braided sheath and elastic inner tube and between the strands of the sheath themselves. The sum of these two forces composes the last term (t_f) of Eq. (1) which has the general form.

$$t_f = (u_t + u_s)\, N$$

u_t, u_s and N are, respectively, the coefficient of friction between the braided sheath and the elastic inner tube, the coefficient of friction between the fibers of the braided sheath, and the normal force between the surfaces in question. The normal force is created by the pressure within the actuator acting on the total area exposed to it. This area is the lateral surface area of the actuator excluding the end elements. If the shape of the actuator is neglected as its ends are approached, this force can be expressed as

$$N = P''\,(\pi L d)$$

P" is the effective pressure acting on the lateral surface area. This pressure is slightly less than P by the amount of pressure necessary to maintain equilibrium in the elastic inner tube at a given configuration of the actuator. This partial pressure was previously used to define F".

Substituting into the expression for t_f and letting $U = (u_t+u_s)$

$$t_f = P''\, U\pi L d \qquad (14)$$

Now using Eqs. (11), (12), (13), and (14), Eq. (1) becomes

$$T = \frac{L}{2n}\frac{\cos\theta}{\sin\theta}\left[Pd - 2\pi k_e\,(d - d_o)\right] + \pi k_e\, d\,(L - L_o) - \frac{\pi P d^2}{4} - P''ULd$$

where

$$(d - d_o) > 0$$
$$(L - L_o) > 0$$

n can be eliminated from this equation by solving Eqs. (2) and (3) for n and substituting. d can be eliminated by using Eq. (4). On rearranging T takes the final form.

$$T = \frac{\pi D^2 P}{4}\left[3\cos^2\theta - 1\right] + \pi D k_e\left[(L - L_o)\sin\theta - \frac{\pi\cos^2\theta}{\sin\theta}\,(D\sin\theta - d_o)\right] - \pi\, L\, D\, U\, P''\sin\theta \qquad (15)$$

where

$$(L - L_o) > 0$$
$$(D\sin\theta - d_o) > 0$$

This equation can be represented by

$$T = T_p + T_r - T_f \qquad (15a)$$

T_p, T_r and T_f are the three major terms of Eq. (15). The first term represents the portion of T due to the action of the pressure of the actuator, the second term the portion due to the action of the elastic inner tube, and the third term the portion due to frictional effects.

If ideal materials are used in constructing an actuator with its force output defined by Eq. (15), k_e and U will be small and approximately equal to zero.* Under these conditions

$$T = \frac{\pi D^2 P}{4} [3 \cos^2 \Theta - 1] \qquad (16)$$

Or by substituting Eq. (2)

$$T = \frac{\pi D^2 P}{4} \left[3 \left(\frac{L}{L_h} \right)^2 - 1 \right] \qquad (16a)$$

From these equations it can be seen that

T = Maximum when $L = L_h$ or $\Theta = 0°$

T = Zero when $L = L_h/\sqrt{3}$ or $\Theta = 54°44'$**

T = Maximum negative pull or maximum push when $L = 0$ or $\Theta = 90°$

The three regions characterized by Θ as defined above can be classed as follows: (1) pressure retractive, (2) pressure stable and (3) pressure extensive. Experiments have verified this reasoning. If an actuator is extended such that Θ tends toward 0° and pressure is applied from within, it will retract with the travel stopping as Θ approaches 54°44'. Conversely, if its ends are restrained such that Θ approaches 90°, the tubing will elongate under pressure with the travel stopping as Θ approaches 54°44'. These relationships are shown in Fig. B-4 (p. 114). Since the majority of the applications of the BFA will utilize its retractive characteristics, only that portion of the force spectrum will be considered in this report.

The only retracting device comparable at this time to the BFA is a conventional pneumatic cylinder having a force output (T') defined by the equation

$$T' = PA_s \qquad (17)$$

*Portions of the following discussion are abstracted from Ref. 1.
**Since cos 54°44' = .5774 = $1/\sqrt{3}$.

P and A_s are, respectively, the internal pressure in the cylinder and the area of its piston.

The maximum tension (T_{max}) exerted by an ideal BFA can be put in a form for comparison to Eq. (17) by designating the value of the stable cross section as (A_s) (i.e., when $\theta = 54°44'$) and that of the diameter of the stable cross section by (D_s). From the geometry of the helical sheath,

$$D_s = D \sin 54°44' = .8165\ D \tag{18}$$

and

$$A_s = \frac{\pi D_s^2}{4} = \frac{1}{6}\pi D^2 \tag{19}$$

As previously stated, T becomes a maximum when $L = L_h$ or $\theta = 0°$. Utilizing this point and substituting Eq. (19) into Eq. (16) yields

$$T_{max} \approx 3\ P\ A_s \tag{20}$$

Thus, the BFA is ideally capable of yielding a force which is three times that of a pneumatic cylinder having a piston area equal to its stable cross section.

MODIFICATION OF THE EQUATION FOR PRACTICAL USE

For practical use Eq. (15) can be put in terms of easily measured parameters which are the free length of the braided sheath and the angle θ at this length (i.e., the angle at which the braided sheath is woven). Let these parameters be designated by L_o and θ_o, respectively. The L_o defined here is identical to the L_o previously defined as the unelongated length of the elastic inner tube. From Eq. (3), L_o can be specifically defined as

$$L_o = L_h \cos \theta_o \tag{21}$$

Solving Eq. (3) for cos θ and substituting the value of L_h from Eq. (21) yields

$$\cos \theta = \frac{L \cos \theta_o}{L_o} \tag{22}$$

By trigonometry

$$\sin \theta = \left(1 - \left[\frac{L \cos \theta_o}{L_o}\right]^2\right)^{1/2} \tag{23}$$

From Eq. (19) it is seen that

$$D^2 = \left(\frac{3}{2}\right) D_s^2 \text{ or } D = D_s\sqrt{\frac{3}{2}}$$

Substituting Eqs. (21), (22), and (23) into Eq. (15) and simplifying yields the final form of the equation for the force output of the BFA.

$$T = 1.178D_s^2 P\,[3\,BL^2 - 1] + 3.848\,D_s k_e \left[(L - L_o)C - \frac{BL^2\pi}{C}(1.225D_sC - d_o)\right]$$

$$- 3.848D_sL\,UP''C$$

where $$B = \left(\frac{\cos\,\theta_o}{L_o}\right)^2$$

$$C = (1 - BL^2)^{1/2}$$

and $$(L - L_o) > 0$$

$$(1.225D_sC - d_o) > 0$$

In this equation there are two parameters K_e and U which are difficult to evaluate accurately analytically or empirically. In the BFA's under study the elastic inner tube is composed of latex rubber and the braided sheath of nylon strands. Due to the triaxial nature of the elongation in rubber, the further it is elongated in a given direction the greater k_e becomes. Thus k_e is not a constant but a function of L and d. Similarly, due to imbedding of the rubber into the asperities of the helical sheath, u_t increases as P increases and as θ changes from a small to a large angle. This effect is greatest when θ = 45° at high pressures and it decreases as θ becomes greater or less than 45° at constant pressures. Thus U is not a constant but a function of P and θ. Empirical attempts at evaluating U under the conditions as they exist in the operation of the BFA have proven unsuccessful.

If the effects of k_e and U are considered negligible, as previously discussed, Eq. (24) takes the simplified form

(25) $$T = 1.178\,D_s^2\,P\,(3\,BL^2 - 1)$$

where $$B = \left(\frac{\cos\,\theta_o}{L_o}\right)^2$$

Tensile force—length characteristics as determined by this equation are compared to experimentally determined values in Fig. B-5. It is clearly seen that Eq. (25) does not accurately predict the output of the device. Further, since k_e and U cannot be determined accurately, Eq. (24) cannot be evaluated.

In view of the findings of this study, prediction of the tensile force—length characteristics for the BFA by analytical methods was set aside in favor of the empirical methods used.

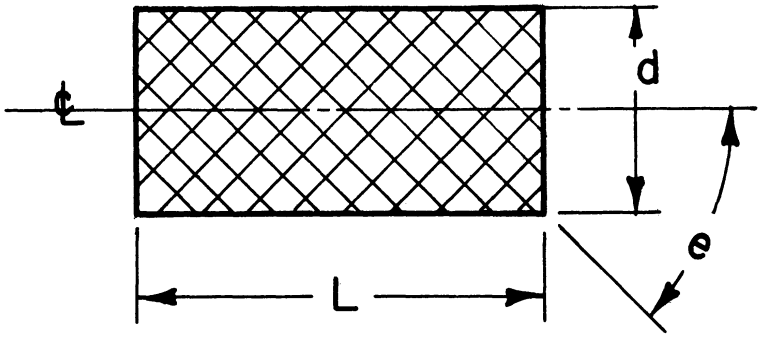

Fig. B-1. Geometrical parameters of the braided sheath.

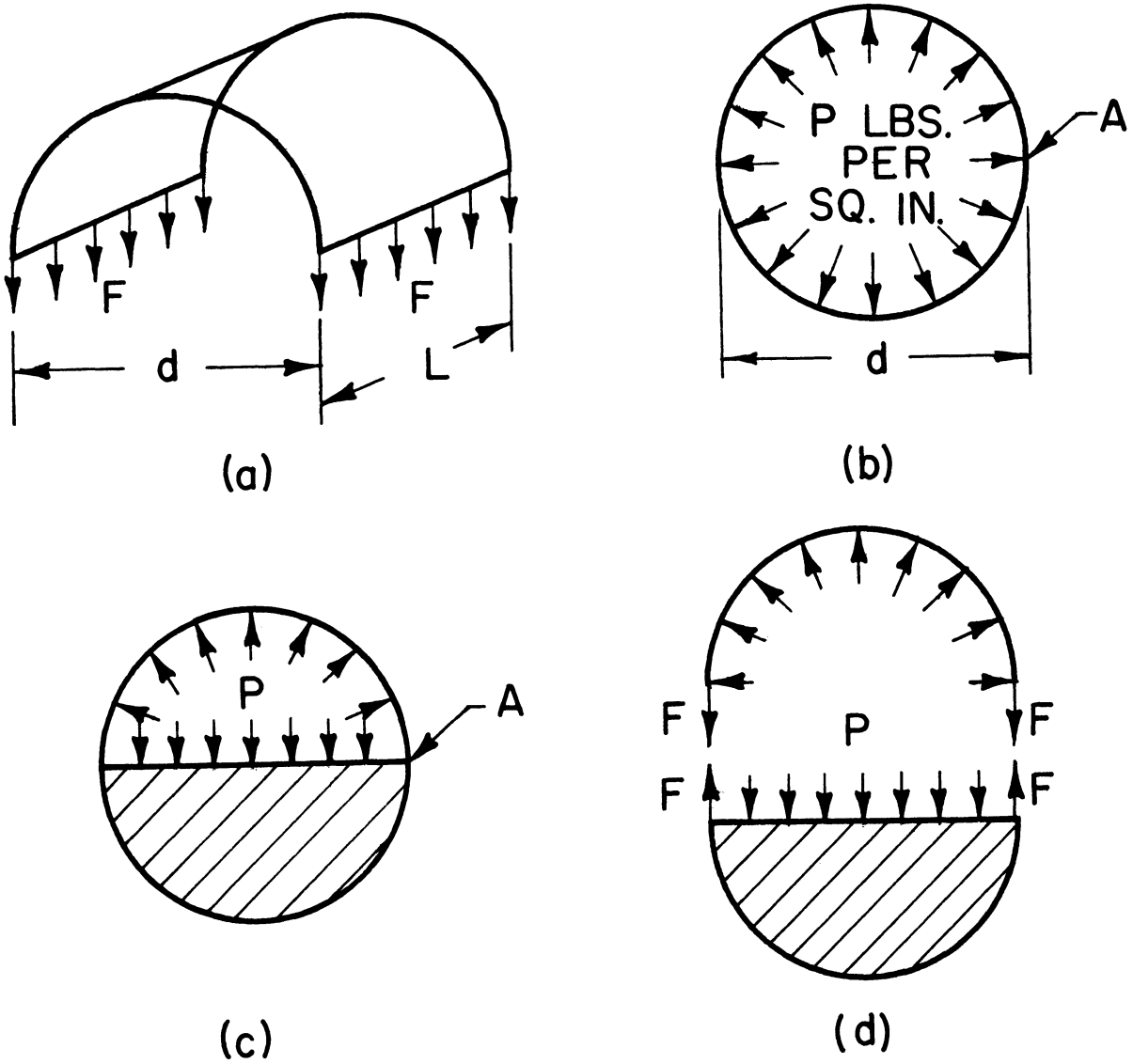

Fig. B-2. The relationship between the force created by the internal pressure (P) and the circumferential force (F) in the walls of the actuator.

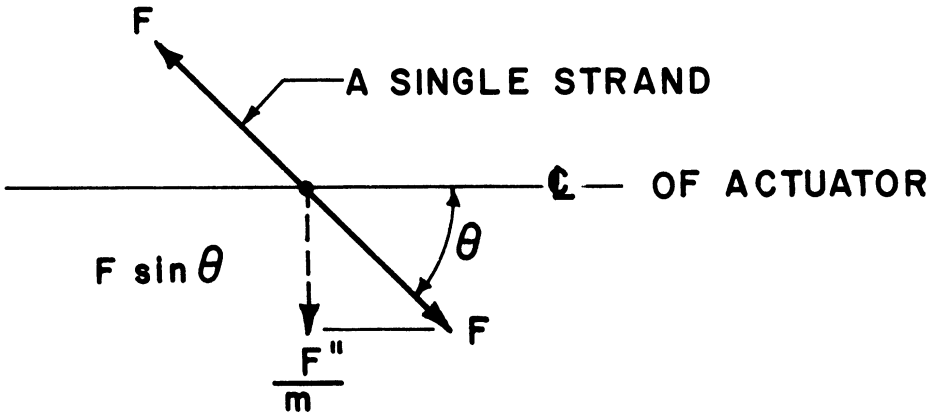

Fig. B-3. Force relationships in a single strand of the braided sheath.

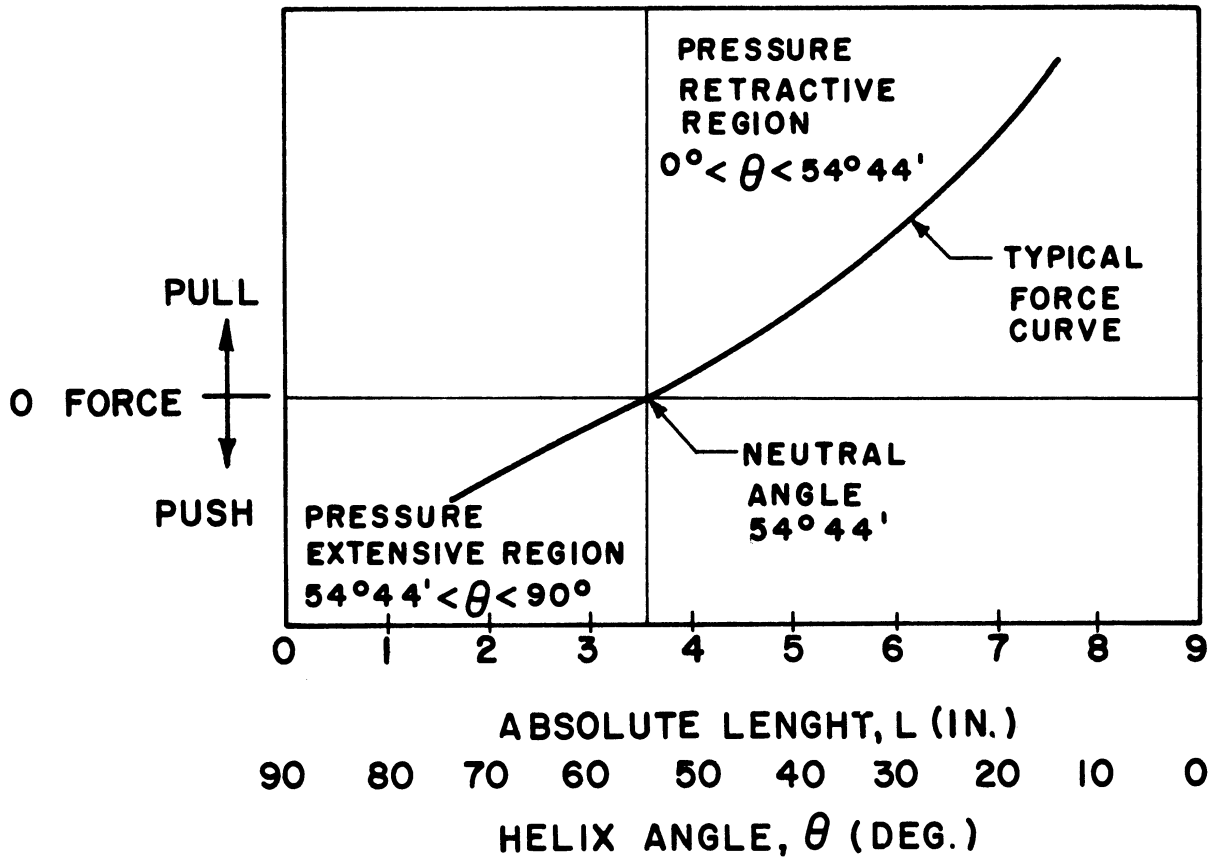

Fig. B-4. The three force regions of the actuator as defined by the helix angle (θ). Diagram not to scale.

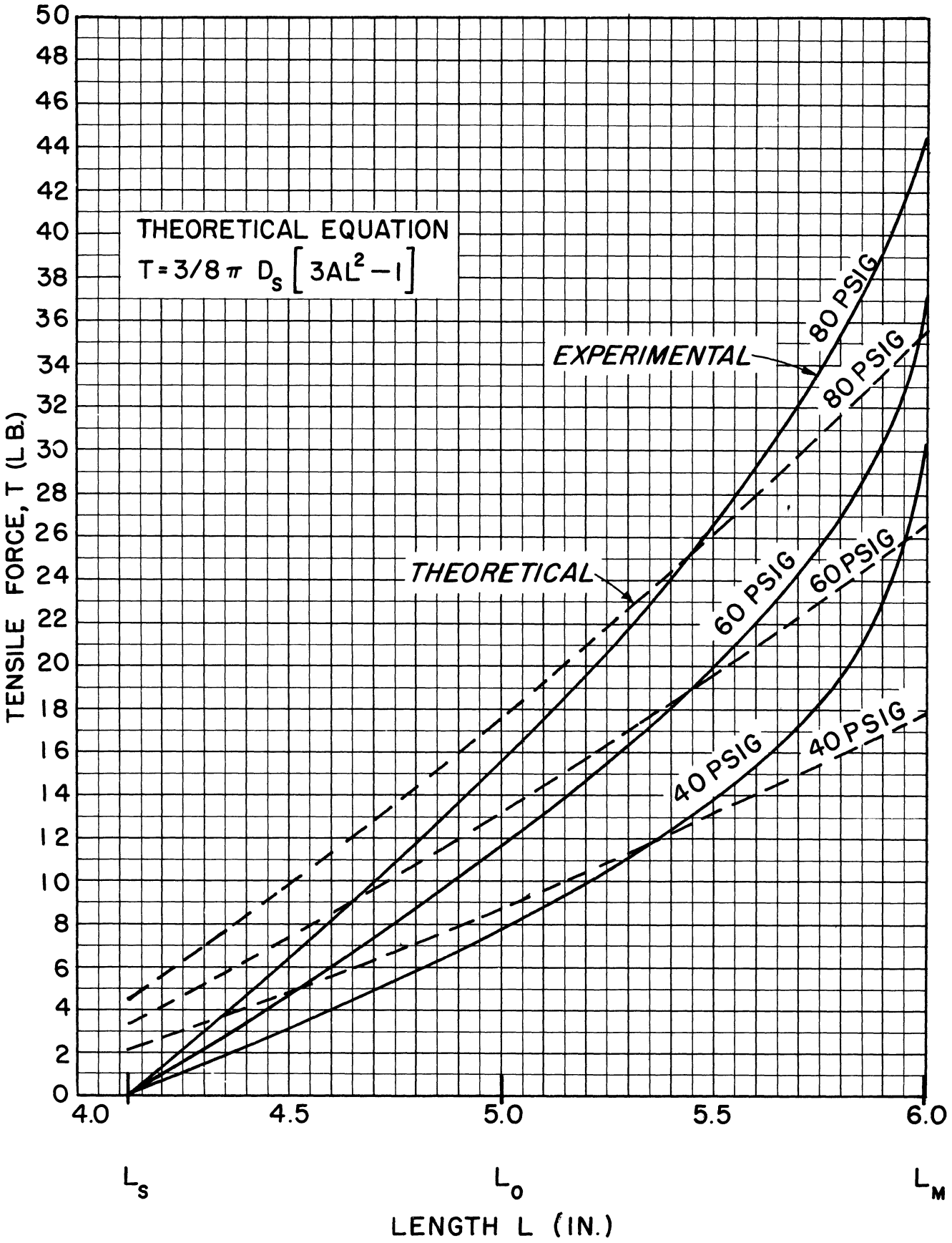

Fig. B-5. Comparison of the theoretical and experimental force—length characteristics of the BFA: L_o = 5.00 in., W = .63 in., D_s = .48 in.

APPENDIX C

DERIVATION FOR THE TENSILE FORCE OF THE BRAIDED FLUID ACTUATOR

The derivation of the expression for tension as a function of pressure, diameters, helix angle, and length accounts for strain of the elastic tubing in axial and tangential directions by use of the specially defined constant, k_e. This device simplifies the final expression considerably, but it is an unconventional term, the evaluation of which would require special experimentation.

In the interests of using conventional concepts, and accessible material data, a further derivation, utilizing the conventional plane strain concepts of elasticity theory is appended here. The terminology is the same as that of the derivation in the report with the addition of the stress terms σ_x and σ_y; the strain terms, ϵ_x and ϵ_y; the modulus of elasticity of the elastic tubing, E; and Poisson's ratio, the usual dimensions holding. The axis orientation is with x in the axial direction and y in the tangential direction.

The equations include the equation of equilibrium of forces in the axial (x) direction;[1] the equation of equilibrium of forces in the tangential direction (y); the equations for σ_x and σ_y as functions of modulus, strain, and Poisson's ratio; the definitions of strain; a relation between length, diameter, and helix angle; and a relation between an arbitrary diameter and the constant D, the diameter when the helix angle, Θ, is zero.

The so-called solution is the algebraic manipulation that was used to establish the equation for tension T, in the same form as in the body of the report. It might be noticed that the first and third terms on the right are the same as the previous equation. The second is more complicated, but a more exact and accessible term, in that the modulus and Poisson ratio for the tubing should be available without test. The relative influence of the tubing should then be more easily determined.

DERIVATION FOR THE TENSILE FORCE OF THE BRAIDED PNEUMATIC ACTUATOR

(1) $$-T + mF\cos\theta + \sigma_x \pi dt - \frac{P\pi d^2}{4} - \mu P_c \pi dL = 0$$

(2) $$-2mnF\sin\theta - 2\sigma_y tL + PdL = 0$$

(3) $$\sigma_x = \frac{E}{(1+\nu)(1-2\nu)}\left[(1-\nu)\epsilon_x + \nu(\epsilon_y)\right]$$

(4) $$\sigma_y = \frac{E}{(1+\nu)(1-2\nu)}\left[(\nu\epsilon_x + (1-\nu)\epsilon_y\right]$$

(5) $$\epsilon_x = \frac{L}{L_o} - 1$$

(6) $$\epsilon_y = \frac{d}{d_o} - 1$$

(7) $$L = \pi Dn\cos\theta$$

(8) $$d = D\sin\theta$$

SOLUTION

(a) $$\frac{mF\cos\theta}{2mnF\sin\theta} = \frac{T - \sigma_x\pi dt + \frac{P\pi d^2}{4} + \mu P_c \pi dL}{PdL - 2\sigma_y tL}$$

(b) $$T = \frac{L\cos\theta}{2n\sin\theta}\left[Pd - 2\sigma_y t\right] + \sigma_x\pi dt - \frac{P\pi d^2}{4} - \mu P_c\pi dL$$

(c) $$T = \frac{\pi D n\cos^2\theta}{2n\sin\theta} \times PD\sin\theta - \frac{\pi D\cos^2\theta \times 2\sigma_y t}{2\sin\theta} + \sigma_x\pi dt - \frac{P\pi D^2}{4}(1-\cos^2\theta)$$

$$- \mu P_c \pi DL\sin\theta$$

(d) $$T = \frac{P\pi D^2}{4}(3\cos^2\theta - 1) - \frac{\sigma_y \pi Dt \cos^2\theta}{\sin\theta} + \sigma_x \pi Dt \sin\theta - \mu P_c \pi DL \sin\theta$$

(e) $$T = \frac{P\pi D^2}{4}(3\cos^2\theta - 1) - \pi Dt\left[\frac{\sigma_y \cos^2\theta}{\sin\theta} + \sigma_x \sin\theta\right] - \mu P_c \pi DL \sin\theta$$

(f) $$\left[\frac{\sigma_y \cos^2\theta}{\sin\theta} + \sigma_x \sin\theta\right] = \sigma_y\left[\frac{1}{\sin\theta} - \sin\theta\right] + \sigma_x \sin\theta$$

$$= \sigma_y/\sin\theta + (\sigma_x - \sigma_y)\sin\theta$$

$$= \frac{E}{(1+\nu)(1-2\nu)\sin\theta}\left[\nu\epsilon_x + (1-\nu)\epsilon_y\right]$$

$$+ \frac{E\sin\theta}{(1-\nu)(1-2\nu)}\left[(1-\nu)\epsilon_x + \nu\epsilon_y - \nu\epsilon_x - (1-\nu)\epsilon_y\right]$$

$$= \frac{E}{(1+\nu)(1-2\nu)}\left\{\frac{\nu\epsilon_x + (1-\nu)\epsilon_y}{\sin\theta} + \left[(1-\nu)\epsilon_x + \nu\epsilon_y - \nu\epsilon_x - (1-\nu)\epsilon_y\right]\sin\theta\right\}$$

$$= \frac{E}{(1+\nu)(1-2\nu)}\left\{\frac{\epsilon_y + \nu(\epsilon_x - \epsilon_y)}{\sin\theta} + \left[(\epsilon_x - \epsilon_y) - 2\nu(\epsilon_x - \epsilon_y)\right]\sin\theta\right\}$$

$$= \frac{E}{(1+\nu)(1-2\nu)}\left\{\frac{\epsilon_y + \nu(\epsilon_x - \epsilon_y)}{\sin\theta} + \left[(\epsilon_x - \epsilon_y)(1-2\nu)\right]\sin\theta\right\}$$

(g) $$= \frac{E}{(1+\nu)(1-2\nu)}\left\{\frac{\epsilon_y}{\sin\theta} + (\epsilon_x - \epsilon_y)\left[\frac{\nu}{\sin\theta} + (1-2\nu)\sin\theta\right]\right\}$$

(h) $$\epsilon_y = \frac{d}{d_o} - 1$$

(i) $$\epsilon_x - \epsilon_y = \frac{L}{L_o} - 1 - \frac{d}{d_o} + 1 = \left(\frac{L}{L_o} - \frac{d}{d_o}\right)$$

(j) $$\left[\frac{\sigma_y \cos^2\theta}{\sin\theta} + \sigma_x \sin\theta\right] = \frac{E}{(1+\nu)(1-2\nu)}\left[\frac{d/d_o - 1}{\sin\theta} + \left(\frac{L}{L_o} - \frac{d}{d_o}\right)\left(\frac{\nu}{\sin\theta} + (1-2\nu)\sin\theta\right)\right]$$

(k) $$= \frac{E}{(1+\nu)(1-2\nu)}\left\{\frac{L}{L_o}\left[\frac{\nu}{\sin\theta} + (1-2\nu)\sin\theta\right] - \frac{d}{d_o}\left[\frac{1+\nu}{\sin\theta} + (1-2\nu)\sin\theta\right] - \frac{1}{\sin\theta}\right\}$$

(l) $$T = \frac{P\pi D^2}{4}(3\cos^2\theta - 1) - \frac{\pi DtE}{(1+\nu)(1-2\nu)}\left\{\frac{L}{L_o}\left[\frac{\nu}{\sin\theta} + (1-2\nu)\sin\theta\right] - \frac{d}{d_o}\left[\frac{1+\nu}{\sin\theta} + (1-2\nu)\sin\theta\right] - \frac{1}{\sin\theta}\right\} - \mu P_c \pi DL \sin\theta.$$

APPENDIX D

DETAIL DRAWINGS OF THE END ELEMENTS

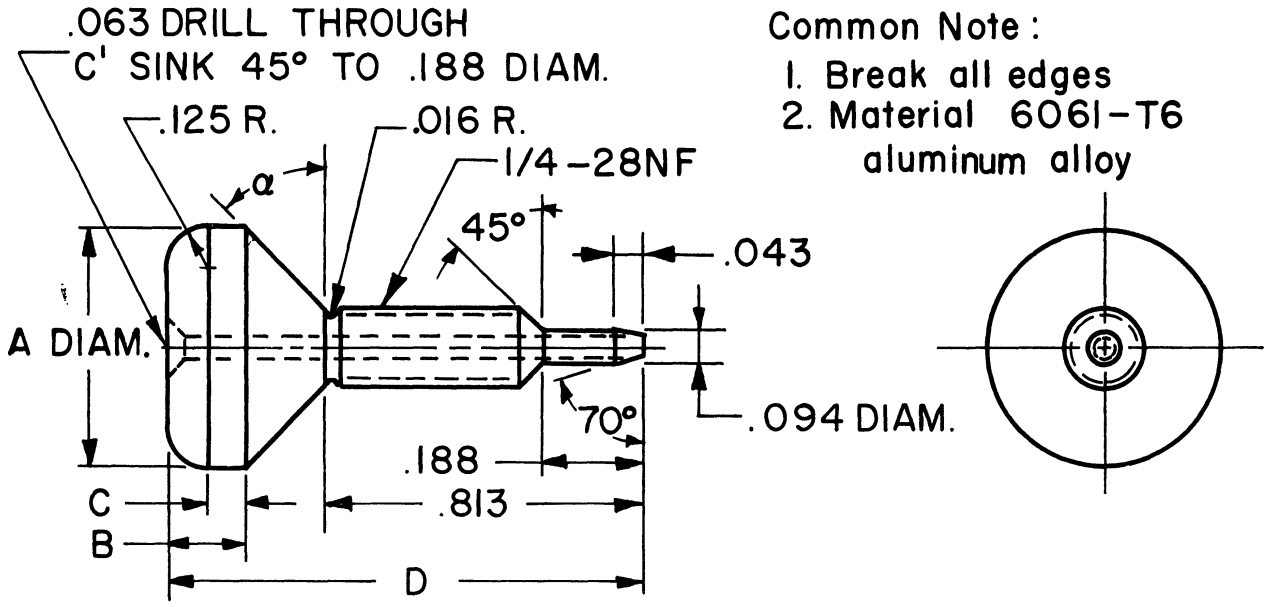

MALE ELEMENT - GAS INLET END

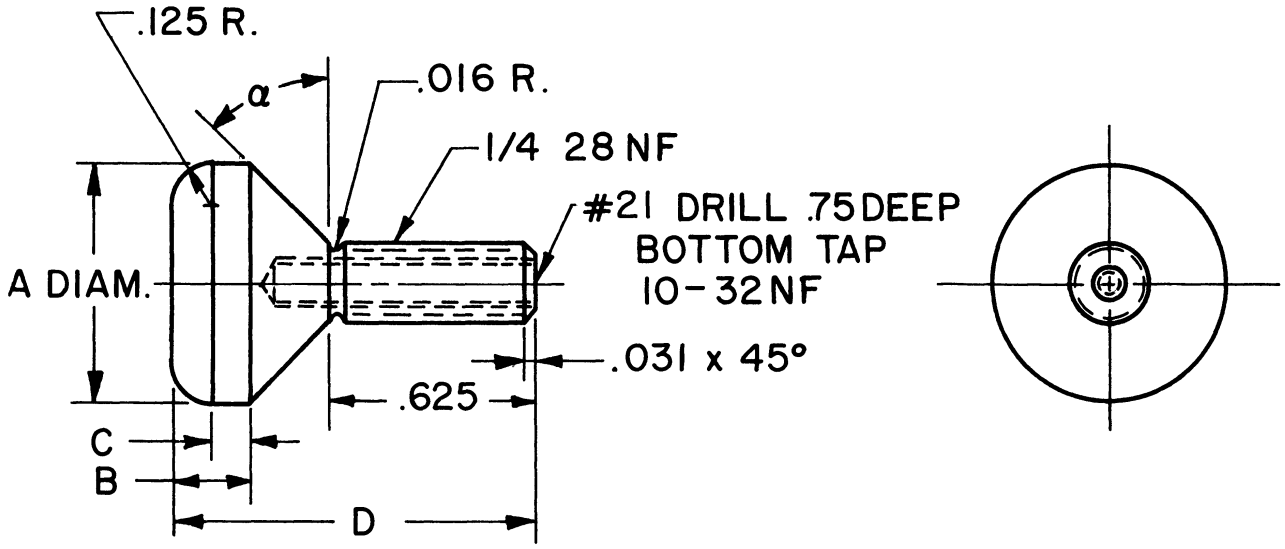

MALE ELEMENT—BLIND END

COMMON LETTERED DIMENSIONS			
DEVICE CODE NO. / FLAT WIDTH(W)	W-1 / .63	W-1 / .70	W-2 / .95
A	.391	.438	.563
B	.250	.188	.188
C	.125	.063	.063
D	1.257	1.163	1.157
α	70°	60°	45°

Fig. D-1. Details—male elements of the cone type ends used on the W-1 and W-2 BFA's. Drawings not to scale.

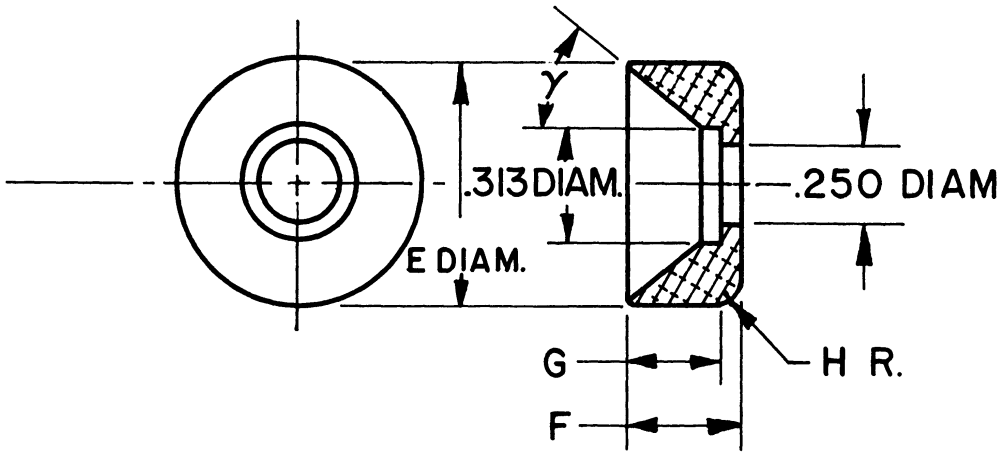

COMMON LETTERED DIMENSIONS			
DEVICE CODE NO. / FLAT WIDTH(W)	W-1 .63	W-1 .70	W-2 .95
E	.500	.625	.750
F	.341	.369	.329
G	.278	.306	.266
H	.016	.063	.094
γ	20°	30°	45°

FEMALE ELEMENT — COMMON BOTH ENDS

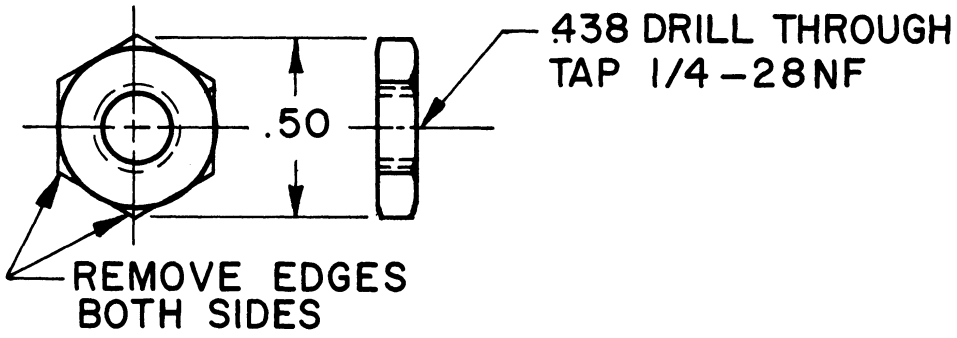

NUT — COMMON ALL ENDS

Common Note:

1. Break all edges
2. Material 6061-T6 aluminum alloy

Fig. D-2. Details—female elements and common nut of the cone type ends used on the W-1 and W-2 BFA's. Drawing not to scale.

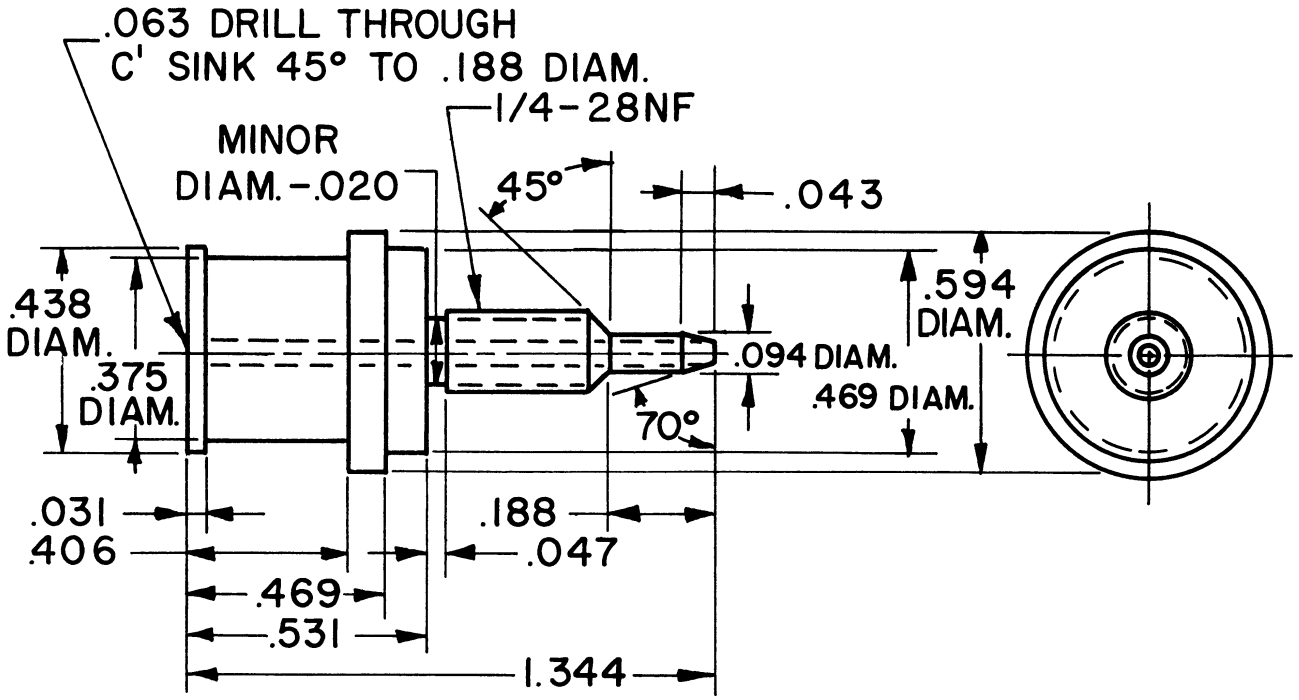

MALE ELEMENT—GAS INLET END

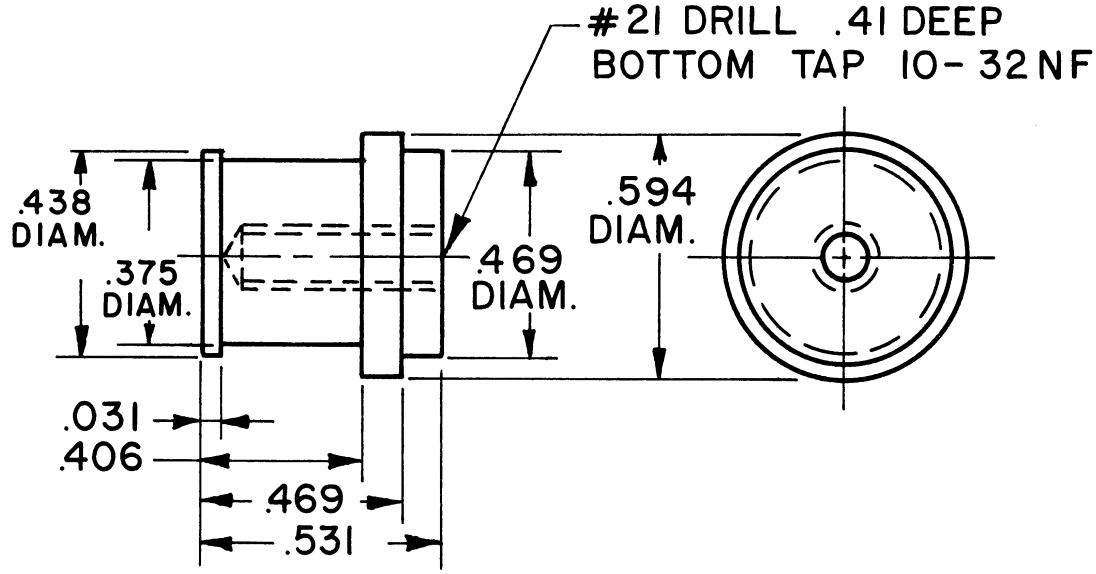

MALE ELEMENT — BLIND END

Common Note:

1. Break all edges

2. Material 6061-T6 aluminum alloy

Fig. D-3. Details—male elements of the cylindrical crimped type ends used on the W-4 and W-3I BFA's. Drawing not to scale.

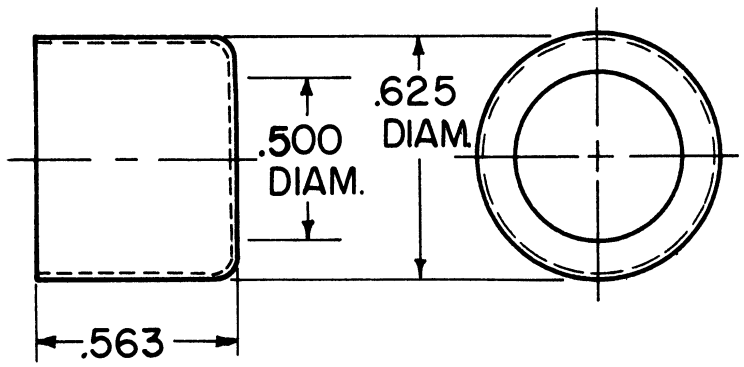

NOTE:

1. Material #28 Gage Brass-Chrome Plated
2. This is a Standard Commercial Hose end Fitting
3. Crimp on Male Element with Standard Commercial Tool for this Purpose

FEMALE ELEMENT—COMMON BOTH ENDS

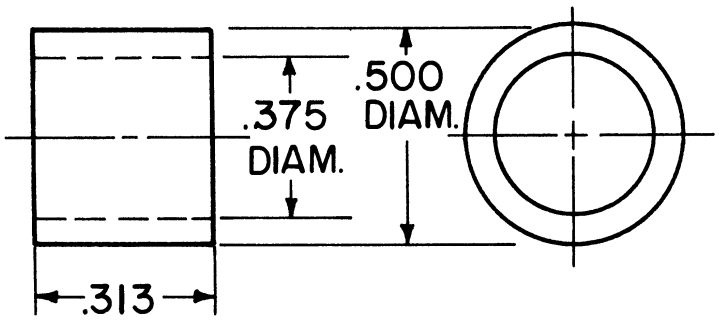

NOTE:

1. Material-Poly-Styrene Tubing

GROMMENT FOR MALE ELEMENTS

Fig. D-4. Details—female element and grommet of the cylindrical crimped type ends used on the W-4 and W-3I BFA's. The grommet fits over the cylindrical end of the male element which in turn fits inside the rubber inner tube. Drawing not to scale.

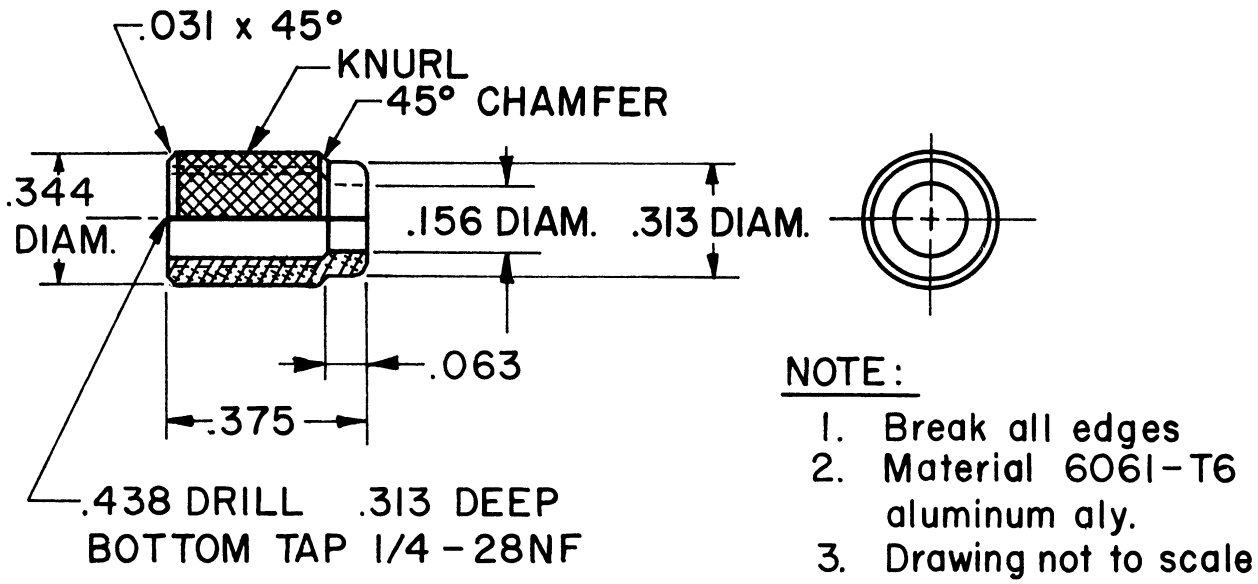

DETAIL-GAS-SUPPLY-LINE CLAMP-COMMON TO ALL TYPES OF GAS SUPPLY ENDS

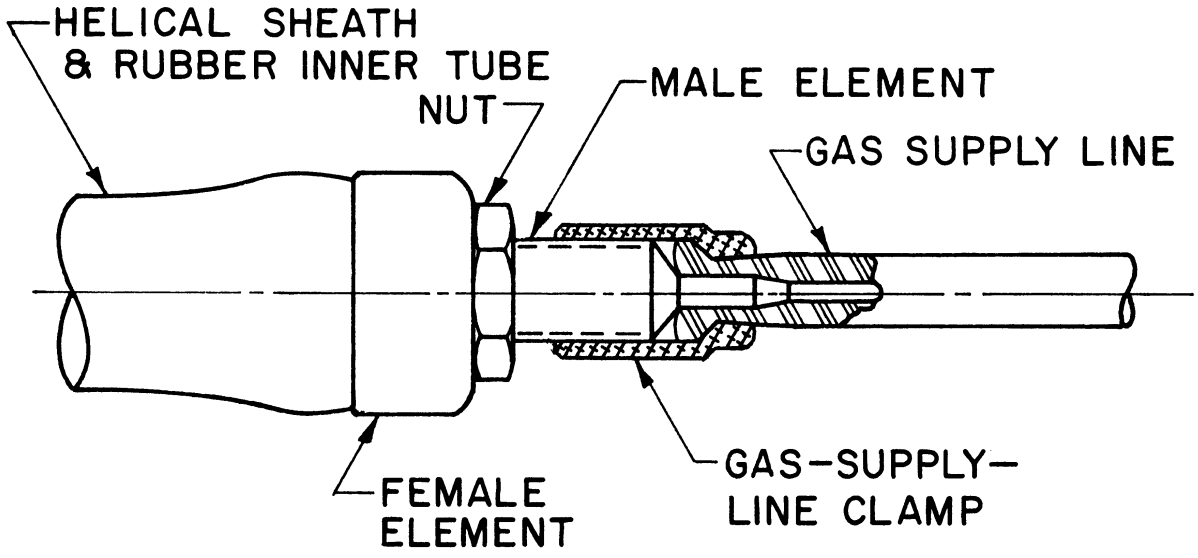

GAS-SUPPLY END ASSEMBLY

Fig. D-5. Details and application of the gas supply line clamp to the BFA. Drawing not to scale.

REFERENCES

1. National Foundation For Infantile Paralysis, Conference Report on the "Artificial Muscle," Downey, California, 1958.

2. Klopsteg, P. E., and Wilson, P. D., Human Limbs and Their Substitutes, McGraw-Hill Book Co., New York, 1954.

3. Dow Corning Corporation, "Preliminary Information on Silastic," Bulletin No. P-9-303, January, 1958.

4. Kececioglu and Opperthauser, "Construction of Alignment Nomograms," Product Engineering, McGraw-Hill, Mid-September, 1959.

5. Meeusen, H. J., "The Application of Nomograms to The Solution of an Engineering Problem," Reprint from the General Motors Engineering Journal, Detroit, Michigan, 1960.

6. Snelson, R., personal communication, Rancho Los Amigos Hospital, Downey, California, 1960.

7. Schulte, H. F., "Characteristics of the McKibben Artificial Muscle," In The Application of External Power in Prosthetics and Orthotics, Comm. on Prosthetics Research and Development. National Academy of Sciences—National Research Council, Publication 874, September, 1960.

8. Mills, F. C., Statistical Methods, 3rd ed., Henry Holt and Co., New York, 1955.

9. Timoshenko, Stephen, Theory of Elasticity, McGraw-Hill, New York, 1934.